Communauté UNIVERSITÉ Grenoble Alpes
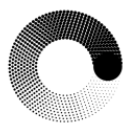
moscow polytech

THÈSE

Pour obtenir le grade de

DOCTEUR DE LA COMMUNAUTÉ UNIVERSITÉ GRENOBLE ALPES

préparée dans le cadre d'une cotutelle entre la Communauté Université Grenoble Alpes et l'Université Polytechnique de Moscou

Spécialité : Physique Subatomique et Astroparticules
Arrêté ministériel : 25 mai 2016

Présentée par

Aleksandr NEZVANOV

Thèse dirigée par **Valery NESVIZHEVSKY**, Institut Laue-Langevin et codirigée par **Valery ARTEM'EV**, Research Institute of Materials Technology
préparée au sein du **Laboratoire Institut LAUE LANGEVIN** dans **l'École Doctorale de Physique**

Particularités de l'interaction et de la propagation de neutrons à basse énergie dans des milieux nano-dispersés (l'exemple de la nano-poudre de diamant)

Peculiarities of interaction and propagation of low-energy neutrons in nano-dispersed media (the example of diamond nano-powder)

Thèse soutenue publiquement le **29 octobre 2018**, devant le jury composé de :

Monsieur KEN ANDERSEN
DIRECTEUR DE RECHERCHE, ESS - SUEDE, Examinateur
Monsieur ALEXEÏ BOSAK
MAITRE DE RECHERCHE, ESRF GRENOBLE, Examinateur
Monsieur BENOÎT CLEMENT
MAITRE DE CONFERENCES, UNIVERSITE GRENOBLE ALPES, Examinateur
Monsieur MARC DUBOIS
PROFESSEUR, UNIVERSITE CLERMONT AUVERGNE, Rapporteur
Monsieur ALEXEÏ VORONIN
DIRECTEUR DE RECHERCHE, ACADEMIE DES SCIENCES DE RUSSIE, Rapporteur
Monsieur KONSTANTIN PROTASSOV
PROFESSEUR, UNIVERSITE GRENOBLE ALPES, Président

Aleksandr Nezvanov, Université Grenoble Alpes, 2018
Peculiarities of interaction and propagation of low-energy neutrons in nano-dispersed media (the example of diamond nano-powder)

2

CONTENTS

Aleksandr Nezvanov, Université Grenoble Alpes, 2018
**Peculiarities of interaction and propagation of low-energy neutrons in nano-dispersed media
(the example of diamond nano-powder)**   *3*

ACKNOWLEGMENTS

Aleksandr Nezvanov, Université Grenoble Alpes, 2018
Peculiarities of interaction and propagation of low-energy neutrons in nano-dispersed media
(the example of diamond nano-powder) 5

INTRODUCTION

Efficient devices and facilities based on intense neutron sources are irreplaceable for research in physics, biology, chemistry, materials science, nuclear physics, the study of real monuments of cultural heritage, and in many other areas. The research is carried out in the fundamental fields of science, but is even more widely applied to application areas of work in various sectors, making the basis of methods of control and certification in materials science, the development of new technologies, including nanotechnology and biotechnology (possible to use on living organisms – *in vivo*). That is, they are the engine of the innovative development of the modern economy, including the long-term perspective.

The present-day most intense sources of neutrons – are unique powerful nuclear reactors and spallation sources on the basis of particle accelerators. They have a very high cost, built only in a single unique copies for collective use by many countries. The instrument base and infrastructure make up the main part of the costs for the creation and operation of research neutron facilities. In some countries, one or several lower-cost neutron sources with lower intensity are working to ensure current research and the educational process.

"Useful" are only the neutrons delivered from a neutron source through neutron guides to the experimental facility. On the present stage of development of the experimental technique, the number of "useful" neutrons is only a very small fraction of the total number of neutrons produced. If it were possible to increase the percent of delivered neutrons, a large yield of "useful" neutrons can be obtained even from low-cost neutron sources of low power.

A significant increase in the fraction of "useful" neutrons became possible in principle through the use of the method of nanoparticle neutron reflectors. This method was first proposed, theoretically developed, and experimentally implemented in [1]–[4], [140], [5], [6], [14], [7], [141-144], [105], [60], [145], [35]. In the experiment, an increase

Aleksandr Nezvanov, Université Grenoble Alpes, 2018

6 **Peculiarities of interaction and propagation of low-energy neutrons in nano-dispersed media (the example of diamond nano-powder)**

in the flux density of cold neutrons (CN) and very cold neutrons (VCN) was achieved, which is equivalent to a multiple increase in the power of research nuclear reactor used as a neutron source.

The method is based on using wave properties of neutrons and nanotechnologies. In the design of the new reflectors, diamond nanopowder was applied as the main functional material. Reflectors are most effective for CN and VCN with energies in the range from 100 neV to 1 meV, or in the neutron wavelength range from 1 nm to 100 nm. In this energy range, all conventional (massive) materials are transparent to neutrons - the reflection coefficient of such neutrons (albedo) from all materials is close to zero. That is, VCN and CN are practically not reflected from common materials, they freely pass through them. While the reflectors made of nanostructured materials allow to reflect and even to store very slow neutrons in closed traps.

The initial theoretical models justified the choice of the correct functional material (diamond nanopowder), and correctly predicted the basic regularities of the interaction of slow neutrons with diamond nanopowder. These models allowed us to theoretically calculate the main expected quantitative characteristics of the interaction results with an acceptable level of accuracy, and this allowed us to successfully plan and conduct the main experiments. The basic model approximations were assumed: neutron scattering occurs on isolated nanoparticles, neutron scattering is calculated using perturbation theory (Born equation), and nanopowder has a monodisperse homogeneous composition [1]–[3], [8], [4], [140], [5], [14], [7], [141-144], [105], [60], [145], [35].

However, such a level of idealization of objects and interaction processes no longer makes it possible to carry out a quantitative analysis of the various data of modern experiments with a satisfactory level of accuracy. Therefore, further theoretical development of quantitative models is required, that will take into account a more realistic interaction of neutrons with nanopowder particles. Also, the properties of a real diamond nanopowder should be taken into account in calculations. This approach will provide a more complete understanding of the most significant physical processes in the interaction of nanopowders with neutrons.

Aleksandr Nezvanov, Université Grenoble Alpes, 2018
Peculiarities of interaction and propagation of low-energy neutrons in nano-dispersed media | 7
(the example of diamond nano-powder) |

Neutrons in powder interact with individual nanoparticles that are surrounded by other nanoparticles in a dense medium. Therefore, for the correct calculation of the interaction of neutrons with powder, it is necessary to apply the methods of the theory of multiple scattering of the waves, and take into account the effects of the medium density [9]–[12].

Using the Born approximation [9] significantly accelerates and simplifies calculations. It is necessary to make preliminary quantum-mechanical calculations [13] of neutron scattering at different energies by particles of different sizes, and determine quantitatively the region of applicability of the Born approximation.

In carrying out of neutron experiments [14], which results will be considered in the present thesis, used the diamond nanopowder of the trademark *"ultradiamond90"* [15], made on the basis of patents [16], [17]. Diamond nanoparticles have spherical shape and sizes from 0.5 to 10 nm. Nanoparticles are heterogeneous by structural and chemical composition, surrounded by a non-diamond shell with a thickness of 0.5 to 0.7 nm [18], [19], [20]. Diamond nanoparticles form inside the nanopowder volume hard-to-destroy agglomerations [21], [22], [23], [24], [25]. The total porosity of the diamond nanopowder is 80–90% [7], [14]. Diffraction on inhomogeneities of the medium becomes the main mechanism determining the processes of neutron propagation with wavelengths $\lambda > \lambda_d$, where $\lambda_d \sim (a / n_{at})^{1/4}$, a and n_{at} are the radius and atomic (nuclear) density of the dispersed nanoparticle matter, respectively [6]. Therefore, when the dispersion by the size of the powder particles is significant, this fact must be taken into account in theoretical models to correctly interpret real experiments in a wide energy range.

The **<u>aim of the present study</u>** is to develop a quantitative model for the interaction and propagation of low-energy neutrons in nanodispersed media (using the diamond nanopowder as an example), which takes into account the influence of the nanodispersed medium density on the processes of propagation and scattering of low-energy neutrons, and the information about the structure of a diamond nanopowder.

The **<u>urgency</u>** of the problem being solved is due to the lack of information about the completeness of the concepts of the systems under study, about the mechanisms of

Aleksandr Nezvanov, Université Grenoble Alpes, 2018

8 | ***Peculiarities of interaction and propagation of low-energy neutrons in nano-dispersed media (the example of diamond nano-powder)***

interaction of low energy neutrons with nanostructured materials, about the features of the properties of the structure of nanodispersed media, about the evolution of nanodispersed systems under the influence of radiation. The development of the proposed quantitative model is necessary for qualitative evaluation and interpretation of various experimental data. The development of a quantitative model and methods for the quantitative calculation of the interaction and propagation of low-energy neutrons in nanodispersed media will allow to interpret independent experimental data within the frames of unified concepts, and will significantly reduce the amount of empirical parameters in the quantitative interpretation of experimental results.

Scientific novelty. The research suggests a quantitative model of low-energy neutron transfer in nanodispersed media, which takes into account data on the features of the diamond nanopowder structure. The model takes into account the influence of the medium density and the features of coherent and incoherent interaction of neutrons with nanopowder. The research defines the boundary conditions for the neutron transfer equation in diffusion approximation with allowance for the quantum effects of neutron interaction with the material boundaries. A set of computer programs was written and implemented to calculate the neutron transfer according to the proposed quantitative model. Independent experimental data is interpreted within the framework of a global view.

The research has brought **new scientific results**, which the author puts forward for defense.

The main statements to be defended

1. The thesis suggests a neutron transfer equation in diamond nanopowders, which takes into account the internal small-scale material structure and coherent and incoherent processes of interaction between low-energy neutrons and nanopowder material.

2. The research allowed to define the boundary conditions for the neutron transfer equation in the diffusion approximation, which accounts for coherent and incoherent processes of interaction between neutrons and the material.

Aleksandr Nezvanov, Université Grenoble Alpes, 2018
Peculiarities of interaction and propagation of low-energy neutrons in nano-dispersed media | *9*
(the example of diamond nano-powder)

3. The thesis uses the variation method to suggest an analytical solution for the radiation transfer equation, which accounts for the absorption in the small-angle scattering approximation.

4. The thesis proposes and justifies the low-energy neutron interaction model with diamond nanopowder, taking into account the features of the nanopowder structure, and the features of the coherent and incoherent interaction between neutrons and nanopowders.

5. A set of computer programs was designed and implemented to calculate the interaction and propagation of neutrons in diamond nanopowders, taking into account the features of the nanopowder structure, diamond nanoparticles and the processes of coherent and incoherent interaction of neutrons with nanopowders.

6. Theoretical numerical calculations were conducted with the proposed model for the interaction of low-energy neutrons with diamond nanopowders, and the calculation results were compared with experimental results.

Personal Contribution of the Author

The author of the thesis was directly involved in the work at all stages of the research. He also participated in writing academic articles and conference reports. He presented a few reports at different conferences.

Personal contribution of the author to the obtained results that are to be defended:

1. Participation in the literature research about the structure and properties of diamond nanopowders. Participation in carrying out analytical and numerical calculations that substantiated the neutron transfer equation.

2. Participation in the conduct of analytical calculations.

3. Participation in the conduct of analytical and numerical calculations.

4. Participation in discussions while enunciating and substantiating the model. Participation in the analytical and numerical calculations.

5. Participation in computer program algorithms design. Implementation of computational algorithms in the programming language. Writing and debugging computer programs. Carrying out numerical calculations.

Aleksandr Nezvanov, Université Grenoble Alpes, 2018

10 | **Peculiarities of interaction and propagation of low-energy neutrons in nano-dispersed media (the example of diamond nano-powder)**

6. Conducting numerical calculations with the designed model on the computer. Participation in the analysis, interpretation and comparison of the obtained numerical results with experimental data.

Practical implications. The author recommends using the proposed quantitative model and the designed set of computer programs for qualitative and quantitative estimates and interpretation of various experimental results, and for preliminary quantitative calculations at the stage of experiment planning.

The thesis consists of an introduction, four chapters, a bibliography and conclusions.

The first chapter presents the results of the research into the level of current global technical development of nuclear nanotechnologies. It is noted that in the world today there are practically no nanotechnological inventions designed for specific applications in the nuclear industry. At present, the nuclear nanotechnologies are at the stage of fundamental and exploratory academic research, predominantly focused on the extraction and accumulation of new knowledge.

The research goals and objectives were defined.

The second chapter suggests a model for the propagation of low-energy neutrons in a nanodispersed medium. An expression is obtained for the neutron transfer equation, i.e. Boltzmann type equation. Expressions are obtained for the average effective potential of the nanodispersed powder, effective potentials for nanoparticles and interparticle space. The chapter defines the equation of neutron transfer in the diffusion form. The neutron transfer equations are based on the theory of multiple wave scattering, and allow for the medium density. The boundary conditions are analyzed and established for the neutron transfer equation in the diffusion approximation, accounting for coherent and incoherent processes of neutron interaction with the material. The variational method enables an analytical solution of the transfer equation for the neutron distribution function in the approximation of small angle neutron scattering by nanoparticles in the powder. The experimental data allows to develop a model of diamond nanopowder, which is to be used in calculations.

Aleksandr Nezvanov, Université Grenoble Alpes, 2018
Peculiarities of interaction and propagation of low-energy neutrons in nano-dispersed media | *11*
(the example of diamond nano-powder)

The third chapter describes the design of an algorithm for numerical simulation of neutron tranfer in a diamond nanopowder. Model calculations of the cross section for elastic coherent scattering of neutrons by spherical nanoparticles are carried out: 1) precise quantum-mechanical calculations by the phase-function method; 2) calculations in the Born approximation. The calculations are performed for different values of neutron energies and nanoparticle radii, and the results are compared. For reference, we briefly describe standard methods for simulating random values of scattering angles and transformations of coordinate systems in computer Monte Carlo method simulation of neutron propagation in nanopowder.

The fourth chapter presents the results of numerical calculations carried out after the suggested quantitative model. The results of numerical calculations are analyzed and compared with experimental data. The comparison shows a satisfactory agrement of calculations with the data of independent experiments.

Research approbation. The main research results were presented by the author of the thesis at international and national academic conferences, seminars and meetings:

1. Meeting and Youth Conference on the Use of Neutron Scattering and Synchrotron Radiation in Condensed Matter, NRC 'Kurchatov Institute' — PNPI, 2014, Gatchina, Russia;

2. 23rd International Seminar on Interaction of Neutrons with Nuclei, FLNP JINR, **2016**, Dubna, Russia;

3. Dautreppe Seminar: Demain l'Énergie, SFP, **2016**, Grenoble, France [26];

4. 25th International Seminar on Interaction of Neutrons with Nuclei, FLNP JINR, **2017**, Dubna, Russia;

5. Young researchers conference 'Innovations in Nuclear Energy', JSC Research and Design Institute of Power Engineering named after N.A. Dollezhal, **2017**, Moscow, Russia;

6. LI School on Condensed Matter Physics, NRC 'Kurchatov Institute' — PNPI, **2017**, Saint Petersburg, Russia;

Aleksandr Nezvanov, Université Grenoble Alpes, 2018

12 | ***Peculiarities of interaction and propagation of low-energy neutrons in nano-dispersed media (the example of diamond nano-powder)***

7. 11th International Conference 'Carbon: The Fundamental Problems of Science, Materials Science, Technology', Federal State Institution Technological Institute for Superhard and Novel Carbon Materials, **2018**, Moscow, Troitsk, Russia;

Publications containing the main research results. The following works were based on the thesis materials: [27], [26], [28], [29], [30], [31], [32], [33], [34], [35], [36], [37], among them:

7 abstracts of reports for academic conferences, seminars, meetings;

3 reports in collected works of international and national academic seminars and conferences:

1. Artem'ev V.A., Nesvizhevsky V.V., **Nezvanov A.Yu.**, Proskuryakov A.L. A Solution of the Kinetic Equation for the Propagation of Radiation in Nanodispersed Absorbing Medium in the Approximation of Small Scattering Angles // Proceedings of the XXIII International Seminar on Interaction of Neutrons with Nuclei. Dubna: JINR, 2016. pp. 111–118.

2. Artem'ev, V. A., **Nezvanov, A. Y.** (2017). Nanotechnology for nuclear energy and industry [in Russian]. In Proceedings of the conference of young specialists "Innovations in Nuclear Energy" (pp. 362–368). Moscow: Publishing house of NIKIET.

3. Artem'ev V.A., Nesvizhevsky V. V., **Nezvanov A.Yu.** Estimations of the Inelastic Interaction of Neutrons with Nanostructures Media at Low Energies and Temperatures // Proceedings of the XXV International Seminar on Interaction of Neutrons with Nuclei. Dubna: JINR, 2018. pp. 23–30.

2 articles in academic journals:

1. Artem'ev, V. A., **Nezvanov, A. Yu.**, & Nesvizhevsky, V. V. (2016). Precise calculations in simulations of the interaction of low energy neutrons with nano-dispersed media. Crystallography Reports, 61(1), 84–88. DOI: 10.1134/S1063774516010028;

2. Nesvizhevsky V.V., Dubois M., Gutfreund Ph., Lychagin E.V., **Nezvanov A.Yu.** and Zhernenkov K.N. Effect of nanodiamond fluorination on the efficiency of quasispecular

Aleksandr Nezvanov, Université Grenoble Alpes, 2018

Peculiarities of interaction and propagation of low-energy neutrons in nano-dispersed media 13
(the example of diamond nano-powder)

reflection of cold neutrons // Phys. Rev. A. American Physical Society, 2018. Vol. 97, i. 2. pp. 1–8. DOI: 10.1103/PhysRevA.97.023629;

2 certificates of state registration for a computer program:

1. Nezvanov, A. Yu. (2015). 2015618099. RU: Russian Agency for Patents and Trademarks;

2. Nezvanov, A. Yu. (2016). 2016612455. RU: Russian Agency for Patents and Trademarks.

CHAPTER 1. REVIEW OF THE RESEARCH WORK ON INTERACTIONS BETWEEN IONIZING RADIATIONS AND NANODISPERSED MEDIA

1.1. The level of technical development of nanotechnologies in nuclear energy and industry

In 1952 exponential growth in the number of registered nanotechnological patents started which pointed to the start of conversion of the primary academic skills gained earlier in a set of technological applications and their implementation in economic turnover [38]. As it's considered, nanotechnology is the most probable initiator of a new long economic wave in the world [39]. The shift of long economic waves is related to technological paradigm (waves of innovation) — a set of technologies typical of a certain level of production development [40]. Revolutionary technologies generate new industries, provide opportunities for expansion in the production and formulate new sectors of economy. A significant impact of nanotechnologies is foreseen on the global economy, as in every industry sector they possess practical applications.

A work has been published by the beginning of the thesis work [41]. It summarizes results of the research on the existing level of the technical development of nanotechnologies in nuclear industries and technology in the world. The subject of the research has been the dynamics in the occurrence of new nanotechnological patents in the period of 1950-2012, as well as the distribution of these patents by thematic areas of technologies in nuclear industries. The research has been carried out on databases and funds of national patent offices around the world. The research method is described in [38], [41].

The patent information of interest refers to the section of nuclear technologies and is contained in the class G21 "Nuclear Physics; nuclear engineering" of the International Patent Classification – IPC. Statistical studies on patenting dynamics have been implemented in the fields of nuclear technologies in the class G21. The database esp@cenet of the European Patent Office (EPO) has been applied.

Aleksandr Nezvanov, Université Grenoble Alpes, 2018
Peculiarities of interaction and propagation of low-energy neutrons in nano-dispersed media
(the example of diamond nano-powder) | *15*

In the result of the research carried out, statistical data are obtained and the following conclusions are made [38], [41].

In the period of 1960–2012, in the total number of patents in the class G21 the number of patents on nuclear nanotechnologies amounted to a percentage less than 1%. For the period of 1950–2012, the number of nanotechnological patents in the field of nuclear technologies composed less than 15% of the total number of the world's registered nanotechnological patents on all economic sectors. A considerable number of existing patents on nuclear nanotechnologies is for the application of electronic industry (X-ray and electronic lithography, etc.). Nanotechnological patents with respect to the areas: nuclear reactors (class G21C); protection from X-ray, gamma- and corpuscular radiation, bombardments with particles, materials processing with radioactive contamination, devices aimed at eliminating the radioactive contamination of such materials (class G21F); energy production from radioactive sources, application of radiation of radioactive sources, usage of cosmic radiation (class G21H); and others – are represented in single documents. Objectively, well-known nanotechnological solutions, intended for the specific application in nuclear industry, don't actually exist in the world.

Currently, in the field of nuclear nanotechnologies both on separate areas and industry on the whole, there exists a stage of fundamental and exploratory scientific research, on the basis of which procurance and accumulation of new knowledge mainly takes place. An important contribution to this activity was done, in particular, by my supervisors [61], [42], [56], [57], [43], [44], [47-52], [55], [53], [45], [46], [1], [54], [59], [2-4], [8], [5-7], [58], [60].

The absence of satisfactory results of the research in the following area, as well as, insufficient data on radiation resistance impedes the creation of new nuclear nanotechnologies and patents for the aim of effective use in nuclear industry.

Aleksandr Nezvanov, Université Grenoble Alpes, 2018

16 | **Peculiarities of interaction and propagation of low-energy neutrons in nano-dispersed media (the example of diamond nano-powder)**

1.2. Formulation of tasks and goals of the research in the thesis work

The review of the research work implemented above allows to draw the following conclusions.

The results gained by now confirm the credibility of initial theoretical models on pattern of interactions between IR and nanodispersed media.

In present, most intensively develops the research area on studying the interactions of low-energy neutrons with nanodispersed powders. All this indicates the importance of developing model perceptions about nanodispersed media properties. The tasks and goals of the research in the current thesis work can be formulated as follows.

1. It's necessary to record neutron transfer equation with respect to effects of the medium density. The model (approximation) of isolated nanoparticles being applied currently leads to a significant error at calculating kinetic processes.

2. It's necessary to analyze and clarify the boundary conditions of low-energy neutron transfer equation.

3. It's necessary to get an approximate solution of the transfer equation in the small-angle scattering approximation with the smallest rejection from the exact solution.

4. It's necessary to develop updated model of nanodispersed powder of the diamond, taking into account the experimental data about the structure of nanopowder.

5. It's necessary to calculate the exact cross-sections of neutron scattering on nanoparticles.

6. It's necessary to develop algorithms and a set of programs for the numerical simulation of neutron transfer in the diamond nanopowder.

7. It's necessary to make numerical calculations and make comparison with experimental data.

Aleksandr Nezvanov, Université Grenoble Alpes, 2018
Peculiarities of interaction and propagation of low-energy neutrons in nano-dispersed media | *17*
(the example of diamond nano-powder)

CHAPTER 2. DEVELOPING A MODEL OF LOW-ENERGY NEUTRONS PROPAGATION IN THE NANODISPERSED MEDIUM

For definiteness, we will choose detonation nanodispersed diamonds ([62], [63], [64], [65], [66]) as a material (nanodispersed medium). We will consider neutrons with wavelengths $\lambda > 0.4$ nm. It means that the energies of all neutrons will have values below the Bragg cut-off energy in diamond [67]. Such a choice of the energy range excludes from further consideration all the interaction processes caused by the phenomenon of Bragg neutron diffraction in the material.

2.1. Derivation of a neutron transport equation in a nanodispersed medium

Consider the basic regularities of low-energy neutrons propagation through nanodispersed medium using the example of nanodispersed powder.

For clarity of presentation we choose a model of a homogeneous nanopowder in the form of a composition of bulk identical sphere nanoparticles of radius a, filling with substance the relative volume fraction γ (γ is the powder packing coefficient [68]). We assume that the substance is chemically homogeneous. From purely mathematical point of view, identical incompressible balls might take their places in disordered form, generating configurations, for which the values of γ variable lie in the interval ([69], [70], [71]):

$$0.54 < \gamma < 0.64; \tag{2.1.1}$$

for bulk powder of identical particles, the average value is $\bar{\gamma} \approx 0.59$, for packed powder it is $\bar{\gamma} \approx 0.637$.

Denoting through V_1 the volume of one nanoparticle:

$$V_1 = 4\pi a^3 / 3 , \tag{2.1.2}$$

we obtain the average nanoparticles concentration N_0 of a homogenous nanopowder:

Aleksandr Nezvanov, Université Grenoble Alpes, 2018

18 ***Peculiarities of interaction and propagation of low-energy neutrons in nano-dispersed media (the example of diamond nano-powder)***

$$N_0 = \gamma / V_1 = 3\gamma / 4\pi a^3 \ . \tag{2.1.3}$$

A generalization of results obtained below to more realistic cases of the substances of the complex chemical composition, accounting the structuring of nanoparticle agglomerations in a powder, and the distribution of nanoparticles by size, is mainly of a technical nature and is set forth in the following text of the thesis.

For the neutrons with a wave length $\lambda \sim a$, a coherent elastic scattering on powder nanoparticles is essential. The cross-section of coherent elastic scattering of a neutron on a single nanoparticle is $\sigma_1^{coh} \sim N_1^2 \cdot \sigma_n^{coh}$, where N_1 is the total number of atoms (nuclei) in one nanoparticle; and σ_n^{coh} is the cross-section of coherent elastic scattering of a neutron on a single atomic nucleus. The cross section of incoherent elastic neutron scattering on a single nanoparticle is $\sigma_1^{inc} = N_1 \cdot \sigma_n^{inc}$ (the crystalline atomic structure of the nanoparticle), or $\sigma_1^{inc} \sim N_1 \cdot \sigma_n$ (the completely disordered atomic structure of the nanoparticle), where σ_n^{inc} and σ_n are incoherent elastic and completely elastic cross-sections of a neutron on a single atomic nucleus, respectively. It is seen that $\sigma_1^{coh} / \sigma_1^{inc} \sim N_1 \gg 1$, and therefore the coherent elastic scattering of neutrons by powder nanoparticles is the main type of interaction for neutron scattering.

Coherent elastic scattering of neutrons by nanoparticles can be described using an optical potential (pseudo-potential) [72], [73]:

$$U_0 = (2\pi\hbar^2 / m)n_0 b_c \sim 10^{-7} \ \text{eV} \ , \tag{2.1.4}$$

where m is the neutron mass, n_0 is the concentration of atoms (atomic nuclei) in the nanoparticle; and b_c is the coherent scattering length of a neutron on the bounded atomic nucleus.

The neutron scattering events on different nanoparticles can be considered as independent if the free path length l_s of a neutron in a nanodispersed medium is $l_s \gg a$. The cross-section of coherent elastic scattering of a neutron on a single nanoparticle in the Born approximation for $ka > 1$ has the form [9]:

Aleksandr Nezvanov, Université Grenoble Alpes, 2018
Peculiarities of interaction and propagation of low-energy neutrons in nano-dispersed media
(the example of diamond nano-powder)

19

$$\sigma_1^{coh} \cong \frac{2\pi}{k^2} \left(\frac{mU_0 a^2}{\hbar^2} \right)^2 , \qquad (2.1.5)$$

where we have introduced the notations: $k = 2\pi / \lambda$ the neutron wavevector, E the neutron energy, and $k^2 = 2mE / \hbar^2$. Expression (2.1.5) can be converted to the following form:

$$\sigma_1^{coh} \cong \pi a^2 \cdot \frac{U_0}{E} \cdot \left[\frac{U_0}{(\hbar^2 / ma^2)} \right] . \qquad (2.1.6)$$

The mean free path length l_s of a neutron in powder before scattering equals:

$$l_s = (N_0 \cdot \sigma_1^{coh})^{-1} . \qquad (2.1.7)$$

Taking into account expressions (2.1.3), (2.1.6) and (2.1.7) we obtain:

$$l_s \cong \frac{a}{\gamma} \cdot \frac{E}{U_0} \cdot \frac{(\hbar^2 / ma^2)}{U_0} \gg a , \qquad (2.1.8)$$

since the quantities have the characteristic numerical values: $E \sim 10^{-6} - 10^{-3} \, \text{eV}$, $U_0 \sim 10^{-7} \, \text{eV}$; and a applicability condition of the Born approximation is met $(\hbar^2 / ma^2) / U_0 \gg 1$. Using accurate quantitative calculations, it was previously found that the Born approximation (perturbation theory) is applicable in all relevant cases [34]. Therefore, the neutron scattering events by individual nanoparticles can be considered as independent for the process of propagation of neutrons in the nanoparticle powder.

The methods of multiple scattering of waves and particles have been justified and developed over the past decades. The research findings are presented in numerous scientific articles, monographs and textbooks (including [9]–[12], [75], [76], [77], [78], [79], [80], [81], [82]). Two main theoretical directions were developed: multiple wave scattering by continuous random fields and that by ensemble of discrete scattering centers (particles). The both theoretical methods give equivalent results [12], while the perturbation theory is applicable to wave-medium interactions.

Results of application of the known methods of the theory of multiple wave scattering to the problem of slow neutron propagation in a nanodiamond powder can be formulated in a simple form.

Aleksandr Nezvanov, Université Grenoble Alpes, 2018

20 | ***Peculiarities of interaction and propagation of low-energy neutrons in nano-dispersed media (the example of diamond nano-powder)***

The interaction of neutrons with a single nanoparticle is described by an optical potential $U_1(\mathbf{r})$:

$$U_1(\mathbf{r}) = \begin{cases} U_0, & r \le a \\ 0, & r > a \end{cases}. \qquad (2.1.9)$$

Consider the material is a nanopowder. Assume that a sample of our material occupies a volume V_t, and denote by N_t the total number of nanoparticles of the sample material in volume V_t:

$$N_t = N_0 V_t. \qquad (2.1.10)$$

Denote by $\{\mathbf{R}_j\}$ the complete set of vectors, by $\mathbf{R}_j$ the radius-vector of location of center of a jth nanoparticle in the powder, $j = 1, 2, ..., N_t$. $\{\mathbf{R}_j\}$ is a set of coordinates describing the first and other scatterers (nanoparticles).

The interaction of a neutron with the entire volume V_t of a material is described by a random potential field:

$$U\left(\mathbf{r}, \{\mathbf{R}_j\}\right) = \sum_{j=1}^{N_t} U_1\left(\left|\mathbf{r} - \mathbf{R}_j\right|\right). \qquad (2.1.11)$$

The Schrödinger equation for the wave function of a neutron interacting with a nanopowder in a volume V_t has the form:

$$-\frac{\hbar^2}{2m} \Delta_{\mathbf{r}} \psi\left(\mathbf{r}, \{\mathbf{R}_j\}\right) + \sum_{j=1}^{N_t} U_1\left(\left|\mathbf{r} - \mathbf{R}_j\right|\right) \cdot \psi\left(\mathbf{r}, \{\mathbf{R}_j\}\right) = E\psi\left(\mathbf{r}, \{\mathbf{R}_j\}\right). \qquad (2.1.12)$$

For elastic neutron scattering,

$$E = \hbar^2 k_0^2 / 2m, \qquad (2.1.13)$$

where k_0 is the initial neutron wave vector outside the volume of the sample.

If the condition $f_S N_0^{1/3} \ll 1$ is met [83], where f_S is an amplitude of s–scattering of a neutron on a single nanoparticle; or $\sigma_1^{coh} \ll \pi a^2$ ($\sigma_1^{coh} \ll N_0^{-2/3}$); or $l_s \gg a$ ($l_s \gg N_0^{-1/3}$), the correlations in random arrangement of nanoparticles are insignificant. The above conditions are practically equivalent. Considering the interaction of neutrons with a nanopowder, nanoparticles of the powder can be considered as a "gas" of low

Aleksandr Nezvanov, Université Grenoble Alpes, 2018
Peculiarities of interaction and propagation of low-energy neutrons in nano-dispersed media | 21
(the example of diamond nano-powder)

density, similar to [83]. Therefore, we assume that the positions N_t of the powder nanoparticles are chaotically (equiprobably) with a uniform density N_0 distributed in space of the volume V_t.

The equation for a coherent wave $\langle \psi(\mathbf{r}) \rangle$ is obtained by averaging over the coordinates $\mathbf{R}_j$. The averaging procedure reduces to integrating over $\mathbf{R}_j$ with weight $\left(V_t^{N_t}\right)^{-1}$ in the volume V_t, occupied by the sample. Assuming that all the scatterers are in the ground state, we obtain:

$$\langle \psi(\mathbf{r}) \rangle = \frac{1}{V_t^{N_t}} \int ... \int \psi\left(\mathbf{r}, \{\mathbf{R}_j\}\right) d\mathbf{R}_1 .. d\mathbf{R}_{N_t} \ . \tag{2.1.14}$$

Averaging the fields $U_1\left(|\mathbf{r} - \mathbf{R}_j|\right)$ for all configurations N_t of nanoparticles by volume V_t leads to the emergence of a constant potential energy $\langle U \rangle$ in the entire volume of our sample:

$$\langle U \rangle = \left\langle \sum_{j=1}^{N_t} U_1\left(|\mathbf{r} - \mathbf{R}_j|\right) \right\rangle = \frac{1}{V_t} \sum_{j=1}^{N_t} \int U_1\left(|\mathbf{r} - \mathbf{R}_j|\right) d\mathbf{R}_j =$$

$$= \frac{N_t}{V_t} \int_{r \leq a} U_0 dV = \frac{N_t}{V_t} \cdot \left(U_0 \cdot \frac{4\pi}{3} a^3\right) \ . \tag{2.1.15}$$

Taking into account (2.1.3), (2.1.10), we obtain from (2.1.15) for $\langle U \rangle$:

$$\langle U \rangle = \gamma U_0 = \gamma \left(\frac{2\pi \hbar^2}{m}\right) n_0 \, b_c \ . \tag{2.1.16}$$

Thus, $\langle U \rangle = \gamma U_0$ is the average constant homogeneous effective potential field (pseudo-potential), in which a coherent neutron wave propagates within nanopowder.

If we consider the propagation of neutrons in a nanopowder as the result of wave multiple scattering by an ensemble of discrete scattering centers (nanoparticles), another method can be used to determine the average effective field (pseudo-potential) impacting neutrons from the matter side [9]. The main type of neutron interaction with the nanopowder matter is coherent elastic neutron scattering by dispersed nanoparticles. The amplitude of neutron scattering by a single nanoparticle $f_1(\theta)$ in the Born approximation:

Aleksandr Nezvanov, Université Grenoble Alpes, 2018

22 | **Peculiarities of interaction and propagation of low-energy neutrons in nano-dispersed media (the example of diamond nano-powder)**

$$f_1(\theta) = -\frac{m}{2\pi\hbar^2} \int\limits_{r\leq a} U_1(\mathbf{r})e^{-i\mathbf{q}\mathbf{r}}dV \ . \tag{2.1.17}$$

The amplitude of neutron scattering "forward" (with angle $\theta=0$) on one nanoparticle in the Born approximation is:

$$f_1(0) = -\frac{m}{2\pi\hbar^2} \int\limits_{r\leq a} U_0 dV \ . \tag{2.1.18}$$

For the average effective field in the material we have [9]:

$$\langle U \rangle = -\left(\frac{2\pi\hbar^2}{m}\right)f_1(0)\,N_0 \ . \tag{2.1.19}$$

Taking into account (2.1.4) and (2.1.18):

$$f_1(0) = -b_c\,N_1 \ , \tag{2.1.20}$$

and then $\langle U \rangle = (2\pi\hbar^2/m)b_c N_1 N_0 = (2\pi\hbar^2/m)b_c \tilde{n}_0$, where $\tilde{n}_0 = N_1 N_0 = \gamma n_0$ is the average concentration of atoms (atomic nuclei) of a substance in the volume V_t, occupied by the material (nanopowder). This expression completely coincides with (2.1.16).

Thus, the Schrödinger equation (2.1.12) for the propagation of a coherent neutron wave $\langle \psi(\mathbf{r}) \rangle$ in a nanopowder has the following form:

$$-\frac{\hbar^2}{2m}\Delta_\mathbf{r}\langle \psi(\mathbf{r}) \rangle = \left[E-\langle U \rangle\right]\langle \psi(\mathbf{r}) \rangle \ . \tag{2.1.21}$$

The value $\langle U \rangle$ is no longer dependent on the coordinate $\mathbf{r}$ due to the homogeneity of the medium at these coordinates, and has the meaning of the effective potential energy of interaction of neutrons with medium (with nanopowder).

The random field (2.1.11), associated with the substance of dispersed nanopowder particles:

$$U(\mathbf{r}) = \sum_{j=1}^{N_t} U_1\left(\left|\mathbf{r}-\mathbf{R}_j\right|\right), \tag{2.1.22}$$

can be written as:

$$U(\mathbf{r}) = \langle U \rangle + U(\mathbf{r}) . \tag{2.1.23}$$

Aleksandr Nezvanov, Université Grenoble Alpes, 2018
Peculiarities of interaction and propagation of low-energy neutrons in nano-dispersed media | 23
(the example of diamond nano-powder)

The fluctuation part $U(\mathbf{r})$ of a random potential field $U(\mathbf{r})$ is determined by the relation:

$$U(\mathbf{r}) = U(\mathbf{r}) - \langle U \rangle. \tag{2.1.24}$$

From definition (2.1.24) it follows:

$$\langle U(\mathbf{r}) \rangle = \langle U(\mathbf{r}) - \langle U \rangle \rangle = \langle U \rangle - \langle U \rangle = 0. \tag{2.1.25}$$

Denote by $\mathbf{M}$ the part of the total volume V_t of the material, occupied by the substance of all N_t dispersed particles:

$$\mathbf{M} = \bigcup_{j=1}^{N_t} \left\{ \left| \mathbf{r} - \mathbf{R}_j \right| \le a \right\}. \tag{2.1.26}$$

$\mathbf{R}_j$ is a radius-vector of the center of jth powder nanoparticle, and $d = 2a$ is a diameter of the nanoparticle. The fluctuation part $U(\mathbf{r})$ of the random potential field in volume V_t of the material, taking into account (2.1.16), is:

$$U(\mathbf{r}) = \begin{cases} (1-\gamma)U_0, & \text{if} \quad \mathbf{r} \in \mathbf{M} \\ -\gamma U_0, & \text{if} \quad \mathbf{r} \notin \mathbf{M} \end{cases}. \tag{2.1.27}$$

Assuming for certainty $U_0 > 0$, we obtain:

$U(\mathbf{r}) = (1-\gamma)U_0 > 0$, if the point $\mathbf{r}$ falls into the space area, occupied by the matter, i.e. lies inside the volume of one of the nanoparticles ;

$U(\mathbf{r}) = -\gamma U_0 < 0$, if the point $\mathbf{r}$ falls into the interparticle space, i.e. into the pore, the empty space between particles of nanopowder, free of matter.

In the stationary case, the Schrödinger equation for the neutron wave function in the random field $U(\mathbf{r})$ (2.1.23) will be:

$$\frac{\hbar^2}{2m} \Delta_{\mathbf{r}} \psi(\mathbf{r}) + \left[\left(E - \langle U \rangle \right) - U(\mathbf{r}) \right] \psi(\mathbf{r}) = 0. \tag{2.1.28}$$

We note once again that averaging $\langle U \rangle$ here means averaging over the random realization $\{\mathbf{R}_j\}$ of nanoparticles positions in our material (in nanopowder). $E = \hbar^2 k_0^2 / 2m$ is the neutron energy in vacuum (outside the volume of a nanopowder V_t).

Aleksandr Nezvanov, Université Grenoble Alpes, 2018

24 | ***Peculiarities of interaction and propagation of low-energy neutrons in nano-dispersed media (the example of diamond nano-powder)***

We assume that condition $E > \langle U \rangle$, necessary for the neutron to propagate inside the nanopowder, is met.

From the Schrödinger equation (2.1.28), it can be seen that the process of neutron propagation in a nanopowder can be interpreted as follows. The neutron inside the nanopowder due to the effects of multiple elastic potential scattering on the structural elements of the medium (nanoparticles) has an effective (renormalized) energy of motion (kinetic energy) E_{eff} :

$$E_{eff} = E - \langle U \rangle = E - \gamma U_0 . \tag{2.1.29}$$

A coherent wave describes the motion of a neutron with an effective energy E_{eff} in a dispersed medium, to which the effective wave vector k_{eff} of a free (wave) neutron motion corresponds:

$$k_{eff} = \frac{1}{\hbar}\sqrt{2m\left(E - \langle U \rangle\right)} . \tag{2.1.30}$$

The effects of the medium density are taken into account in $\langle U \rangle$ via the nanopowder packing coefficient γ.

When the coherent neutron wave $\exp\left(i\mathbf{k}_{eff}\mathbf{r}\right)$ propagates in nanodispersed medium it is attenuated due to scattering on the fluctuation part $U(\mathbf{r})$ of a random potential field; due to other scatterers and in consequence of inelastic processes. The elastic coherent neutron scattering by the fluctuation potential $U(\mathbf{r})$ is an elastic incoherent process with respect to the propagation of the coherent wave $\exp\left(i\mathbf{k}_{eff}\mathbf{r}\right)$, and causes its decay in the material.

The description of neutron propagation in nanodispersed media, correctly considering coherent, incoherent, elastic and inelastic processes, is possible within the frames of kinetic theory. To do this, it is necessary to formulate the neutron transport equation (the Boltzmann-type kinetic equation).

Aleksandr Nezvanov, Université Grenoble Alpes, 2018
Peculiarities of interaction and propagation of low-energy neutrons in nano-dispersed media
(the example of diamond nano-powder) | 25

For definiteness, let us consider a model of a bulk nanopowder consisting of homogeneous sphere nanoparticles of radius a. Assume the packing coefficient of the nanopowder equal γ. Denote the porosity of the powder by p. The porosity p is the relative fraction of the powder volume that is not occupied by the substance. The following relation is met:

$$\gamma + p = 1.$$

Pores in the powder forms a complex branched spatial structure, free of matter. For the purposes of our description, introduce the concept of an individual pore as follows.

Dispersed particles of matter in a nanopowder form a spatial structure, at the nodes of which there are individual nanoparticles (similar to the visual model of an atomic crystal lattice formed of contacting balls [atoms] [68], [84]). An empty interstitial space (free of matter) inside a nanopowder bounded by the surfaces of the nearest neighboring nanoparticles will be called a separate interstitial space (individual pore, single pore). The boundaries of a single pore are the material surfaces of the nearest neighboring nanoparticles, as well as imaginary surfaces (planes) drawn at the sites of closest approach of the material surfaces of the nearest neighboring nanoparticles, which mentally delineate the distinguished interstitial space.

Establish dependences of the size and the number of pores on the nanopowder packing coefficient γ. Idealize the problem.

Assume that the identical sphere powder nanoparticles are located in the nodes of regular cubic cells forming a three-dimensional cubic lattice. Using the data of the works [68], [69], [84], it is possible to draw a Table 2.1 of properties of such cubic cells.

Introduce the notation: z_n is the coordination number, i.e. the number of nearest neighboring particles surrounding the powder particle and having contact with it; N_{dp} is the number of dispersed particles of powder per one cubic cell (per elementary volume); N_{int} is the number of interstitial positions (number of pores) per one elementary volume; α_z is the coefficient of proportionality in relation $z_n = \alpha_z \cdot \gamma$. The average value $\bar{\alpha}_z = (11.7647 + 11.5385 + 11.7647)/3 \approx 11.69$.

Aleksandr Nezvanov, Université Grenoble Alpes, 2018

26 | **Peculiarities of interaction and propagation of low-energy neutrons in nano-dispersed media (the example of diamond nano-powder)**

Obtain approximation for the powder of random structure from data of Table 2.1:

$$\bar{z}_n = \bar{\alpha}_z \cdot \gamma = 11.69 \cdot \gamma, \qquad (2.1.32)$$

where $\bar{z}_n$ is an average number of nearest neighboring nanoparticles surrounding the given nanoparticle of the powder, depending on the packing coefficient over the range $0.34 \leq \gamma \leq 0.68$.

Write down relation $N_{int} = P_p \cdot N_{dp}$. With increasing the number of powder particles that surround and contact the given particle, the number of interstitial volumes (pores) also increases. Simultaneously with increasing the number of particles in the powder volume, the total porosity of the material p decreases. Using data of Table 2.1, taking into account relation (2.1.31), we choose the approximation in the following form:

$$P_p = 0.48/p = 0.48/(1 - \gamma). \qquad (2.1.33)$$

Aleksandr Nezvanov, Université Grenoble Alpes, 2018
Peculiarities of interaction and propagation of low-energy neutrons in nano-dispersed media | *27*
(the example of diamond nano-powder)

Table 2.1.

Structural characteristics of an idealized powder, forming regular cubic spatial lattices of monodisperse particles.

Lattice type	Tetrahedral (diamond type)	Simple cubic	Body-centered cubic
z_n	4	6	8
γ	0.34	0.52	0.68
p	0.66	0.48	0.32
N_{dp}	—	1	2
N_{int}	—	1	3
α_z	11.7647	11.5385	11.7647

Notes to Table 2.1:

1) $\alpha_z = z_n / \gamma$.

2) Simple cubic packing of powder $(\gamma = 0.52)$: the particles are located in the vertices (nodes) of the cubic unit cell. The pore is in the center of the elementary cubic cell. In such a packing, one particle is associated with one pore.

3) Body-centered cubic powder packing $(\gamma = 0.68)$: particles are located in the vertices (nodes) and one particle is in the center of the cubic unit cell. The pores are located in the centers of the six side faces of the elementary cubic cell. In such a packing, one-unit cell has two powder particles and three pores.

Aleksandr Nezvanov, Université Grenoble Alpes, 2018

28 | **Peculiarities of interaction and propagation of low-energy neutrons in nano-dispersed media (the example of diamond nano-powder)**

Denote by N_p the average number of individual pores per unit volume of nanopowder (average concentration of pores).

Assume that the nanopowder has an average concentration N_0 of identical nanoparticles (2.1.3), the value of the powder packing density is γ and the porosity is p. The average concentration of individual (single) pores N_p of such powder will be approximated by expression:

$$N_p = P_p \cdot N_0 = \frac{0.48}{p} \cdot N_0 = \frac{0.48}{1-\gamma} \cdot N_0 \,, \tag{2.1.34}$$

in the range of values $0.52 \le \gamma \le 0.68$ and $0.32 \le p \le 0.48$. The specified interval includes values γ (2.1.1).

A neutron propagating in nanopowder with an effective wave vector $\mathbf{k}_{eff}$ (2.1.30), interacts with an individual nanoparticle of a powder through a potential $U_m = (1-\gamma)U_0$, and, with a separate pore of nanopowder, through a potential $U_p = -\gamma U_0$; see equations (2.1.27).

Taking into account the above estimates $l_s \gg a$ (2.1.8), one can assume neutron scattering by individual nanopores and nanoparticles to be independent. In this case, the process of neutron propagation in a nanopowder can be described using the transfer equation (Boltzmann equation) [85] for the neutron flux density $\Phi_n(\mathbf{r},\mathbf{\Omega},t)$ with the wave vector k_{eff}.

The transfer equation of low energy monenergistic neutrons in nanodispersed materials has the following form:

$$\frac{1}{\upsilon_{eff}} \cdot \frac{\partial \Phi_n}{\partial t} = -\mathbf{\Omega}\nabla\Phi_n - \Sigma_t \Phi_n + \int d\mathbf{\Omega}' \cdot \Phi_n(\mathbf{r},\mathbf{\Omega}',t) \Big[\Sigma_s W_s (\mathbf{\Omega}' \to \mathbf{\Omega}) +$$

$$+ \Sigma_{coh}^{(m)} W_{coh}^{(m)} (\mathbf{\Omega}' \to \mathbf{\Omega}) + \Sigma_{coh}^{(p)} W_{coh}^{(p)} (\mathbf{\Omega}' \to \mathbf{\Omega}) \Big] + q(\mathbf{r},\mathbf{\Omega},t) \,. \tag{2.1.35}$$

Here we introduce the notation:

υ_{eff} is the effective neutron velocity in nanopowder, $m\upsilon_{eff}^2 = 2(E - \langle U \rangle)$;

$\mathbf{\Omega}$ is the unit vector in the direction of neutron motion (velocity);

Aleksandr Nezvanov, Université Grenoble Alpes, 2018
Peculiarities of interaction and propagation of low-energy neutrons in nano-dispersed media
(the example of diamond nano-powder)   29

the total macroscopic cross-section of neutron interaction with nanopowder $\Sigma_t = \Sigma_a + \rho\sigma_s + N_0\sigma_{coh}^{(m)} + N_p\sigma_{coh}^{(p)}$, Σ_a takes into account inelastic processes (neutron absorption by nuclei, heating and cooling of neutrons, neutron decay);

$\rho = \gamma\, n_0$ is the concentration of atoms in the nanopowder, n_0 is the concentration of atoms (atomic nuclei) of the nanoparticle matter; σ_s is the neutron scattering cross-section by nuclei of the matter, describes the incoherent scattering by individual atomic nuclei of a nanoparticles matter;

$\sigma_{coh}^{(m)}$ and $\sigma_{coh}^{(p)}$ are the cross-sections for elastic coherent (potential) neutron scattering by individual nanoparticles and by nanopores, respectively;

$\Sigma_s = \rho\sigma_s$, $W_s(\boldsymbol{\Omega}' \to \boldsymbol{\Omega})$ is the probability of elastic scattering of a neutron, that moved before scattering in the direction $\boldsymbol{\Omega}'$, in the solid angle element $d\boldsymbol{\Omega}$ about the direction $\boldsymbol{\Omega}$ on the atomic nuclei of the nanoparticle matter (refers to elastic incoherent scattering processes);

$\Sigma_{coh}^{(m)} = N_0\,\sigma_{coh}^{(m)}$, $\Sigma_{coh}^{(p)} = N_p\,\sigma_{coh}^{(p)}$;

$W_{coh}^{(m)}(\boldsymbol{\Omega}' \to \boldsymbol{\Omega})$ and $W_{coh}^{(p)}(\boldsymbol{\Omega}' \to \boldsymbol{\Omega})$ are the probabilities of elastic coherent (potential) scattering of a neutron that moved before scattering in the direction $\boldsymbol{\Omega}'$, in the solid angle element $d\boldsymbol{\Omega}$ about the direction $\boldsymbol{\Omega}$ by nanoparticles (m) and nanopores (p) respectively;

$q(\mathbf{r}, \boldsymbol{\Omega}, t)$ is the distribution function of an external neutron source.

Pores in the powder have different volumes bounded by surfaces of complex shape, and are randomly oriented in space. Denote by $\{b\}$ the cumulative set of parameters characterizing the size and shape of the pores in the nanopowder, and by $f_p(b)$ we denote the distribution function of pores by these parameters.

Dispersed particles in a real nanopowder have various sizes and shapes, different from the shape of an ideal ball. Denote by $\{a\}$ the cumulative set of parameters characterizing the size and shape of the nanoparticles, $f_m(a)$ the distribution function of

Aleksandr Nezvanov, Université Grenoble Alpes, 2018

30 | **Peculiarities of interaction and propagation of low-energy neutrons in nano-dispersed media (the example of diamond nano-powder)**

dispersed nanoparticles by these parameters. $\int db \cdot f_p(b) = 1$, $\int da \cdot f_m(a) = 1$; the integration is performed over the areas of allowed values of parameters $\{b\}$ and $\{a\}$.

Taking into account the inhomogeneity of the nanopowder by the size of the dispersed particles, the neutron transport equation (2.1.35) takes the form:

$$\frac{1}{v_{eff}} \cdot \frac{\partial \Phi_n}{\partial t} = -\mathbf{\Omega}\nabla\Phi_n - \Sigma_t \Phi_n + \int d\mathbf{\Omega}' \cdot \Phi_n(\mathbf{r}, \mathbf{\Omega}', t)\left[\Sigma_s W_s(\mathbf{\Omega}' \to \mathbf{\Omega}) + \right.$$

$$\left. + \int da \cdot f_m(a) \cdot \Sigma_{coh}^{(m)} W_{coh}^{(m)}(\mathbf{\Omega}' \to \mathbf{\Omega}) + \int db \cdot f_p(b) \cdot \Sigma_{coh}^{(p)} W_{coh}^{(p)}(\mathbf{\Omega}' \to \mathbf{\Omega})\right] + \quad (2.1.36)$$

$$+ q(\mathbf{r}, \mathbf{\Omega}, t),$$

where denoted:

$$\Sigma_t = \Sigma_a + \rho\sigma_s + \int da \cdot f_m(a) \, N_0 \sigma_{coh}^{(m)} + \int db \cdot f_p(b) \, N_p \sigma_{coh}^{(p)}. \quad (2.1.37)$$

2.2. Boundary conditions analysis for the neutron transport equation

Assume that the material has a shape of a infinite flat plate of thickness H (Figure 2.2.1). The left plane of the plate is aligned with the plane xOy of the rectangular coordinate system, and the Z axis is directed inside the plate perpendicularly to the left surface (Figure 2.2.2). The average effective potential of a substance of the material equals

$$U = \langle U(\mathbf{r}) \rangle. \quad (2.2.1)$$

The material is supposed to be homogenous on average, therefore, $U = $ const. The average effective potential of the neutron interaction with the substance of the plate is equal to:

$$U(z) = \begin{cases} U > 0, & 0 \leq z \leq H \\ 0, & z < 0, \, z > H \end{cases}. \quad (2.2.2)$$

A neutron gas is to the left of the material. We denote its density by n_0. In the neutron gas, the motions of neutron are uniformly distributed by directions. The

Aleksandr Nezvanov, Université Grenoble Alpes, 2018
Peculiarities of interaction and propagation of low-energy neutrons in nano-dispersed media
(the example of diamond nano-powder)

31

probability of a neutron to move in the direction if a vector $\mathbf{\Omega}$, determined by the angles θ, φ, in the cone of solid angle $d\mathbf{\Omega}$ about vector $\mathbf{\Omega}$, is

$$dP(\theta, \varphi) = d\mathbf{\Omega}/4\pi. \tag{2.2.3}$$

Monoenergetic neutron flux with energy E falls on the surface of the material from the left:

$$E = \hbar^2 k_0^2/2m, \tag{2.2.4}$$

where $\mathbf{k_0} = (k_{0x}, k_{0y}, k_{0z})$ is a wave vector, m is the neutron mass, $\hbar$ is the Planck constant. Neutron wavelength λ_0 (in vacuum) is

$$\lambda_0 = 2\pi/k_0. \tag{2.2.5}$$

If the relation

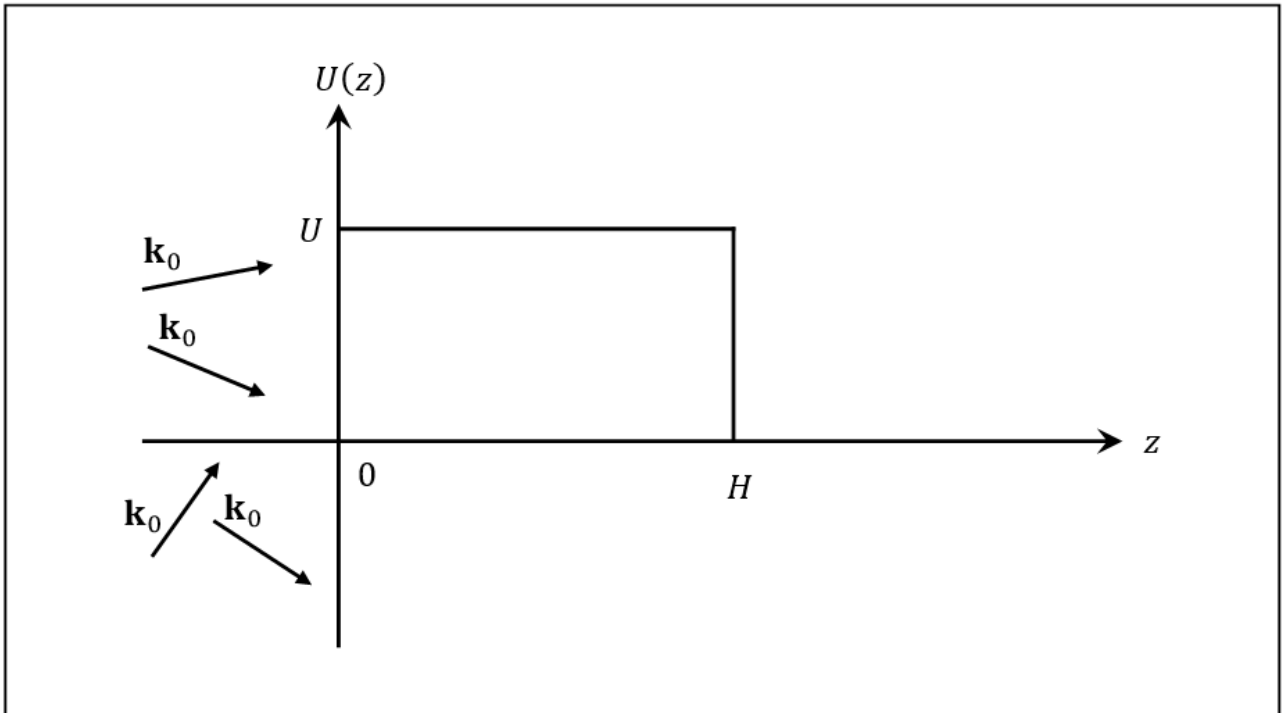$$\hbar^2 k_{oz}^2/2m < U \tag{2.2.6}$$

is valid then a total potential (mirror coherent) reflection of the neutron with a wave vector $\mathbf{k_0}$ from the surface of the material takes place (k_{oz} is the projection of vector $\mathbf{k_0}$ on Z-axis).
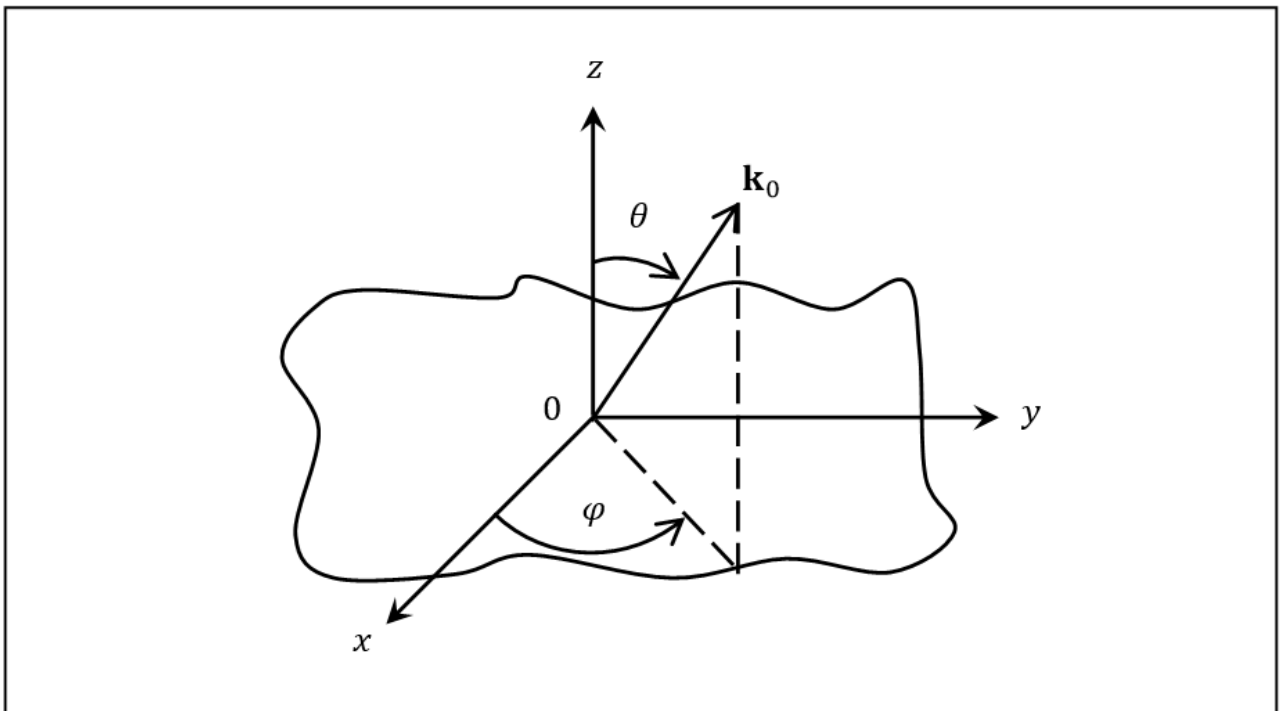
If

$$\hbar^2 k_{oz}^2/2m > U, \tag{2.2.7}$$

then a partial reflection of incident neutron wave from the surface of the material will occur [9].

Suppose that the material of the plate is nanostructured and represents itself a composition of sphere nanodispersed particles of characteristic radius a. The thickness of plate $H \gg l_s$, where l_s is a mean neutron path before interaction in the material. The neutron wavelength in the material is $\lambda \ll l_s$. Under this condition, it is possible to correctly determine the very concept of the mean free path. The typical values are: $a \cong 2$–3 nm, $\lambda \sim 3$–30 nm and $l_s \sim 10$–10^2 μm in nanodispersed diamond powder for neutron energies $E \sim 10^{-4}$–10^{-6} eV.

Aleksandr Nezvanov, Université Grenoble Alpes, 2018

32 | **Peculiarities of interaction and propagation of low-energy neutrons in nano-dispersed media (the example of diamond nano-powder)**

Fig. 2.2.1. The flux of neutrons with wave vectors $\mathbf{k_0}$,

falling on an infinite flat plate of thickness H.

Fig. 2.2.2. The coordinate system used

Aleksandr Nezvanov, Université Grenoble Alpes, 2018
Peculiarities of interaction and propagation of low-energy neutrons in nano-dispersed media
(the example of diamond nano-powder) | **33**

Suppose that the material of the plate is nanostructured and represents itself a composition of round nanodispersed particles of characteristic radius a. The thickness of plate $H \gg l_s$, where l_s – is a mean neutron path length before interaction in material. The neutron wavelength in the material $\lambda \ll l_s$. Under this condition it is possible to correctly determine the very concept of the mean free path. The typical values: $a \cong 2$–3 nm, $\lambda \sim 3$–30 nm and $l_s \sim 10$–10^2 μm in nanodispersed diamond powder for neutron energies $E \sim 10^{-4}$–10^{-6} eV.

The boundaries of material (the plate surface) have a transition area ("blurring") with the thickness $\sim a$. We will neglect this area and suppose that boundaries of the material are "sharp" at $z = 0$ and $z = H$. Such approximation is justified by the following arguments. The processes of propagation and scattering of neutrons on local potential inhomogeneities of size $\sim a$ are essential for distances $z \sim l_s$ and larger, and described by the Boltzmann-type transport equations.

For distances $z < l_s$, the neutron motion is described by the Schrödinger equation with mean field potential U. As shown in [9], «boundary blurring» of the potential does not affect the wave reflection and transmission coefficient trough the potential barrier. It is only the asymptotic height of the barrier that is important in the potential interaction.

In the plate of the material, the potential reaches its asymptotic value U beyond the boundaries of the transition layer with thickness $\sim a$ near the surfaces $z = 0$ and $z = H$. Therefore, the boundaries of the material (the plate surfaces) can be assumed as «sharp» and «smooth» (without roughness), when calculating the potential coherent reflection of neutrons from boundaries, if the condition $a \ll l_s$ is met.

Taking into account that $k_{oz} = k_0 \cdot \cos \theta$ (see Figure 2.2.2), the total reflection condition (2.2.6) will take form:

$$(\hbar^2 k_{oz}^2 / 2m) \cos^2 \theta = E \cos^2 \theta < U. \qquad (2.2.8)$$

The neutron transport onto the area $z > 0$ is possible only under condition $E \cdot \cos^2 \theta > U$, or

$$\cos \theta > \sqrt{U/E}. \qquad (2.2.9)$$

Only the neutrons that fall from vacuum at the angle θ to the surface normal propagate in material (Figure 2.2.2):

$$0 \leq \theta \leq \theta_U, \tag{2.2.10}$$

where

$$\cos \theta_U = \sqrt{U/E}. \tag{2.2.11}$$

The coefficients of neutron transmission D_{coh} and elastic potential (coherent) reflection R_{coh} from the boundary of material are related to each other by the ratio:

$$R_{coh}(\mathbf{k}_0) + D_{coh}(\mathbf{k}_0) = 1. \tag{2.2.12}$$

The coefficient of coherent transmission through material boundary for the neutron falling to the surface from the left in the direction of the vector $\mathbf{k}_0$, characterized by polar angles θ and φ, under condition $l_s \ll H$, equals [9]:

$$D_{coh}(\mathbf{k}_0) = \frac{4\cos\theta\sqrt{\cos^2\theta - U/E}}{\left(\cos\theta + \sqrt{\cos^2\theta - U/E}\right)^2}, \tag{2.2.13}$$

for $0 \leq \theta \leq \theta_U$, $0 \leq \varphi \leq 2\pi$.

The total neutron reflection coefficient from the material boundary can be given in form [6]:

$$R = R_{coh} + R_{inc}, \tag{2.2.14}$$

where $R_{coh}(\mathbf{k}_0)$ is the coefficient of elastic potential (mirror coherent) reflection of neutrons from the material surface; R_{inc} is the total coefficient of incoherent neutron reflection from the material boundary.

Albedo (reflection coefficient), by definition, is the ratio of the number of back scattered particles to the number of incident particles, i.e. the ratio of the back current of particles to the incident current of particles.

The coefficient of elastic potential (coherent) reflection under the condition $l_s \ll H$ equals to [9]:

$$R_{coh}(\mathbf{k}_0) = 1 \ ,$$
$$\text{for } \theta_U \leq \theta \leq \pi/2 \ , \quad 0 \leq \varphi \leq 2\pi \ ; \tag{2.2.15}$$

and

Aleksandr Nezvanov, Université Grenoble Alpes, 2018
Peculiarities of interaction and propagation of low-energy neutrons in nano-dispersed media
(the example of diamond nano-powder) | 35

$$R_{coh}(\mathbf{k}_0) = \frac{\left(\cos\theta - \sqrt{\cos^2\theta - U/E}\right)^2}{\left(\cos\theta + \sqrt{\cos^2\theta - U/E}\right)^2} \quad,$$

(2.2.16)

$$\text{for } 0 \le \theta \le \theta_U \;, \quad 0 \le \varphi \le 2\pi \;.$$

The potential reflection is a coherent scattering of neutrons from the matter, and it cannot be described in frames of kinetic and diffusion approximations (for the processes of incoherent scattering), since it is described by the Schrodinger equation with the potential energy U (2.2.1), (2.2.2) for the coherent part of the neutron wave function, valid for distances smaller than the value $\sim l_s \gg a$ from the material boundary.

Denote by $N(\mathbf{r}, \boldsymbol{\Omega}, v)$ the neutron angular density; $N(\mathbf{r}, \boldsymbol{\Omega}, v) \, dV \, d\boldsymbol{\Omega} \, dv$ the number of neutrons in the volume element dV near the point $\mathbf{r}$ with velocity in the interval $(v, v + dv)$, moving in the solid angle $d\boldsymbol{\Omega}$ about the direction of vector $\boldsymbol{\Omega}$; where $\boldsymbol{\Omega} = \mathbf{v}/v$ is a unit vector on the direction of velocity vector $\mathbf{v}$ [87].

The density of the neutron flux at the point $\mathbf{r}$ denote:

$$\Phi(\mathbf{r}, \boldsymbol{\Omega}, v) = v \cdot N(\mathbf{r}, \boldsymbol{\Omega}, v).$$

(2.2.17)

In a neutron gas, the directions of neutron motion are equiprobable (2.2.3). Therefore, the angular density of a gas of monoenergetic neutrons in vacuum will be (at $z < 0$):

$$N(\mathbf{r}, \boldsymbol{\Omega}, v) = \frac{n_0}{4\pi v^2} \, \delta(v - v_0),$$

(2.2.18)

where n_0 is a neutron gas density in vacuum (the number of neutrons per unit volume); v_0 is a neutron velocity in a vacuum,

$$E = mv_0^2/2.$$

(2.2.19)

Denote:

$$d\mathbf{j}_{\boldsymbol{\Omega}} = \mathbf{v} \cdot N(\mathbf{r}, \boldsymbol{\Omega}, v) \, dv,$$

(2.2.20)

neutron current (neutron gas current vector) at point $\mathbf{r}$ with velocity in the interval $(v, v + dv)$, moving in the solid angle $d\boldsymbol{\Omega}$ about the direction of vector $\boldsymbol{\Omega}$; $d\mathbf{v} = v^2 dv \, d\boldsymbol{\Omega}$; $d\boldsymbol{\Omega} = \sin\theta \, d\theta d\varphi$.

Aleksandr Nezvanov, Université Grenoble Alpes, 2018

36 | **Peculiarities of interaction and propagation of low-energy neutrons in nano-dispersed media (the example of diamond nano-powder)**

Denote **e** the unit vector in the direction of the Z-axis. Then the total neutron current from vacuum towards the left surface of the plate (at $z = 0$) in the direction of Z-axis (Figure 2.2.1) will be:

$$I_0^{(+)} = \int_{\Omega \cdot \mathbf{e} > 0} \mathbf{e} \cdot d\mathbf{j}_{\Omega} =$$

$$= \int_{\Omega \cdot \mathbf{e} > 0} \frac{n_0}{4\pi v^2} \cdot \delta(v - v_0) \cdot (\mathbf{v} \cdot \mathbf{e}) \, d\mathbf{v} =$$

$$= \int_0^{\pi/2} d\theta \int_0^{2\pi} d\varphi \cdot \frac{n_0}{4\pi} \cdot \sin\theta \cdot v_0 \cdot \cos\theta = \frac{n_0 v_0}{4}.$$

(2.2.21)

The total, or "global", neutron flux from the volume dV near the point **r** for the monoenergetic neutron gas, taking into account (2.2.17) and (2.2.18), will be [85]:

$$\Phi_0(\mathbf{r}) = \int \Phi(\mathbf{r}, \Omega, v) dv =$$

$$= \int_0^{2\pi} d\varphi \int_0^{\pi} d\theta \int_0^{\infty} dv \cdot v^2 \cdot \sin\theta \cdot v \cdot \frac{n_0}{4\pi v^2} \cdot \delta(v - v_0) =$$

$$= n_0 v_0 = \Phi_0 = \text{const},$$

(2.2.22)

and then

$$I_0^{(+)} = \frac{\Phi_0}{4}.$$

(2.2.23)

In the case of a coherent reflection from the material boundary, the velocity component v_z of the neutron reverses its sign. Therefore, the projection of the total neutron coherent reflected current from material boundary on Z-axis (at $z = 0$), taking into account (2.2.12), (2.2.13), (2.2.15), (2.2.16), (2.2.18), (2.2.20), will be:

$$I_{coh}^{(-)} = \int_{\Omega \cdot \mathbf{e} > 0} (-\mathbf{e} \cdot d\mathbf{j}_{\Omega}) \cdot R_{coh}(\mathbf{k}) =$$

$$= \int_0^{2\pi} d\varphi \int_0^{\pi/2} d\theta \int_0^{\infty} dv \cdot v^2 \cdot \sin\theta \cdot \frac{n_0}{4\pi v^2} \cdot \delta(v - v_0) \cdot (-v \cdot \cos\theta) \cdot R_{coh}(\mathbf{k}) =$$

(2.2.24)

Aleksandr Nezvanov, Université Grenoble Alpes, 2018
Peculiarities of interaction and propagation of low-energy neutrons in nano-dispersed media
(the example of diamond nano-powder) | 37

$$= -\frac{n_0 v_0}{2} \int_0^{\frac{\pi}{2}} R_{coh}(\mathbf{k}_0)\cdot \cos\theta \cdot \sin\theta \cdot d\theta \ =$$

$$= -\frac{n_0 v_0}{2} \int_0^{\frac{\pi}{2}} [1 - D_{coh}(\mathbf{k}_0)] \cdot \cos\theta \cdot \sin\theta \cdot d\theta \ =$$

$$= -\frac{n_0 v_0}{4} + \frac{n_0 v_0}{4} \cdot D_n(E).$$

Here, $D_n(E)$ denotes the total transmission coefficient of the incident gas current of monoenergetic neutrons with energy E from vacuum on the material through the boundary at $z = 0$ (Figure 2.2.1):

$$D_n(E) = 2 \int_0^{\theta_U} D_{coh}(\mathbf{k}_0) \cdot \cos\theta \cdot \sin\theta \cdot d\theta. \tag{2.2.25}$$

From (2.2.21), (2.2.24), (2.2.25) we obtain:

$$I_{coh}^{(-)} = -I_0^{(+)} \cdot [1 - D_n(E)]. \tag{2.2.26}$$

By definition, the albedo of coherent reflected neutron gas that enters into formula (2.2.14), will be equal to:

$$R_{coh}(E) = \frac{\left| I_{coh}^{(-)} \right|}{I_0^{(+)}} = 1 - D_n(E). \tag{2.2.27}$$

A current of neutron gas passing from vacuum the boundary $z = 0$ (Figure 2.2.3) is:

$$I^{(+)} = I_0^{(+)} + I_{coh}^{(-)} = I_0^{(+)} - I_0^{(+)} \cdot [1 - D_n(E)] = I_0^{(+)} \cdot D_n(E) \tag{2.2.28}$$

inside the plate material.

Let's calculate $D_n(E)$, taking into account relations (2.2.11), (2.2.13), (2.2.25) and condition $E \geq U$. Introducing notations

$$x = \cos\theta, \tag{2.2.29}$$

$$B \equiv \cos\theta_U = \sqrt{U/E} \ , \tag{2.2.30}$$

we get from (2.2.25):

$$D_n(E) = 8 \int_B^1 \frac{x^2\sqrt{x^2 - B^2}}{\left(x + \sqrt{x^2 - B^2}\right)^2} dx.$$

Aleksandr Nezvanov, Université Grenoble Alpes, 2018

38 | **Peculiarities of interaction and propagation of low-energy neutrons in nano-dispersed media (the example of diamond nano-powder)**

Finally, we obtain:

$$D_n(E) = \frac{4}{3} \cdot \left[\frac{2(1-U/E)^{3/2} - 2 + 3 \cdot U/E}{(U/E)^2} - \frac{U}{E} \right]. \qquad (2.2.31)$$

In limiting cases, we have from (2.2.31):

a) if $E \gg U$, i.e. $(U/E) \rightarrow 0$:

$$D_n(E) \cong 1 - \frac{7}{6} \cdot \frac{U}{E} \rightarrow 1, \qquad (2.2.32)$$

b) if $(U/E) \rightarrow 1$:

$$D_n(E) \cong \frac{8}{3} \cdot (1 - U/E)^{3/2} \rightarrow 0. \qquad (2.2.33)$$

Coherent reflection coefficient of a neutron gas (coherent albedo), following formula (2.2.14), will be equal:

$$R_{coh}(E) = 1 - D_n(E). \qquad (2.2.34)$$

Now let`s discuss the procedure for calculating elastic incoherent albedo $R_{inc}(E)$, the coefficient of total neutron elastic incoherent reflection from the boundary of our material, using formula (2.2.14).

For a wide range of problems in the theory of neutron transport, the so-called diffusion approximation for the neutron transport equation (the Boltzmann equation) is sufficient.

We consider the case of monoenergetic neutrons, or all neutrons having the same energy (in a homogeneous medium). In this case, the neutron distribution function $\Phi(\mathbf{r}, \mathbf{\Omega}, v)$ in formula (2.2.17) can be expanded in a series of spherical harmonics, and it is possible to limit ourselves with two first terms of the expansion [85], [87], [88]:

$$\Phi(\mathbf{r}, \mathbf{\Omega}, v) \cong \frac{\Phi(\mathbf{r}, v)}{4\pi} + \frac{3}{4\pi} \cdot \mathbf{i}(\mathbf{r}, v) \cdot \mathbf{\Omega}. \qquad (2.2.35)$$

Here is left the icon for neutron velocity v, to distinguish cases:

a) neutron velocity in vacuum $v = v_0$ and is given by the relation $E = mv_0^2/2$ of formula (2.2.19);

b) neutron velocity in the material $v = v_m$ and is given by relation:

$$mv_m^2/2 = E - U. \qquad (2.2.36)$$

Aleksandr Nezvanov, Université Grenoble Alpes, 2018
Peculiarities of interaction and propagation of low-energy neutrons in nano-dispersed media
(the example of diamond nano-powder) | 39

Inside the material through the boundary ($z = 0$) from vacuum passes the neutron gas (Figure 2.2.3), which projection on Z-axis is defined by formula (2.2.28):

$$I^{(+)} = \frac{n_0 v_0}{4} \cdot D_n(E) \qquad (2.2.37)$$

The neutrons transmitted inside the material are incoherently elastically scattered on the fluctuations of the potential $\delta U(\mathbf{r})$ and on individual atoms (nuclei), partially absorbed by the material, heated by inelastic interactions and get a different energy, and a backward current of monoenergetic incoherently scattered neutrons $\mathbf{i}_n^{(-)}$ leaks from the material to vacuum..

By definition, the coefficient of non-coherent elastic reflection of neutrons (albedo) $R_{inc}(E)$ will be equal (for the plane $z = 0$):

$$R_{inc} = \frac{\left|i_n^{(-)}\right|}{I_0^{(+)}} = \frac{\left|i_n^{(-)}\right|}{I^{(+)}/D_n(E)} = D_n(E) \cdot \beta_{inc}(E) \qquad (2.2.38)$$

Here $i_n^{(-)}$ is a projection of backward current $\mathbf{i}_n^{(-)}$ on z-axis;

$$\beta_{inc}(E) = \left|i_n^{(-)}\right|/I^{(+)}, \qquad (2.2.39)$$

– is the coefficient of incoherently reflected neutrons from the material of the plate (at $z = 0$), referred to the neutron current that has transmitted inside the material (2.2.28), (2.2.37).

The processes of incoherent neutron propagation in the material can be described by neutron transport equation (the Boltzmann equation).

For the material in the diffuse approximation from the neutron distribution function $\Phi_m(\mathbf{r}, \mathbf{\Omega}, v_m)$ (2.2.35) we have [85], [87], [88]:

$$\Phi_m(\mathbf{r}, v_m) = \int d\mathbf{\Omega} \cdot \Phi_m(\mathbf{r}, \mathbf{\Omega}, v_m), \qquad (2.2.40)$$

– total neutron flux in the material at point $\mathbf{r}$;

$$\mathbf{i}_m(\mathbf{r}, v_m) = \int d\mathbf{\Omega} \cdot \mathbf{\Omega} \cdot \Phi_m(\mathbf{r}, \mathbf{\Omega}, v_m), \qquad (2.2.41)$$

– neutron current in the material at point $\mathbf{r}$;

the following relation is fulfilled

$$\mathbf{i}_m(\mathbf{r}, v) = -D \cdot \nabla \Phi_m(\mathbf{r}, v_m), \qquad (2.2.42)$$

Aleksandr Nezvanov, Université Grenoble Alpes, 2018

40   **Peculiarities of interaction and propagation of low-energy neutrons in nano-dispersed media (the example of diamond nano-powder)**

where the neutron diffusion coefficient in the material:

$$D = 1/(3\Sigma_{tr}), \tag{2.2.43}$$

Σ_{tr} – transport macroscopic cross-section on neutrons in the material;

$$l_{tr} = 1/\Sigma_{tr}, \tag{2.2.44}$$

– transport path length of neutron in the material.

Index m denotes the values related to the material.

Submitting the neutron albedo in form (2.2.14), we take into account the wave properties of the neutron as a quantum particle (via a coefficient R_{coh}).

It follows from the general principles of quantum mechanics [9], that when neutrons leave the material in a vacuum, a part of the neutron flux is coherently reflected "from the vacuum" and returns back to the material.

Consider the left boundary of the material at $z = 0$ (Figure 2.2.3). From the left from vacuum the current of neutron gas $I^{(+)}$ flows into material in direction of Z axis. From the material, the neutron diffusion current $\mathbf{i}_{dif}^{(-)}$ approaches the boundary, and a part of this current $\mathbf{i}_n^{(-)}$ leaves the material and flows into vacuum, and the part of the current $\mathbf{i}_{dif}^{(-)}$ is spectacularly (coherently) reflected from the vacuum, and returns back in the material. Denote this coherently reflected part of the current by $\mathbf{i}_{coh}^{(+)}$. The current $\mathbf{i}_{coh}^{(+)}$ is directed along the Z-axis. The following relation is fulfilled (at $z = 0$):

$$\mathbf{i}_n^{(-)} = \mathbf{i}_{dif}^{(-)} + \mathbf{i}_{coh}^{(+)} . \tag{2.2.45}$$

Then the total neutron current entering the material from the vacuum on the boundary $z = 0$, will be equal:

$$\mathbf{I}_{tot}^{(+)} = \mathbf{I}^{(+)} + \mathbf{i}_{coh}^{(+)} . \tag{2.2.46}$$

The total diffusion current of neutrons in the material is determined by (2.2.42).

The continuity condition of the neutron current at the material boundary at $z = 0$ has form:

$$-D \cdot \frac{d\Phi_m(z, v_m)}{dz}\bigg|_{z=0} = I^{(+)} + i_{coh}^{(+)}(z, v_m)\bigg|_{z=0} \tag{2.2.47}$$

Aleksandr Nezvanov, Université Grenoble Alpes, 2018
Peculiarities of interaction and propagation of low-energy neutrons in nano-dispersed media | 41
(the example of diamond nano-powder)

When $E \gg U$ the coherently reflected neutron current $\mathbf{i}_{coh}^{(+)} \to 0$ and the condition (2.2.47) becomes a usual boundary condition at $z = 0$ [89]:

$$-D \cdot \frac{d\Phi(z)}{dz}\bigg|_{z=0} = I_0^{(+)} = \frac{n_0 v_0}{4} \tag{2.2.48}$$

On the right boundary of the material (plane $z = H$) we have the following. From the material, the neutron diffusion current $\mathbf{i}_{dif}^{(+)}$ approaches the boundary. Part of this current $\mathbf{i}_n^{(+)}$ current leaves the material and flows into vacuum, and the part of the current $\mathbf{i}_{dif}^{(+)}$ is spectacularly (coherently) reflected from the vacuum, and returns back in the material. Denote this coherently reflected part of the current by $\mathbf{i}_{coh}^{(-)}$. The current $\mathbf{i}_{coh}^{(-)}$ is directed against Z-axis (from vacuum into material).

The following relation is fulfilled (at $z = H$):

$$\mathbf{i}_n^{(+)} = \mathbf{i}_{dif}^{(+)} + \mathbf{i}_{coh}^{(-)} . \tag{2.2.49}$$

In the diffusion approximation, the current $\mathbf{i}_m^{(-)}(z)$, нdirected from the boundary $z = H$ inside the material, in projection on Z-axis has the form [85]:

$$i_m^{(-)}(z, v_m) = -\frac{\Phi_m(z, v_m)}{4} + \frac{1}{2} \cdot i_m(z, v_m) \tag{2.2.50}$$

Taking into account the continuity condition for the neutron current at the boundary of the material at $z = H$, we have:

$$i_m^{(-)}(z, v_m)\bigg|_{z=H} = i_{coh}^{(-)}(z, v_m)\bigg|_{z=H} . \tag{2.2.51}$$

Taking into account the relation (2.2.42), we obtain a boundary condition for $z = H$:

$$-\frac{\Phi_m(z, v_m)}{4}\bigg|_{z=H} - \frac{1}{2} \cdot D \cdot \frac{d\Phi_m(z, v_m)}{dz}\bigg|_{z=H} = i_{coh}^{(-)}(z, v_m)\bigg|_{z=H} \tag{2.2.52}$$

When $E \gg U$ coherently reflected neutron current $i_{coh}^{(-)} \to 0$, and a boundary condition (2.2.52) turns into famous Marshak condition – the requirement of no current (of current absence) from the vacuum [85], [87], [88]:

$$i^{(-)}(z)\Big|_{z=H} = -\frac{\Phi(z)}{4}\Big|_{z=H} - \frac{1}{2}\cdot D \cdot \frac{d\Phi(z)}{dz}\Big|_{z=H} = 0 \qquad (2.2.53)$$

The boundary conditions (2.2.47), (2.2.52) make it possible to calculate coefficient $\beta_{inc}(E)$ (2.2.39) correctly in diffusion approximation.

It is necessary to calculate the coherent reflected neutron currents in explicit form $i_{coh}^{(+)}(z, v_m)\Big|_{z=0}$ and $i_{coh}^{(-)}(z, v_m)\Big|_{z=H}$.

Preliminary calculate the coefficients of coherent reflection and transmission of neutrons from the material to the vacuum. The values of the neutron wave vectors are given by the following relations: in vacuum $\mathbf{k}_0$ (2.2.4) and in the material $\mathbf{k}$

$$\hbar^2 k^2/2m = E - U . \qquad (2.2.54)$$

The neutron velocities, respectively: v_0 in vacuum – (2.2.19); v_m in the material – (2.2.36).

It can be shown [9], that for given values $\hbar^2 k_z^2/2m$, $\hbar^2 k_{0z}^2/2m > U$, coherent reflection coefficients are the same for neutrons, moving from material to vacuum or from vacuum into material.

Reflection coefficient:

$$R_m(\mathbf{k}) = (k_{0z} - k_z)^2/(k_{0z} + k_z)^2 ; \qquad (2.2.55)$$

Transmission coefficient $D_m(\mathbf{k})$:

$$D_m(\mathbf{k}) = 4k_{0z}k_z/(k_{0z} + k_z)^2 . \qquad (2.2.56)$$

If we enter a designation (Figure 2.2.4):

$$k_{0z}^2 = k_0^2 \cdot \cos^2 \theta_{\mathbf{k}_0} , \qquad (2.2.57)$$

Then from (2.2.55), (2.2.56) we come to the formulas (2.2.13), (2.2.15), (2.2.16) for the coefficients R and D. In this form, the formulas are convenient to use in case of neutron transmission from vacuum to the material.

Here are denoted: $\theta_{\mathbf{k}_0}$ – the angle between the directions of the vector $\mathbf{k}_0$ and z-axis in vacuum; $\theta_{\mathbf{k}}$ – the angle between the directions of the vector $\mathbf{k}$ and z-axis in the material (Figure 2.2.4). The plate of the material is located at values of z: $0 \leq z \leq H$.

Aleksandr Nezvanov, Université Grenoble Alpes, 2018
Peculiarities of interaction and propagation of low-energy neutrons in nano-dispersed media
(the example of diamond nano-powder)
43

When studying the propagation of neutrons from material to vacuum, it is more convenient to use other variables that are more consistent with the considering physical phenomena.

We denote the kinetic energy ε of neutron in the material:

$$\varepsilon = E - U = \hbar^2 k^2 / 2m . \tag{2.2.58}$$

Then

$$\hbar^2 k_z^2 / 2m = \varepsilon \cdot \cos^2 \theta_{\mathbf{k}} , \tag{2.2.59}$$

and

$$\hbar^2 k_{0z}^2 / 2m = \varepsilon \cdot \cos^2 \theta_{\mathbf{k}} + U. \tag{2.2.60}$$

The average potential energy (2.2.2) of a neutron $U(z)$ does not depend on coordinates along the axes, parallel to the planes of material boundaries $z = 0$ and $z = H$. Therefore, the projection of neutron pulse on these planes is preserved [91], and relations (2.2.59), (2.2.60) are valid.

Introduce the notation: $R_m(\mathbf{k})$ – coefficient of neutron coherent reflection («from vacuum») upon the transition of a neutron with a wave vector $\mathbf{k}$ from material to vacuum; $D_m(\mathbf{k})$ – coefficient of coherent transition of a neutron with a wave vector $\mathbf{k}$ from material to vacuum. The relation similar to (2.2.12) takes place:

$$R_m(\mathbf{k}) + D_m(\mathbf{k}) = 1 . \tag{2.2.61}$$

For the boundary plane $z = H$ we have $0 \leq \theta_{\mathbf{k}} \leq \pi/2$, $\cos \theta_{\mathbf{k}} \geq 0$. Then, taking into account (2.2.58) – (2.2.60), from (2.2.55), (2.2.56) we obtain:

$$R_m(\mathbf{k})|_{z=H} = \frac{\left(\sqrt{\cos^2 \theta_{\mathbf{k}} + (U/\varepsilon)} - \cos \theta_{\mathbf{k}}\right)^2}{\left(\sqrt{\cos^2 \theta_{\mathbf{k}} + (U/\varepsilon)} + \cos \theta_{\mathbf{k}}\right)^2} \tag{2.2.62}$$

$$D_m(\mathbf{k})|_{z=H} = \frac{4 \cdot \cos \theta_{\mathbf{k}} \cdot \sqrt{\cos^2 \theta_{\mathbf{k}} + (U/\varepsilon)}}{\left(\sqrt{\cos^2 \theta_{\mathbf{k}} + (U/\varepsilon)} + \cos \theta_{\mathbf{k}}\right)^2} \tag{2.2.63}$$

For the boundary plane $z = 0$ we have $\pi/2 \leq \theta_{\mathbf{k}} \leq \pi$, $\cos \theta_{\mathbf{k}} \leq 0$ and $\sqrt{\cos^2 \theta_{\mathbf{k}}} = -\cos \theta_{\mathbf{k}}$. From (2.2.55), (2.2.56) obtain:

Aleksandr Nezvanov, Université Grenoble Alpes, 2018

44 | **Peculiarities of interaction and propagation of low-energy neutrons in nano-dispersed media (the example of diamond nano-powder)**

$$R_m(\mathbf{k})|_{z=0} = \frac{\left(\sqrt{\cos^2\theta_\mathbf{k} + (U/\varepsilon)} + \cos\theta_\mathbf{k}\right)^2}{\left(\sqrt{\cos^2\theta_\mathbf{k} + (U/\varepsilon)} - \cos\theta_\mathbf{k}\right)^2} \tag{2.2.64}$$

$$D_m(\mathbf{k})|_{z=0} = \frac{-4\cdot\cos\theta_\mathbf{k}\cdot\sqrt{\cos^2\theta_\mathbf{k} + (U/\varepsilon)}}{\left(\sqrt{\cos^2\theta_\mathbf{k} + (U/\varepsilon)} - \cos\theta_\mathbf{k}\right)^2} \tag{2.2.65}$$
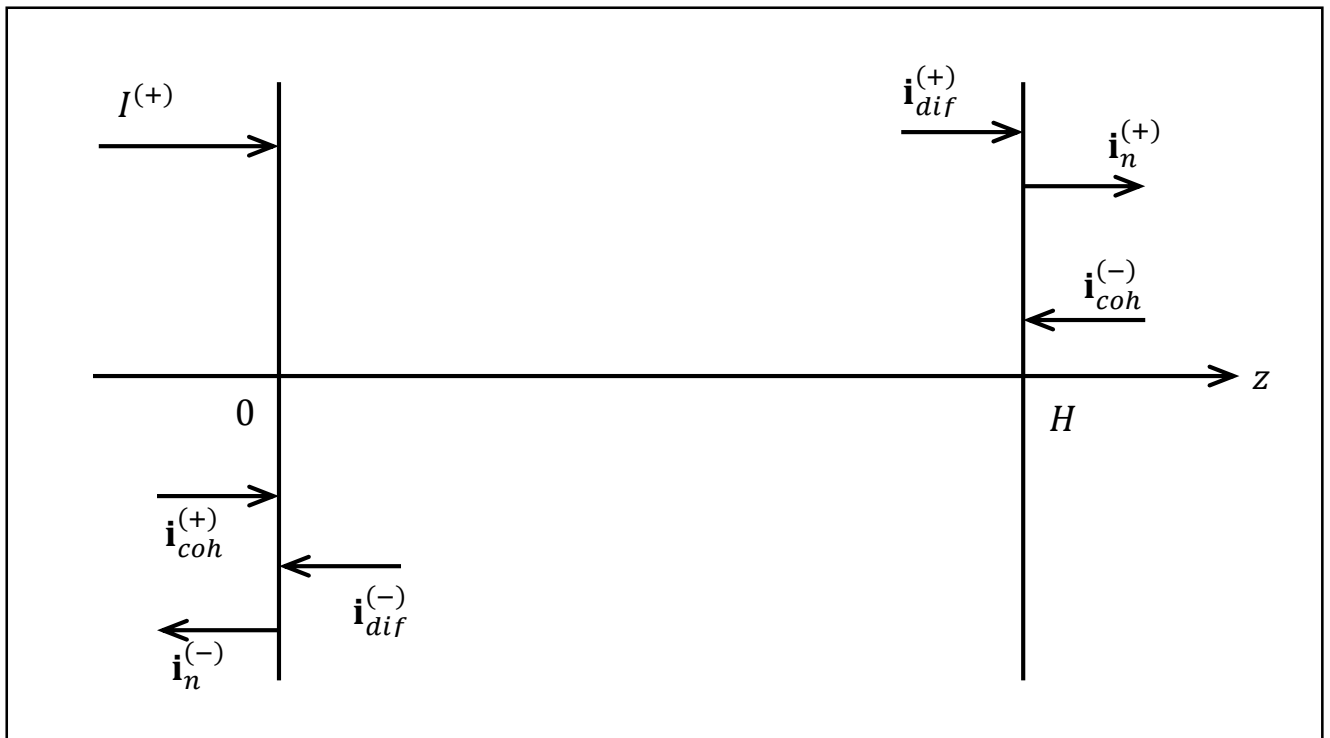
From the symmetry of the problem (Figure 2.2.4) the neutron current (2.2.41) $\mathbf{i}_m(\mathbf{r}, v_m)$ in material will be directed along Z-axis. The angle between vector $\mathbf{i}_m(\mathbf{r}, v_m)$ and the direction of the neutron velocity vector $\mathbf{\Omega}$ in material will be $\theta_\mathbf{k}$. The neutron distribution function in the material, taking into account (2.2.35), (2.2.40), (2.2.41), will be equal:

$$\Phi_m(\mathbf{r}, \mathbf{\Omega}, v_m) = \frac{\Phi_m(\mathbf{r}, v_m)}{4\pi} + \frac{3}{4\pi}\cdot i_m(\mathbf{r}, v_m)\cos\theta_\mathbf{k} \tag{2.2.66}$$
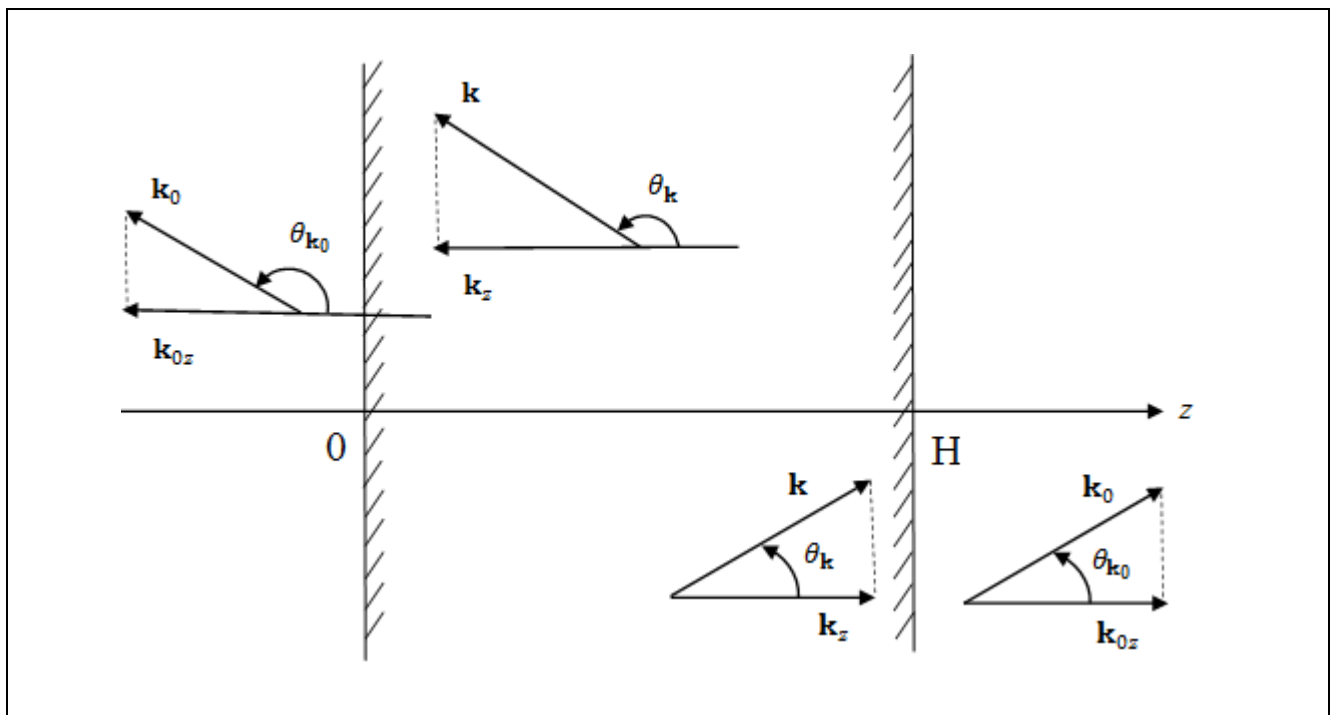
Let`s consider the neutron propagation near the boundary material-vacuum, to the left of the plane $z = H$ (i.e. in plane $z = H - 0$).

The neutron current $d\mathbf{j}_\mathbf{\Omega}$ at point $\mathbf{r}$, moving in the material at a velocity v_m in a solid angle $d\mathbf{\Omega}$ near the direction of vector $\mathbf{\Omega}$, в соответствии с (2.2.41) in accordance with (2.2.41) will be:

$$d\mathbf{j}_\mathbf{\Omega} = \mathbf{\Omega} \cdot \Phi_m(\mathbf{r}, \mathbf{\Omega}, v_m) \cdot d\mathbf{\Omega} . \tag{2.2.67}$$

Aleksandr Nezvanov, Université Grenoble Alpes, 2018
Peculiarities of interaction and propagation of low-energy neutrons in nano-dispersed media | 45
(the example of diamond nano-powder)

Fig. 2.2.3. Neutron currents, passing through the material of the of thickness H.

Fig. 2.2.4. The image of directions of neutron motion in coherent reflection and coherent transmission from material to vacuum and from vacuum into material.

At a distance from an interface «material-vacuum» less than l_s – neutron free path in the material before interaction, the neutron motion inside material is described by the Schrödinger equation with an average potential field U. Therefore the neutrons, which are moving from material to vacuum, will experience elastic coherent (mirror) reflection from the vacuum, determined by the coefficient of coherent reflection $R_m(\mathbf{k})$ (2.2.62). Denote the current of such a mirror reflected neutrons by $\mathbf{i}_{coh}^{(-)}$ (Figure 2.2.3). Denoting by $\mathbf{e}$ the unit vector in the direction of Z-axis, similarly to (2.2.24) we write (in projection on Z-axis):

$$
\begin{aligned}
i_{coh}^{(-)} &= \left. \int\limits_{\mathbf{\Omega e}>0} (-\mathbf{e} \cdot d\mathbf{j_\Omega}) \cdot R_m(\mathbf{k}) \right|_{z=H} \\
&= - \int\limits_{\mathbf{\Omega e}>0} d\mathbf{\Omega} \cdot \cos\theta_{\mathbf{k}} \left[\frac{\Phi_m(\mathbf{r}, v_m)}{4\pi} \right. \\
&\quad \left. + \frac{3}{4\pi} i_m(\mathbf{r}, v_m) \cos\theta_{\mathbf{k}} \right] R_m(\mathbf{k}) \Big|_{z=H} \\
&= -\frac{1}{4\pi} \int\limits_0^{2\pi} d\varphi_{\mathbf{k}} \int\limits_0^{\pi/2} d\theta_{\mathbf{k}} \sin\theta_{\mathbf{k}} \cos\theta_{\mathbf{k}} \\
&\quad \times \frac{\left(\sqrt{\cos^2\theta_{\mathbf{k}} + U/\varepsilon} - \cos\theta_{\mathbf{k}}\right)^2}{\left(\sqrt{\cos^2\theta_{\mathbf{k}} + U/\varepsilon} + \cos\theta_{\mathbf{k}}\right)^2} \\
&\quad \times \left[\Phi_m(\mathbf{r}, v_m) + 3 \cdot i_m(\mathbf{r}, v_m) \cdot \cos\theta_{\mathbf{k}}\right]
\end{aligned}
\tag{2.2.68}
$$

Denoting $x = \cos\theta_k$, after transformations we obtain from (2.2.68):

$$
i_{coh}^{(-)} = - \left[\frac{1}{4}\Phi_m(z, v_m) A_\Phi(E) + \frac{1}{2} i_m(z, v_m) A_i(E) \right]\Big|_{z=H}
\tag{2.2.69}
$$

Here we introduce the notation:

$$
A_\Phi(E) = 2 \int\limits_0^1 dx \frac{\left(\sqrt{x^2 + U/E} - x\right)^2}{\left(\sqrt{x^2 + U/E} + x\right)^2}
\tag{2.2.70}
$$

Aleksandr Nezvanov, Université Grenoble Alpes, 2018
Peculiarities of interaction and propagation of low-energy neutrons in nano-dispersed media | 47
(the example of diamond nano-powder)

$$A_i(E) = 3 \int_0^1 dx \frac{x^2 \left(\sqrt{x^2 + U/E} - x\right)^2}{\left(\sqrt{x^2 + U/E} + x\right)^2} \qquad (2.2.71)$$

and $E = \varepsilon + U$ from (2.2.58).

The sign «←» in (2.2.69) means that neutron current $i_{coh}^{(-)}$ is directed against Z-axis, thus, there exists a neutron current from the vacuum to the material at the boundary of the plate $z = H$.

Let`s calculate the integrals (2.2.70), (2.2.71). Going to variable $\varepsilon = E - U$, we get:

$$A_\Phi(E) \equiv A_\Phi(\varepsilon) = \frac{1}{3} \left(\frac{\varepsilon}{U}\right)^2 \left[8 + 12\frac{U}{\varepsilon} + 3\left(\frac{U}{\varepsilon}\right)^2 - 8\left(1 + \frac{U}{\varepsilon}\right)^{3/2}\right] \qquad (2.2.72)$$

$$A_i(E) \equiv A_i(\varepsilon)$$

$$= \frac{8}{35}(U/\varepsilon)^{3/2} - \frac{1}{35}(\varepsilon/U)^2$$

$$\cdot \left[-120 - 168U/\varepsilon - 35(U/\varepsilon)^2\right. \qquad (2.2.73)$$

$$+ 120(1 + U/\varepsilon)^{3/2} - 12U/\varepsilon(1 + U/\varepsilon)^{3/2}$$

$$\left. + 8(U/\varepsilon)^2(1 + U/\varepsilon)^{3/2}\right]$$

In the limiting cases from (2.2.72), (2.2.73) obtain:

a) for $E \gg U$ we have $\varepsilon \gg U$ and

$$A_\Phi(\varepsilon) \cong \frac{1}{6} \cdot \frac{U}{\varepsilon} \to 0 \qquad (2.2.74)$$

$$A_i(\varepsilon) \cong \frac{8}{35} \cdot \left(\frac{U}{\varepsilon}\right)^{3/2} \to 0 \qquad (2.2.75)$$

b) for $E \to U$ we have $\varepsilon \to 0$ and

$$A_\Phi(\varepsilon) \to 1 \qquad (2.2.76)$$

$$A_i(\varepsilon) \to 1 \qquad (2.2.77)$$

Taking into account (2.2.76), (2.2.77) from (2.2.69) we obtain:

$$i_{coh}^{(-)} = -\left[\frac{1}{4}\Phi_m(z, v_m) + \frac{1}{2}i_m(z, v_m)\right]\bigg|_{z=H} \qquad (2.2.78)$$

for $E \to U$ or $\varepsilon \to 0$.

Aleksandr Nezvanov, Université Grenoble Alpes, 2018

48 | **Peculiarities of interaction and propagation of low-energy neutrons in nano-dispersed media (the example of diamond nano-powder)**

Diffusion current of the neutrons $i_{dif}^{(+)}$, в emerging from material into vacuum. At $z = H - 0$ equals [85]:

$$i_{dif}^{(+)} = \frac{1}{4}\Phi_m(z, v_m) + \frac{1}{2}i_m(z, v_m)$$ (2.2.79)

Comparing expressions (2.2.78) and (2.2.79) we conclude, that for neutron energies $E \to U$ we obtain the total mirror reflection of all neutrons inside the material from the boundary of the material with vacuum, i.e. the extremely slow neutrons will never go beyond the boundaries of the material.

At high energies $E \gg U$ from (2.2.74), (2.2.75), (2.2.69) we obtain $i_{coh}^{(-)} \to 0$, т i.e. the current of neutrons coherently reflected «from vacuum» back inside the material, equals zero. The expressions (2.2.69), (2.2.72), (2.2.73) completely determine neutron current $i_{coh}^{(-)}(z, v_m)$, entering the boundary conditions (2.2.52) at $z = H$.

$$A_\Phi(\varepsilon) \cong 0.124 \cdot \frac{U}{E - U}$$ (2.2.80)

$$A_i(\varepsilon) \cong 0.083 \cdot \frac{U}{E - U}$$ (2.2.81)

Let's consider the neutron propagation near the boundary material-vacuum at $z = 0$ (Figure 2.2.3).

Diffusion current of the neutrons $i_{dif}^{(-)}$, emerging from material into vacuum, will be specularly reflected from vacuum with the reflection coefficient $R_m(\boldsymbol{k})$ (2.2.64) from the interface at $z = 0$. Denote the current of such specularly reflected neutrons by $i_{coh}^{(+)}$. In projection on Z-axis we have:

Aleksandr Nezvanov, Université Grenoble Alpes, 2018
Peculiarities of interaction and propagation of low-energy neutrons in nano-dispersed media
(the example of diamond nano-powder) | 49

$$i_{coh}^{(+)} = \int\limits_{\Omega \cdot e < 0} (-e \cdot d\boldsymbol{j}_{\Omega}) R_m(\boldsymbol{k}) \Bigg|_{z=0}$$

$$= -\frac{1}{4\pi} \int\limits_{0}^{2\pi} d\varphi_k \int\limits_{\pi/2}^{\pi} d\theta_k \sin\theta_k \cos\theta_k \qquad (2.2.82)$$

$$\times \frac{\left(\sqrt{\cos^2\theta_k + U/E} + \cos\theta_k\right)^2}{\left(\sqrt{\cos^2\theta_k + U/E} - \cos\theta_k\right)^2}$$

$$\times \left[\Phi_m(\boldsymbol{r}, v_m) + 3 \cdot i_m(\boldsymbol{r}, v_m)\cos\theta_k\right]$$

After transformations (2.2.82) we have:

$$i_{coh}^{(+)} = \left[\frac{1}{4}\Phi_m(z, v_m)A_\Phi(E) - \frac{1}{2}i_m(z, v_m)A_i(E)\right]\Bigg|_{z=0} \qquad (2.2.83)$$

at the interface $z = 0$, where $A_\Phi(E)$ and $A_i(E)$ are defined by expressions (2.2.72), (2.2.73).

In the diffusion approximation between functions Φ_m and i_m is fulfilled:

$$i_m(z, v_m) = -D\frac{d\Phi_m(z, v_m)}{dz} \qquad (2.2.84)$$

Thus, the relations (2.2.69), (2.2.72), (2.2.73), (2.2.83), (2.2.84) completely determine the boundary conditions (2.2.47), (2.2.52) in the diffusion approximation.

Let`s determine the neutron current $\boldsymbol{i}_n^{(-)}$ emerging from material to vacuum at $z = 0$ (рисунок 2.2.3). The current $\boldsymbol{i}_n^{(-)}$ – is a part of the diffusion neutron current $\boldsymbol{i}_{dif}^{(-)}$, that has passed through the interface $z = 0$. The neutron transmission coefficient through the interfaces $D_m(\boldsymbol{k})|_{z=0}$ determined by the expression (2.2.65).

In projection on Z-axis for the current $\boldsymbol{i}_n^{(-)}$ we have:

Aleksandr Nezvanov, Université Grenoble Alpes, 2018

50 | **Peculiarities of interaction and propagation of low-energy neutrons in nano-dispersed media (the example of diamond nano-powder)**

$$i_n^{(-)} = \int\limits_{\Omega \cdot e < 0} (-e \cdot dj_\Omega) D_m(k) \Bigg|_{z=0}$$

$$= \int\limits_0^{2\pi} d\varphi_k \int\limits_{\pi/2}^{\pi} d\theta_k \sin\theta_k \cos\theta_k$$

$$\times \frac{(-4\cos\theta_k)\sqrt{\cos^2\theta_k + U/E}}{\left(\sqrt{\cos^2\theta_k + U/E} - \cos\theta_k\right)^2}$$

$$\times \left[\Phi_m(r, v_m) + \frac{3}{4\pi} \cdot i_m(r, v_m)\cos\theta_k\right]$$

(2.2.85)

After transformations from (2.2.85) we obtain:

$$i_n^{(-)} = \left[-\frac{1}{4}\Phi_m(z, v_m)T_\Phi(E) + \frac{1}{2}i_m(z, v_m)T_i(E)\right]\Bigg|_{z=0}$$

(2.2.86)

where indicated: $\varepsilon = E - U$, E – neutron energy in vacuum

$$T_\Phi(E) = 2\int\limits_0^1 dx \frac{4x^2\sqrt{x^2 + U/E}}{\left(\sqrt{x^2 + U/E} + x\right)^2}$$

(2.2.87)

$$T_i(E) = 3\int\limits_0^1 dx \frac{4x^3\sqrt{x^2 + U/E}}{\left(\sqrt{x^2 + U/E} + x\right)^2}$$

(2.2.88)

Calculating (2.2.87), (2.2.88), we obtain:

$$T_\Phi(E) = -\frac{4}{3}\left(\frac{\varepsilon}{U}\right)^2\left[2 + 3\frac{U}{\varepsilon} - 2\left(1 + \frac{U}{\varepsilon}\right)^{3/2}\right]$$

(2.2.89)

$$T_i(E) = -\frac{8}{35}\left(\frac{U}{\varepsilon}\right)^{\frac{3}{2}} + \frac{4}{35}\left(\frac{\varepsilon}{U}\right)^2$$
$$\cdot \left[30(1 + U/\varepsilon)^{3/2} - 3U/\varepsilon(1 + U/\varepsilon)^{3/2}\right.$$
$$\left. + 2(U/\varepsilon)^2(1 + U/\varepsilon)^{3/2} - 30 - 42U/\varepsilon\right]$$

(2.2.90)

In the limiting cases from (2.2.89), (2.2.90) obtain:

a) for $E \gg U$ or $\varepsilon \gg U$:

$$T_\Phi(E) = 1 - \frac{1}{6} \cdot \frac{U}{\varepsilon} \to 1$$

(2.2.91)

Aleksandr Nezvanov, Université Grenoble Alpes, 2018
Peculiarities of interaction and propagation of low-energy neutrons in nano-dispersed media | 51
(the example of diamond nano-powder)

$$T_i(E) = 1 - \frac{8}{35} \cdot \left(\frac{U}{\varepsilon}\right)^{3/2} \to 1 \qquad (2.2.92)$$

b) for $E \to U$ or $\varepsilon \to 0$:

$$T_\Phi(E) \to 0, T_i(E) \to 0, i_n^{(-)} \to 0 \qquad (2.2.93)$$

By direct calculating one can verify:

$$A_\Phi(E) + T_\Phi(E) \equiv 1 \qquad (2.2.94)$$

$$A_i(E) + T_i(E) \equiv 1 \qquad (2.2.95)$$

The current $i_n^{(-)}$ – is a current of neutrons that enter in vacuum from the surface of the material at the interface $z = 0$, i.e. it is a current of neutrons incoherently (diffusively) reflected from the material of the plate. The current $i_n^{(-)}$ (2.2.86) is included to the formulas (2.2.38), (2.2.39) for the calculation of neutron albedo. In the diffusion approximation the relation (2.2.84) is used.

Thus, all the formulas for calculating of neutron albedo in the diffusion approximation taking account of coherent reflection processes are written in explicit form.

In conclusion, we write down the formulas for calculating at $z = H$ the current $i_n^{(+)}$ of neutrons that passed through the plate (Figure 2.2.3). Taking into account (2.2.63) in projection on Z-axis we have:

$$i_n^{(+)} = \int\limits_{\Omega \cdot e} (e \cdot dj_e) D_m(k) \Bigg|_{z=H}$$

$$= \frac{1}{4\pi} \int\limits_0^{2\pi} d\varphi_k \int\limits_0^{\pi/2} d\theta_k \sin\theta_k \cos\theta_k \qquad (2.2.96)$$

$$\times \frac{4\cos\theta_k \sqrt{\cos^2\theta_k + U/E}}{\left(\sqrt{\cos^2\theta_k + U/E} + \cos\theta_k\right)^2}$$

$$\times [\Phi_m(r, v_m) + 3 \cdot i_m(r, v_m)\cos\theta_k]$$

After transformations from (2.2.96) for the current of neutrons that passed through the plate, we obtain:

Aleksandr Nezvanov, Université Grenoble Alpes, 2018

52   **Peculiarities of interaction and propagation of low-energy neutrons in nano-dispersed media (the example of diamond nano-powder)**

$$i_n^{(+)} = \left[\frac{1}{4} \Phi_m(z, v_m) T_\Phi(E) + \frac{1}{2} i_m(z, v_m) T_i(E) \right]\Bigg|_{z=H} \qquad (2.2.97)$$

where $T_\Phi(E)$, $T_i(E)$ are defined in (2.2.89), (2.2.90).

2.3. Solution of the kinetic equation in the approximation of small scattering angles

The main feature of the propagation of radiation (photons, neutrons) with a wavelength $\lambda \sim 0{,}1$–1 nm in nanodispersed media with a typical size of dispersed particles $a \sim 1$–10 nm in comparison with the conventional (solid) substance is that the radiation undergoes additional intense coherent elastic scattering on dispersed particles. Coherent scattering is substantially the diffraction of radiation on the dispersed nanoparticle. A single-scattering angle ϑ_1 is limited to a certain maximum angle: $\vartheta_1 \leq \vartheta_{max} \sim \lambdabar/a$, where $\lambdabar = \lambda/(2\pi)$. In some cases of practical importance, the basic processes of the interaction of radiation with nanodispersed media are radiation absorption by matter and coherent elastic scattering on dispersed nanoparticles.

We assume for medium a simple structural model: equivalent round nanoparticles with a radius a; the particle density in the medium is N_0 (Figure 1.1). A sample of the nanodispersed material is shaped in the form of a plate of a thickness L.

We consider the following geometry. A broad homogeneous beam of radiation with a wavelength λ falls along the normal to the surface (along the axis z) of a plane nanodispersed layer with a thickness L. Using the condition of smallness of the angle of single scattering of radiation on a single nanoparticle $\vartheta_1 \sim \lambdabar/a \ll 1$, we write the equation of radiation propagation in nanodispersed medium in the differential form (flat geometry, Figure 1.1) [45], [46], [61]:

$$\mu \frac{\partial I(z,\mu)}{\partial z} = -\Sigma_a I(z,\mu) + \frac{\langle \theta_s^2 \rangle}{4} \left[\frac{\partial}{\partial \mu}(1-\mu^2)\frac{\partial I(z,\mu)}{\partial \mu} \right]. \qquad (2.3.1)$$

Aleksandr Nezvanov, Université Grenoble Alpes, 2018
Peculiarities of interaction and propagation of low-energy neutrons in nano-dispersed media   **53**
(the example of diamond nano-powder)

Here $I(z,\mu) = v_0 f(z,\mu)$ is the flux density of radiation (photons, neutrons) with a wavelength λ and the propagation direction $\mathbf{\Omega}$ at the depth z in the nanodispersed medium; $f(z,\mu)$, v_0 are the distribution function and the speed of radiation particles (photons, neutrons) respectively; $\mu = \mathbf{\Omega\Omega_0} = \cos\theta$; $\mathbf{\Omega'}$, $\mathbf{\Omega}$ are unit vectors of the radiation particles before and after scattering, $\mathbf{\Omega_0}$ is unit vector of the particle velocity in the incoming radiation beam; Σ_a is the coefficient of radiation attenuation due to absorption in the medium; $\langle\theta_s^2\rangle = 2\pi\int_0^\pi \vartheta^3 w(\vartheta)\,d\vartheta$ is the mean square of the angle of scattering of radiation with a wavelength λ per unit length; $w(\vartheta)\,d\vartheta = N_0 d\sigma(\vartheta)$ is the probability of scattering of radiation with a wavelength λ to an angle $\vartheta = \arccos(\mathbf{\Omega'\Omega})$ per unit length; ϑ is the angle between the unit vectors of the velocity of radiation particles $\mathbf{\Omega'}$ and $\mathbf{\Omega}$ before and after the scattering of radiation on a nanoparticle; $d\sigma(\vartheta)$ is the differential cross section of elastic coherent scattering of radiation with a wavelength λ on a dispersed nanoparticle.

Because of the symmetry of the problem, the distribution function $f(z,\mu)$ of the radiation particles does not depend on x and y coordinates and the azimuth angle φ (flat geometry), and is determined only by the depth z and the angle θ of deviation from the initial direction $\mathbf{\Omega_0}$ of the radiation beam. Considering the ratio $\dfrac{\partial}{\partial\mu}\left(1-\mu^2\right)\dfrac{\partial I(z,\mu)}{\partial\mu} = \dfrac{1}{\sin\theta}\dfrac{\partial}{\partial\theta}\sin\theta\dfrac{\partial I(z,\theta)}{\partial\theta} = \Delta_\theta I(z,\theta)$, where $\mu = \cos\theta$; Δ_θ is the Laplace operator in spherical coordinates, the transport equation (2.3.1) can be written in the diffusion approximation:

$$\mu\frac{\partial I(z,\theta)}{\partial z} = -\Sigma_a I(z,\theta) + \frac{\langle\theta_s^2\rangle}{4}\Delta_\theta I(z,\theta). \qquad (2.3.2)$$

The diffusion equation (2.3.2) describes the change in the radiation distribution function through the process of diffusion of directions of radiation propagation in the space of scattering angles θ. The boundary conditions on the surfaces of the plate of the nanodispersed medium with a thickness L have the form:

$$I(z=0,\mu) = \{\ (I_0/2\pi)\cdot\delta(1-\mu),\ \text{for}\ 0<\mu<1\ |\ I_1(\mu),\ \text{for}\ -1<\mu<0\ \}, \quad (2.3.3)$$

$$I(z = L, \mu) = \{\ I_2(\mu),\ \text{for}\ 0 < \mu < 1\ |\ 0,\ \text{for}\ -1 < \mu < 0\ \}, \tag{2.3.4}$$

where I_0 is the flux density of the incident radiation. The function $I_1(\mu)$ determines the angular spectrum of the reflected radiation, the function $I_2(\mu)$ determines the angular spectrum of radiation passing through the plate.

For a small plate thickness L, the probability of deviation of radiation to large angles is negligible, and the mean square radiation scattering angle is small: $\langle \theta^2 \rangle_L \ll 1$. For thick plates of absorbing medium, with increasing z coordinate the distribution function $f(z, \theta)$ for large values of angle θ decreases exponentially as a result of additional attenuation. The additional exponential weakening is due to the increase in the optical path length of radiation propagation in the material at high scattering angles θ. This means that the distribution $I(z, \theta)$ is significantly different from zero only for small angles ($\theta \ll 1$). The smallness of the angle of multiple radiation scattering can simplify the problem (2.3.2)–(2.3.4).

The diffusion approximation involves consistent inclusion of small terms, up to $\sim \theta^2$, into the equations. Therefore one assumes $\mu = \cos\theta \cong 1 - \theta^2/2 \cong (1 + \theta^2/2)^{-1}$ in the equation (2.3.2). $\sin\theta \cong \theta$ is replaced in the Laplace operator.

Since the solution $I(z, \theta)$ should decrease rapidly with the increase of θ, we can formally define the range of variation $0 \le \theta < \infty$ and require $I(z, \theta) \to 0$ at $\theta \to \infty$. At normal incidence of radiation the diffusively reflected flux is absent, that is $I_1(\theta) = 0$ in (2.3.3).

As a result of transformations we find that for small-angle scattering, the radiative propagation equation in the diffusion approximation with the boundary conditions (2.3.2)–(2.3.4) takes the form:

$$\frac{\partial I(z, \theta)}{\partial z} = -\left(1 + \frac{\theta^2}{2}\right) \Sigma_a I(z, \theta) + \frac{\langle \theta_s^2 \rangle}{4} \left(1 + \frac{\theta^2}{2}\right) \left[\frac{1}{\theta} \frac{\partial}{\partial \theta} \left(\theta \frac{\partial I(z, \theta)}{\partial \theta}\right)\right], \tag{2.3.5}$$

$$I(z = 0, \theta) = \frac{I_0}{2\pi} \frac{\delta(\theta)}{\theta}, \qquad I(z, \theta) = 0 \ \text{for}\ \theta \to \infty. \tag{2.3.6}$$

Aleksandr Nezvanov, Université Grenoble Alpes, 2018
Peculiarities of interaction and propagation of low-energy neutrons in nano-dispersed media | 55
(the example of diamond nano-powder)

Let us analyze the problem (2.3.5)–(2.3.6). In the initial statement of the problem (2.3.2)–(2.3.4) there were three characteristic length parameters: L – thickness of the plate material; $l_a = 1/\Sigma_a$ – mean free path of the radiation particles till their absorption in the medium; $l_{tr} \cong 2\left(\langle\theta_s^2\rangle\right)^{-1}$ – transport length of the coherent elastic scattering of radiation by nanoparticles. The parameter L was used in the condition $\langle\theta^2\rangle_L \ll 1$; it is not explicitly included in the obtained equations (2.3.5)–(2.3.6).

For the material with low absorption of radiation, the relation $l_a \gg l_{tr}$ is valid, and terms containing the factor Σ_a can be neglected in the equation (2.3.5). For values $z > l_{tr}$, the equation (2.3.5) cannot be used, and the diffusion equation in coordinate space should be solved for describing the propagation of radiation in nanodispersed materials. For values $z \ll l_{tr}$, the equation (2.3.5) reduces to the well-known equation of propagation of radiation in matter without being absorbed [45]: $\partial I(z,\theta)/\partial z = \dfrac{\langle\theta_s^2\rangle}{4}\left[\dfrac{1}{\theta}\dfrac{\partial}{\partial\theta}\left(\theta\dfrac{\partial I(z,\theta)}{\partial\theta}\right)\right]$. For the boundary conditions (2.3.6), we obtain its solution for $z \ll l_{tr}$: $I(z,\theta) = I_0\left(\pi z\langle\theta_s^2\rangle\right)^{-1}$ $\exp\left[-\theta^2/\left(z\langle\theta_s^2\rangle\right)\right]$. The condition of applicability of this solution at small depths will be $z \gg l_s$, where $l_s = (N_0\sigma)^{-1}$ is the mean free path of the radiation in the material before scattering; σ is the total cross section of elastic coherent scattering of radiation with a wavelength λ on a dispersed nanoparticle.

Otherwise, for a material with strong absorption of radiation the following relation is valid:

$$l_a \ll l_{tr}, \quad \text{or} \quad l_a\langle\theta_s^2\rangle/2 \ll 1. \tag{2.3.7}$$

In this case, the equation (2.3.5) reduces to the equation $\partial I(z,\theta)/\partial z = -\Sigma_a I(z,\theta)$, with the solution $I(z) = I_0\exp(-\Sigma_a z)$ for $z \geq 0$. The condition (2.3.7) points to the applicability, for absorbing materials, of the approximation of small-angle scattering of

radiation for all values $z < \infty$. Therefore, it is natural to use below the following dimensionless length variable $\xi = z\Sigma_a$ for solving the problem (2.3.5)–(2.3.6).

The problem (2.3.5)–(2.3.6) will be solved using the variation method analogous to that of Ritz. We introduce the operator $\hat{T}$, which acts on some function $P(z,\theta)$ as follows:

$$\hat{T}[P(z,\theta)] = -\frac{\partial P(z,\theta)}{\partial z} - \left(1 + \frac{\theta^2}{2}\right)\Sigma_a P(z,\theta) + \frac{\langle \theta_s^2 \rangle}{4}\left(1 + \frac{\theta^2}{2}\right)\left[\frac{1}{\theta}\frac{\partial}{\partial\theta}\left(\theta\frac{\partial P(z,\theta)}{\partial\theta}\right)\right].$$

(2.3.8)

Consider the integral

$$S = \int_0^L \rho(z)dz \int_0^\infty \theta\left\{\hat{T}[P(z,\theta)]\right\}^2 d\theta.$$

(2.3.9)

For absorbing materials, it is possible to assume in many cases $L \to \infty$, and consider the problem for the half-space $z \geq 0$. Integral S in the weight function $\rho(z) \geq 0$ is non-negative and vanishes only if the function $P(z,\theta)$ meets the transport equation (2.3.5). Thus, solving the transport equation (2.3.5) is equivalent to the requirement that the value of S have to has the minimum possible value. If the function $P_0(z,\theta)$ is an exact solution of the equation (2.3.5), then $\hat{T}[P_0(z,\theta)] \equiv 0$ and $\hat{T}[F(z,\theta) - P_0(z,\theta)] \equiv \hat{T}[F(z,\theta)]$ for any function $F(z,\theta)$. By approximating the function $P_0(z,\theta)$ with any suitable function $F(z,\theta)$, in which there are parameters with undetermined values, and substituting the function $F(z,\theta)$ in the expression (2.3.9), we obtain an approximate solution of the transport equation meeting the requirement $\delta S = 0$. Equations (2.3.8)-(2.3.9) provide the smallest squared deviation, with a weight $\rho(z)$, of the approximate function $F(z,\theta)$ from the exact solution $P_0(z,\theta)$ of the transport equation.

Taking into account the results of [46], [61], we choose an approximating function to solve the equation (2.3.5) with one dimensionless variable α as follows:

Aleksandr Nezvanov, Université Grenoble Alpes, 2018
Peculiarities of interaction and propagation of low-energy neutrons in nano-dispersed media | 57
(the example of diamond nano-powder)

$$F(z,\theta,\alpha) = \frac{\exp(-\Sigma_a z)}{z\langle\theta_s^2\rangle}\exp(-\Sigma_a z\theta^2\alpha)\exp\left[-\frac{\theta^2}{z\langle\theta_s^2\rangle}\right]. \qquad (2.3.10)$$

Function

$$I(z,\theta,\alpha) = I_0 F(z,\theta,\alpha)/\pi \qquad (2.3.11)$$

meets the boundary conditions (2.3.6) for $\alpha \geq 0$. By finding the numerical value of the parameter α_{min}, at which the minimum of the integral S (2.3.9) is achieved, we obtain an approximate solution of the transport equation (2.3.5) in the form $I(z,\theta,\alpha_{min})$ (2.3.10)-(2.3.11), meeting the requirement $\delta S = 0$.

Let us compute $\hat{T}[F(z,\theta,\alpha)]$. For further references, we write down the explicit calculation result up to the small terms of the order of $\sim \theta^2$ inclusive. Designating the calculation result through function $T(z,\theta,\alpha)$, taking into account (2.3.8), (2.3.10), we get:

$$T(z,\theta,\alpha) = \hat{T}[F(z,\theta,\alpha)] \cong \exp(-\Sigma_a z)\exp(-\Sigma_a z\theta^2\alpha)\exp\left[-\frac{\theta^2}{z\langle\theta_s^2\rangle}\right]t(z,\theta,\alpha), \quad (2.3.12)$$

where

$$t(z,\theta,\alpha) = -\alpha\Sigma_a - \frac{\theta^2\Sigma_a}{2z\langle\theta_s^2\rangle} + \frac{3\theta^2\Sigma_a\alpha}{z\langle\theta_s^2\rangle} - \frac{\theta^2}{2z^2\langle\theta_s^2\rangle} - \frac{\theta^2}{2}\alpha\Sigma_a + \theta^2\alpha^2(\Sigma_a)^2 z. \qquad (2.3.13)$$

For the approximate solution $I(z,\theta,\alpha_{min})$ of the transport equation (2.3.5), we will start to finding the minimum of the integral $S(\alpha)$ with the weight $\rho(z) \geq 0$ for the parameter values $\alpha > 0$. For $L \to \infty$ we get $S(\alpha) = \int_0^\infty \rho(z)dz\int_0^\infty \theta[T(z,\theta,\alpha)]^2 d\theta$.

It is convenient to carry out the calculation $S(\alpha)$ in two steps. We introduce notations: $y = \theta^2$, $Z(z,\alpha) = \int_0^\infty \theta[T(z,\theta,\alpha)]^2 d\theta = \frac{1}{2}\int_0^\infty [T(z,y,\alpha)]^2 dy$, and $S(\alpha) = \int_0^\infty \rho(z)Z(z,\alpha)dz$

.

From (2.3.12)–(2.3.13) we get:

$$[T(z,y,\alpha)]^2 = \exp(-2\Sigma_a z)\exp\left[-2\left(\Sigma_a z\alpha + \frac{1}{z\langle\theta_s^2\rangle}\right)y\right]t_2(z,y,\alpha); \qquad (2.3.14)$$

Aleksandr Nezvanov, Université Grenoble Alpes, 2018

58 | **Peculiarities of interaction and propagation of low-energy neutrons in nano-dispersed media (the example of diamond nano-powder)**

$$t_2(z,y,\alpha)=\alpha^2\Sigma_a^{\;2}+\alpha^2\Sigma_a^{\;2}y+\frac{\alpha^2\Sigma_a^{\;2}}{4}y^2+\frac{y^2}{4\left(\langle\theta_s^2\rangle\right)^2 z^4}-\alpha^3\Sigma_a^{\;3}zy^2+\frac{\Sigma_a}{2\left(\langle\theta_s^2\rangle\right)^2 z^3}y^2-\frac{\alpha^2\Sigma_a^{\;3}}{\langle\theta_s^2\rangle}y^2+$$

$$+\frac{6\alpha^3\Sigma_a^{\;3}}{\langle\theta_s^2\rangle}y^2+\alpha^4\Sigma_a^{\;4}z^2y^2-2\alpha^3\Sigma_a^{\;3}zy+\frac{\Sigma_a^{\;2}}{4\left(\langle\theta_s^2\rangle\right)^2 z^2}y^2+\frac{\alpha\Sigma_a^{\;2}}{2\langle\theta_s^2\rangle z}y^2-\frac{6\alpha^2\Sigma_a^{\;2}}{\langle\theta_s^2\rangle z}y-\frac{3\alpha\Sigma_a^{\;2}}{\left(\langle\theta_s^2\rangle\right)^2 z^2}y^2+$$

$$+\frac{\alpha\Sigma_a}{\langle\theta_s^2\rangle z^2}y-\frac{4\alpha^2\Sigma_a^{\;2}}{\langle\theta_s^2\rangle z}y^2+\frac{9\alpha^2\Sigma_a^{\;2}}{\left(\langle\theta_s^2\rangle\right)^2 z^2}y^2+\frac{\alpha\Sigma_a^{\;2}}{\langle\theta_s^2\rangle z}y+\frac{\alpha\Sigma_a}{2\langle\theta_s^2\rangle z^2}y^2-\frac{3\alpha\Sigma_a}{\left(\langle\theta_s^2\rangle\right)^2 z^3}y^2\,. \tag{2.3.15}$$

Considering expressions (2.3.14)-(2.3.15), the function $Z(z,\alpha)$ is calculated analytically using the known relation $\int_0^\infty y^n \exp(-Gy)dy = n!/G^{n+1} = \Gamma(n+1)/G^{n+1}$. General constant factors in the formula $S(\alpha)$ do not affect the value of the dimensionless parameter $\alpha_{\min}$, at which the minimum of the integral $S(\alpha)$ is achieved.

We introduce the dimensionless function $b(\alpha)=\sqrt{\Sigma_a/\left(\langle\theta_s^2\rangle\alpha\right)}$, use the dimensionless variable $\xi=z\Sigma_a$ and group terms in the derived expression for $Z(z,\alpha)$. We omit common constant terms in the expression $S(\alpha)$, and get dimensionless function $Q(\alpha)$: $S(\alpha)\sim Q(\alpha)$, for which we find the minimum and evaluate $\alpha_{\min}$. As a result of transformations we obtain:

$$Q(\alpha) = (\alpha/2)\,K_1(\alpha)+K_2(\alpha)/4+\left\{(16\alpha)^{-1}-[b(\alpha)]^2/4+(3\alpha/2)[b(\alpha)]^2\right\}K_3(\alpha)+$$

$$+[b(\alpha)]^4(16\alpha)^{-1}K_4(\alpha)-K_5(\alpha)/4+\left[(8\alpha)^{-1}-3/4\right][b(\alpha)]^4 K_6(\alpha)+(\alpha/4)K_7(\alpha)-$$

$$-(\alpha/2)K_8(\alpha)+\left\{[b(\alpha)]^4(16\alpha)^{-1}-(3/4)[b(\alpha)]^4+(9\alpha/4)[b(\alpha)]^4+[b(\alpha)]^2(8\alpha)^{-1}\right\}K_9(\alpha)+$$

$$+\left[(8\alpha)^{-1}-1\right][b(\alpha)]^2 K_{10}(\alpha)+\left[(1/4)-(3\alpha/2)\right][b(\alpha)]^2 K_{11}(\alpha)+[b(\alpha)]^2 K_{12}(\alpha)/4\,.$$

Here we introduced the following notations:

$$K_1(\alpha)=\int_0^\infty d\xi\,\rho(\xi)\xi\exp(-2\xi)\left\{\xi^2+[b(\alpha)]^2\right\}^{-1};\quad K_2(\alpha)=$$

$$\int_0^\infty d\xi\,\rho(\xi)\xi^2\exp(-2\xi)\left\{\xi^2+[b(\alpha)]^2\right\}^{-2};\quad K_3(\alpha)=\int_0^\infty d\xi\,\rho(\xi)\xi^3\exp(-2\xi)\left\{\xi^2+[b(\alpha)]^2\right\}^{-3};$$

Aleksandr Nezvanov, Université Grenoble Alpes, 2018
Peculiarities of interaction and propagation of low-energy neutrons in nano-dispersed media | 59
(the example of diamond nano-powder)

$$K_4(\alpha) = \int_0^\infty d\xi \, \rho(\xi)\xi^{-1}\exp(-2\xi)\left\{\xi^2 + [b(\alpha)]^2\right\}^{-3} ; \quad K_5(\alpha) =$$

$$\int_0^\infty d\xi \, \rho(\xi)\xi^4\exp(-2\xi)\left\{\xi^2 + [b(\alpha)]^2\right\}^{-3} ; \quad K_6(\alpha) = \int_0^\infty d\xi \, \rho(\xi)\exp(-2\xi)\left\{\xi^2 + [b(\alpha)]^2\right\}^{-3} ;$$

$$K_7(\alpha) = \int_0^\infty d\xi \, \rho(\xi)\xi^5\exp(-2\xi)\left\{\xi^2 + [b(\alpha)]^2\right\}^{-3} ; \quad K_8(\alpha) =$$

$$\int_0^\infty d\xi \, \rho(\xi)\xi^3\exp(-2\xi)\left\{\xi^2 + [b(\alpha)]^2\right\}^{-2} ; \quad K_9(\alpha) = \int_0^\infty d\xi \, \rho(\xi)\xi\exp(-2\xi)\left\{\xi^2 + [b(\alpha)]^2\right\}^{-3} ;$$

$$K_{10}(\alpha) = \int_0^\infty d\xi \, \rho(\xi)\xi^2\exp(-2\xi)\left\{\xi^2 + [b(\alpha)]^2\right\}^{-3} ; \quad K_{11}(\alpha) =$$

$$\int_0^\infty d\xi \, \rho(\xi)\xi\exp(-2\xi)\left\{\xi^2 + [b(\alpha)]^2\right\}^{-2} ; \quad K_{12}(\alpha) = \int_0^\infty d\xi \, \rho(\xi)\exp(-2\xi)\left\{\xi^2 + [b(\alpha)]^2\right\}^{-2} .$$

For the weighting function of a type $\rho(\xi) = \xi^\gamma$ for $\gamma > 0$, integrals $K_1(\alpha), \dots, K_{12}(\alpha)$ can be calculated analytically. The minimum $Q(\alpha)$ is defined for the following weight functions: $\rho_1(\xi) = \xi$ and $\rho_2(\xi) = \sqrt{\xi}$, for $\xi \geq 0$.

With the weight functions $\rho_1(\xi)$, $\rho_2(\xi)$, integrals $K_1(\alpha), \dots, K_{12}(\alpha)$ and $Q(\alpha)$ in this paper have been calculated in an explicit analytic form.

For values of the dimensionless parameter $\Sigma_a / \langle \theta_s^2 \rangle$ in the range from 1 to 100, local minima of the function $Q(\alpha)$ were found and values of the parameter α_{min} were directly numerically calculated. Figures 2.3.2, 2.3.3 illustrate calculated values of Q as a function of parameter α. As clear from the Figures, values of Q change only slightly in the vicinity of the minimum of α_{min}. Therefore, in most cases, the value $\alpha_{min} = 1/2$ can be used for approximate estimations. The value of α_{min}, calculated here precisely, confirms validity of estimations and conclusions in [46], [61].

The values of Σ_a and $\langle \theta_s^2 \rangle$ contain information about properties of concrete materials and peculiarities of the interaction of radiation with nanoparticles. Figure 2.3.4

Aleksandr Nezvanov, Université Grenoble Alpes, 2018

60 | **Peculiarities of interaction and propagation of low-energy neutrons in nano-dispersed media (the example of diamond nano-powder)**

presents calculated values α_{min} as a function of parameter $\Sigma_a/\langle\theta_s^2\rangle$ for weight functions $\rho_1(\xi)$ and $\rho_2(\xi)$.
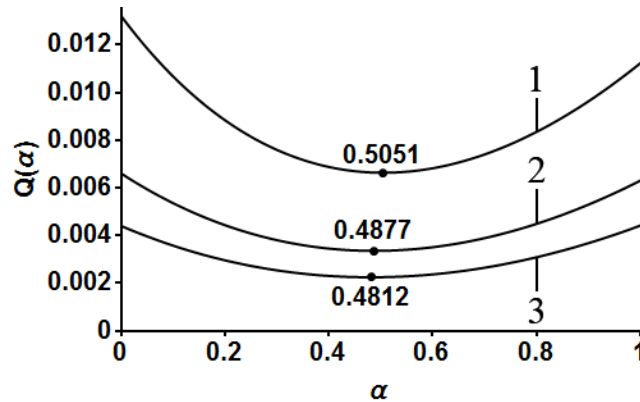
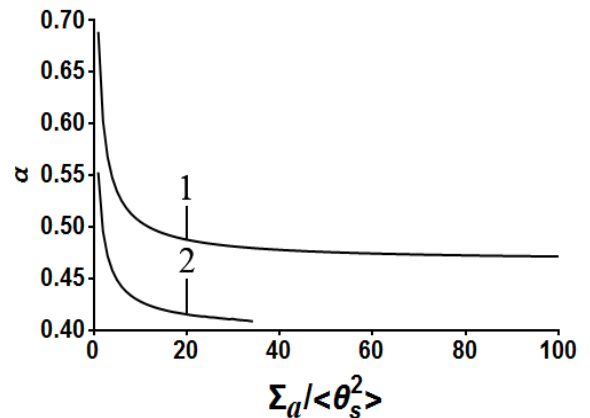**Fig. 2.3.2.** Calculated values Q as a function of parameter α.

1, 2, 3 – values $\Sigma_a/\langle\theta_s^2\rangle$=10, 20, 30 respectively. Points – values α_{min}. $\rho(\xi)=\sqrt{\xi}$.
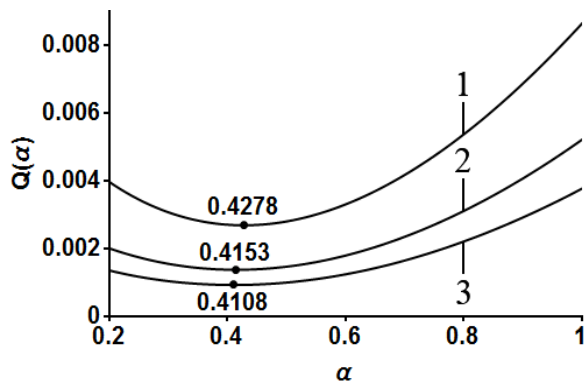
Fig. 2.3.3. Calculated values Q as a function of parameter α.1, 2, 3 – values $\Sigma_a/\langle\theta_s^2\rangle$=10, 20, 30 respectively.

Points – values α_{min}. $\rho(\xi)=\xi$.

Fig. 2.3.4. Calculated values α_{min} as a function of parameter $\Sigma_a/\langle\theta_s^2\rangle$.

$1 - \rho(\xi) = \sqrt{\xi}; \ 2 - \rho(\xi) = \xi.$

Conclusion. An analytical solution of the kinetic equation for the propagation of radiation (photons, neutrons) in nanodispersed absorbing medium is derived using variation method in the approximation of small scattering angles. An approximate solution of the equation (2.3.1) for the radiation propagation has the form:

$$I(z,\theta,\alpha_{min}) = I_0\,\frac{\exp(-\Sigma_a z)}{\pi z\,\langle\theta_s^2\rangle}\,\exp\left(-\Sigma_a z\theta^2\alpha_{min}\right)\exp\left[-\frac{\theta^2}{z\langle\theta_s^2\rangle}\right].$$

Aleksandr Nezvanov, Université Grenoble Alpes, 2018
Peculiarities of interaction and propagation of low-energy neutrons in nano-dispersed media
(the example of diamond nano-powder)

61

This expression can be applied for depths $l_s << z << 2\left(\langle\theta_s^2\rangle\right)^{-1}$ of penetration of radiation into material. For approximate calculations, the value $\alpha_{\min} = \dfrac{1}{2}$ can be used.

2.4. Description of the diamond nanopowder model

Particles of detonation nanodiamond are crystallites with a diameter of 4-5 nm, being formed as a result of blowing explosive substances with a negative oxygen balance in a unoxidized environment [62], [64], [106], [107], [108]. The synthesis conditions determine the shape of the nanoparticles [109]. When the products of denotation are cooled with water vapors, the shape becomes spherical. In the case of dry synthesis, the diamond nanocrystals become ideal in terms of structure. Nanodiamonds are of complex chemical composition. The basic composing elements are carbon C (90.3-93.8 wt. %), oxygen O (2.3-4.5 wt. %), nitrogen N (1.5-2.3 wt. %) and hydrogen H (0.4-4.8 wt. %) [110]. Volatile, difficult-to-remove impurities CO, CO2, N2, H2O [64] consist of the atoms of oxygen, nitrogen and hydrogen.

There may be other impurities in detonation nanodiamonds (up to 4.1 wt. % [111]) – non-combustible metal oxides and carbides, occurring due to corrosion of the walls of the explosive chambers. If there are massive explosive chambers, the amount of non-combustible impurities may reach 26 wt. % [64].

The hydrogen contained in the nanopowder causes heating of cold and very cold neutrons via incoherent scattering. The cross section of neutron capture in hydrogen nuclei is ~ 102 times larger than the cross section of neutron capture in carbon nuclei. The hydrogen reduces the albedo value and deteriorates the conditions for the collection of low-energy neutrons in the vessels made of the diamond nanopowder [7].

Powders of detonation nanodiamonds may adsorb atmospheric moisture [112], [113]. The nanopowder pores contain adsorbed water and its amount may be from 1.3 to 6.6 wt. % [114], [115]. It is possible to partially remove water by heating or vacuum

pumping. Removal of water changes the concentrations of carbon nuclei n_C – hydrogen n_H (n_C / n_H) ration from 7.4 to 12.4 [W14].

Diamond nanopowders contain hydrogen atoms directly related to the nanodiamonds surface stabilizing the carbon nanoparticle in the diamond phase. Hydrogen atoms take up unsaturated bonds of carbon atoms on the surface of crystallites. Thus, there are formed covalent C–H bonds and stabilized electronic sp^3–configurations peculiar for the diamond phase [116].

If speaking about detonation nanodiamonds, the diamond phase with sp^3–configuration of carbon atoms inside the nanoparticle gives place to the graphite-like carbon with sp^2–configuration of bonds on its surface [108], [W16], [117], [118], [119], [120], [121]. A lot of various methods evidence the detection of sp^2–configuration of bonds [122], [123], [124]. The shell thickness is 0.4-1 nm [86], [125], [126], [127].

In order to study the structures of diamond nanoparticles; there has been applied the method of neutrons small-angle scattering [127], [128], [129], [130]. It has been found that there is no strict line between the diamond core and the amorphous shell. The nanodiamond crystal structure deforms gradually, becoming disordered, 'graphite-like' near its surface. Having studied suspensions from detonation nanodiamonds; it has been found that the observed asymptotic behavior of the intensity of neutrons small-angle scattering fails to correspond to the Porod`s law [131]. Thus, the diamond nanoparticle may be characterized as a complex heterogeneous system with a strong diffuse quality, as evidenced by other studies [125], [132].

There are compounds of the elements N, O, H on the surface of the diamond nanoparticle, forming the following functional groups: methine, methyl, methylene, carbonyl, hydroxyl, aldehyde, carboxyl, ether and anhydride, sulfo groups, nitro groups, amine, amide, etc. [133], [W35], [135].

In order to create a theoretical diamond nanopowder model, let us consider the characteristics of the nanopowder "*ultradiamond90*" [15], being used in neutron

Aleksandr Nezvanov, Université Grenoble Alpes, 2018
Peculiarities of interaction and propagation of low-energy neutrons in nano-dispersed media
(the example of diamond nano-powder) | *63*

experiments [14]. The results of these experiments were used for comparison with theoretical calculations.

Nanopowder is produced by Ultradiamond Technologies, USA [16–17]. Nanodiamonds contain 90 wt. % of the carbon diamond phase. Diamond nanoparticles have a spherical shape and a diameter from 0.5 to 10 nm. The average particle diameter is 4–5 nm. The vast majority of particles are from 2 to 8 nm in size. The medium-sized nanodiamonds *"ultradiamond90"* shell thickness is from 0.5 to 0.7 nm [18], [19], [20].

It is important to consider the shell of diamond nanoparticles as it makes additional contribution to the scattering cross section and neutron capture. The nanoparticles shell density has an estimated value of 1.6–1.9 g/cm^3 based on the chemical composition of the nanopowder.

Nanoparticles size distribution is an essential characteristic of diamond nanopowders. Diamonds nanoparticles-size distribution is often approximated by the logarithmic-normal distribution law [131], [136]:

$$f(r) = \frac{1}{r\sigma\sqrt{2\pi}} \exp\left[-\left(\ln r - \mu\right)^2 / 2\sigma^2\right]$$

where μ is the scale parameter (median), $-\infty < \mu < \infty$; σ is the shape parameter (variability), $\sigma > 0$.

The growth of nanodiamonds during detonation synthesis is mainly provided by the coagulation of the explosion products rather than by the diffusion of individual carbon atoms [137]. This process is described by the logarithmic-normal law of particle-size distribution. If the particles grow layer-by-layer thanks to adsorption of new atoms of substance, the particle distribution will be described by the normal law of distribution [138]:

$$f(x) = \frac{1}{\sigma\sqrt{2\pi}} \exp\left[-(x - \mu)^2 / 2\sigma^2\right]$$

where μ is the mathematical expectation, and σ^2 is the variability.

Practically, the consistent pattern in the nanoparticles size distribution is an intermediate form between these two patterns. For extra small particles, the increase in

size is caused by layer-by-layer attaching of new atoms, and only then by coagulation [139]. The exponential power-series distribution is an acceptable approximation for description of the small nanoparticles size distribution.

Let us compare experimentally measured functions of nanopowder *"ultradiamond90"* particles size distribution.
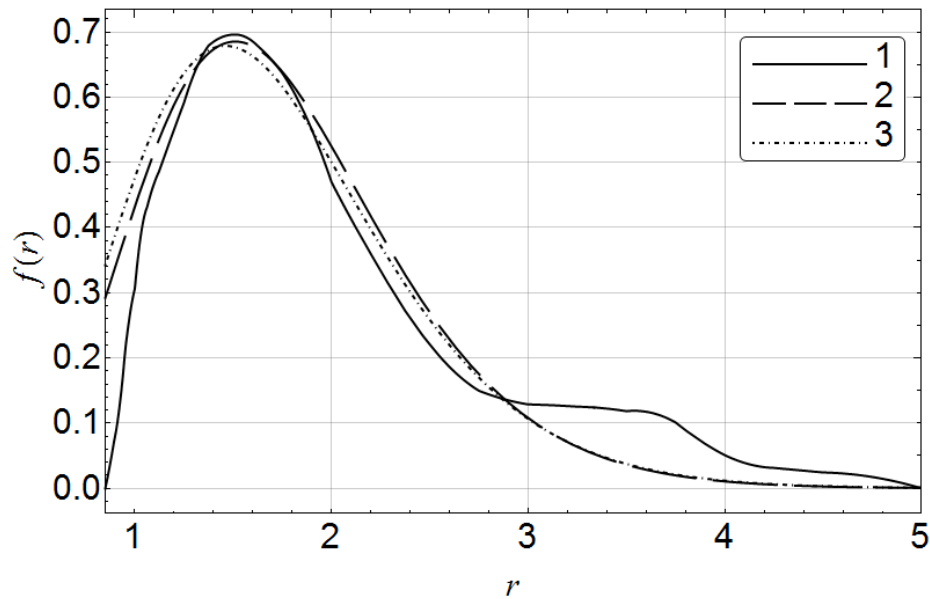
Fig. 2.4.1. Dependence of the distribution density $f(r)$ on the particle radius r, nm.

Figure 2.4.1 demonstrates particles size distributions in the nanopowder *"ultradiamond90"*.

1. Distribution specified on the manufacturer's website of nanopowder. The distribution was obtained by the small-angle X-ray scattering method [15].

2. Exponential-power approximation (2.4.1) of nanoparticles *"ultradiamond90"* size distribution for the most probable radius (mode) of diamond nanoparticle $R_{mode} = 1.51$ nm with distribution parameters $A = 21.33$ nm$^{-6.55}$, $\alpha = 5.55$, $\beta = 3.80$ nm^{-1}, $N_0 = 3.58 \times 10^{24}$ m^{-3}.

3. Exponential-power approximation (2.4.1) of nanoparticles *"ultradiamond90"* size distribution for the average radius of diamond nanoparticle $R_{mean} = 1.8$ nm with the distribution parameters $A = 25.82$ nm$^{-6.55}$, $\alpha = 6.18$, $\beta = 4.09$ nm^{-1}, $N_0 = 3.54 \times 10^{24}$ m^{-3}.

Aleksandr Nezvanov, Université Grenoble Alpes, 2018
Peculiarities of interaction and propagation of low-energy neutrons in nano-dispersed media
(the example of diamond nano-powder) 65

Approximations 2, 3 of the distribution function 1 were obtained for the values of impurity shell density $\rho_{shell} = 1.6$ g/cm^3, shell thickness $h = 0.5$ nm. The average particle radius and the mode of distribution for the nanopowder *"ultradiamond90"* are 1.998 nm and 1.51 nm, accordingly.

Further, we will use information on powder characteristics [15], [16], and the results of approximation $f(r)$ by exponential-power distributions varying the distribution parameters.

We will describe the developed algorithm for determination of the distribution parameters of diamond cores in terms of size.

Let us consider the normalized function $f(r)$ of distribution of nanoparticles in terms of size (radii) of their diamond cores.
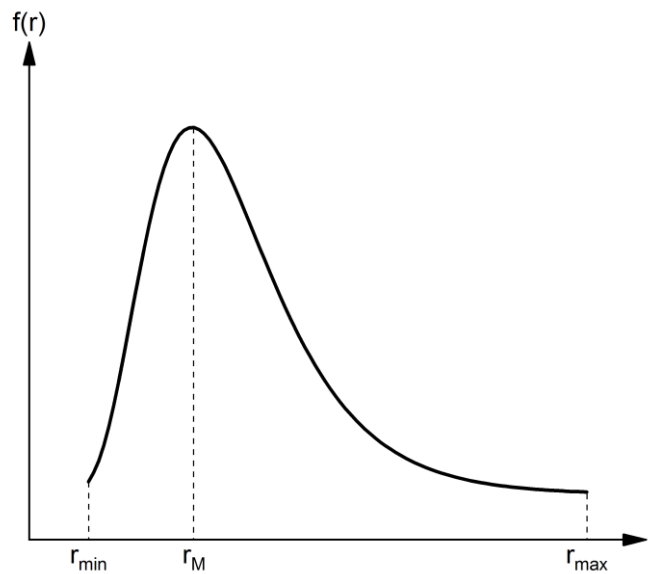
Fig. 2.4.2. Graphic of the distribution function $f(r)$ depending on the radius r of the nanodiamond core.

Let us specify: r is the radius of the nanoparticle diamond core; r_{min}, r_{max} are the lines of the interval of acceptable values r;

$f(r) = f(r; A, \alpha, \beta) = A r^{\alpha} e^{-\beta r}$ is the exponential-power distribution;

Aleksandr Nezvanov, Université Grenoble Alpes, 2018

66 | **Peculiarities of interaction and propagation of low-energy neutrons in nano-dispersed media (the example of diamond nano-powder)**

or $f(r) = f(r; A, \alpha, \beta) = A \dfrac{1}{r\sigma\sqrt{2\pi}} \exp\left[-\left(\ln r - \mu\right)^2 / 2\sigma^2\right]$ is the logarithmically normal distribution.

Let us consider the exponential power law of distribution. We have the same argument for the logarithmically normal distribution.

It is necessary to determine the sets of quantities $\{A, \alpha, \beta\}$ or $\{A, \sigma, \mu\}$. Let us introduce the external parameters of the problem, being determined experimentally:

r_M is the most probable value of the radius of the diamond core of diamond nanoparticle;

$\bar{r}$ is the average value of the radius of the diamond core of diamond nanoparticle.

To determine the distribution parameters:

$$f(r) = f(r; A, \alpha, \beta) = A r^{\alpha} e^{-\beta r}. \tag{2.4.1}$$

the following conditions will be applied.

The first condition is the normalization of the total probability by 1:

$$\int_{r_{min}}^{r_{max}} f(r)\,dr = A \int_{r_{min}}^{r_{max}} r^{\alpha} e^{-\beta r}\,dr = 1. \tag{2.4.2}$$

The second condition can be set in two ways. If one sets the average value of the radius of the diamond core, then the condition will be:

$$\bar{r} = \int_{r_{min}}^{r_{max}} r \cdot f \cdot (r)\,dr = \int_{r_{min}}^{r_{max}} r\, A r^{\alpha} e^{-\beta r}\,dr. \tag{2.4.3}$$

If one sets the value of the most probable radius (mode of distribution), then the second condition will be:

$$\left.\frac{df(r)}{dr}\right|_{r=r_M} = 0. \tag{2.4.4}$$

for $r_{min} \le r_M \le r_{max}$.

Aleksandr Nezvanov, Université Grenoble Alpes, 2018
Peculiarities of interaction and propagation of low-energy neutrons in nano-dispersed media | 67
(the example of diamond nano-powder)

Let us consider the third condition. Let us specify ρ_{core} to be the density of the substance of the diamond core of nanoparticle. Let us consider the following structural model of diamond nanoparticle (Figure 2.4.3).
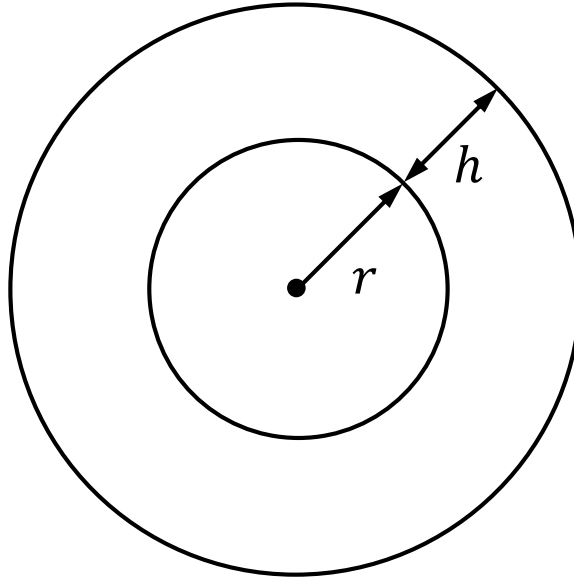
Fig. 2.4.3. The model of the structure of diamond nanoparticle: diamond core without impurities with radius r, an impurity shell with a thickness of h, uniformly surrounding the diamond core; $h = 0.5 \div 0.7$ nm.

Let us introduce the notation:

M is the mass of a unit volume of a diamond nanopowder, in other words the total mass, including diamond nuclei and impurity shells (this value is brought by measurements);

N_0 is the total number of diamond nanoparticles per unit volume of material (in other words in the unit volume of the space occupied by the powder).

M_{core} is the mass of diamond cores of nanoparticles per unit volume of diamond nanopowder;

M_{shell} is the mass of impurity shells of diamond nanoparticles per unit volume of nanopowder.

$$M = M_{core} + M_{shell}. \tag{2.4.5}$$

Sizes:

$$[M] = [M_{core}] = [M_{shell}] = 2 \, / \, cm^3 \, ; \ [N_0] = 1 \, / \, cm^3 \, .$$

The condition for determination of N_0 is received from the known mass of diamond cores for the *"ultradiamond90"* nanopowder (90 wt. %):

$$N_0 \, \rho_{core} \int_{r_{min}}^{r_{max}} \frac{4\pi}{3} r^3 f(r) dr = M_{core} \, . \tag{2.4.6}$$

where $f(r) = A \, r^\alpha e^{-\beta r}$.

This is the third condition for determination of the distribution parameters $f(r)$, as a forth unknown value is added to the unknown values A, α, β.

The fourth condition is written as follows:

$$N_0 \, \rho_{shell} \int_{r_{min}}^{r_{max}} \frac{4\pi}{3} \left[(r+h)^3 - r^3 \right] f(r) dr = M_{shell} \, . \tag{2.4.7}$$

where $f(r) = A \, r^\alpha e^{-\beta r}$.

The condition (2.4.7) is determined by following the balance of impurities mass in the diamond nanopowder.

Here ρ_{shell} means the density of substance of the impurity shell surrounding the diamond core of the nanoparticle.

No direct measures of ρ_{shell} were made. The value ρ_{shell} may be determined from based on the known chemical composition of the impurity shell material of diamond nanoparticles, or estimated using small-angle scattering and diffraction of neutrons or X-rays:

$$\rho_{shell} \cong 1.6 \div 1.9 \, \text{g/cm}^3. \tag{2.4.8}$$

Thus, having determined the unknown quantities A, α, β, N_0 from the system of equations (2.4.2)–(2.4.7), we will be able to determine the parameters of the nanoparticle size distribution (2.4.1). In the same way, the values of A, α, β, N_0 are determined for the logarithmically normal distribution.

Aleksandr Nezvanov, Université Grenoble Alpes, 2018
Peculiarities of interaction and propagation of low-energy neutrons in nano-dispersed media
(the example of diamond nano-powder)   69

Let us make the following explanations:

1. The density of impurity shell material ρ_{shell} may be approximately measured if the density of each substance in the nanoparticle impurity shell content and its percentage are known. For example: impurities – carbine, a fraction 0.3 (30%), density ρ_{carb}; graphite, a fraction 0.27 (27%), density ρ_{grap}; oxygen, a fraction 0.27 (27%), density ρ_O and hydrogen, a fraction 0.03 (3%), density ρ_H in the condensed or bound state;

$$\rho_{shell} = 0.3\rho_{carb} + 0.4\rho_{grap} + 0.27\rho_O + 0.03\rho_H.$$

2. The value of impurity shell thickness was measured experimentally [18], [19], [20]: $h = 0.5 \div 0.7$ nm.

The total packing coefficient of nanodiamond powder is determined γ based on the ratio:

$$\gamma = N_0 \int_{r_{min}}^{r_{max}} \frac{4\pi}{3} (r+h)^3 f(r) dr. \tag{2.4.9}$$

The total porosity of the nanopowder:

$$p = 1 - \gamma. \tag{2.4.10}$$

Usually nanodispersed systems contain heterogeneous and polydispersed particles, form multilevel (multiscale) aggregate structures. Nanodiamonds of detonation synthesis form difficult-to-break agglomerates with sizes $d_2 \sim 100$-200 nm, called 'agglutinates' [21], [22], [23], [24], [25]. Such aggregates consist of primary diamond nanoparticles $d_1 \sim 4$-5 nm in size.

The diamond nanopowder structure was specified at the end of section 2.1 of the thesis. The packing density inside the agglomerates with size d_2 is $\gamma_1 \sim 0,6$. The packing density inside the agglomerates with a characteristic size d_3 (consist of agglomerates with size d_3) is $\gamma_2 \sim 0.6$. The packing density inside the agglomerates d_4 (consist mainly of agglomerates of size d_4 and d_3) is $\gamma_3 \sim 0.6$. Diamond nanopowder consists mainly of a

Aleksandr Nezvanov, Université Grenoble Alpes, 2018

70   **Peculiarities of interaction and propagation of low-energy neutrons in nano-dispersed media (the example of diamond nano-powder)**

mixture of agglomerates d_3 and d_4. The coefficient of packing of diamond nanopowder with agglomerates d_3 and d_4 is $\gamma_4 \sim 0.6 - 0.7$. The total packing coefficient of diamond nanopowder γ is in the range: $\gamma_1\gamma_2\gamma_3\gamma_4 < \gamma < \gamma_1\gamma_2\gamma_3$, i.e. $0.1 < \gamma < 0.2$. The total porosity of the diamond nanopowder is $p = 1 - \gamma = 0.8 - 0.9$, that corresponds to the observed values [7], [14].

In order to make numerical measures, there was applied the experimentally measured size distribution function for nanopowder particles '*ultradiamond90*' $\tilde{f}(r)$, provided by the manufacturer of diamond nanopowder.

There has been made a table of numerical values of $\tilde{f}(r)$ function, the interpolation procedure was used for intermediate values of the radius r of the diamond core.

In order to determine the characteristics of a diamond nanopowder N_0 and γ, there has been used: the normalization condition $\int_{r_{min}}^{r_{max}} \tilde{f}(r)\,dr = 1$, similar to formula (2.4.2), and equations (2.4.6) and (2.4.9).

Aleksandr Nezvanov, Université Grenoble Alpes, 2018
Peculiarities of interaction and propagation of low-energy neutrons in nano-dispersed media | *71*
(the example of diamond nano-powder)

CHAPTER 3. THE DEVELOPMENT OF AN ALGORITHM OF NUMERICAL MODELING OF NEUTRON TRANSPORT IN THE DIAMOND NANOPOWDER

The method of mathematical modeling, the Monte Carlo method, is widely used for the numerical solution of the Boltzmann type neutron transport equation. The algorithm consists of three main blocks in the software implementation of the method. The first block implements algorithms for calculating the scattering angles and cross-section of the interaction of neutrons with matter. The second block implements the conversion algorithms for the coordinate system. The third block simulates the free path of neutrons in the material.

3.1. The cross-section calculation for elastic coherent neutron scattering by spherical nanoparticles

For neutrons with wavelengths $\lambda > \lambda_d$, where $\lambda_d \sim (a/n)^{1/4}$, n is the atomic (nuclear) density of matter of dispersed nanoparticles, the diffraction on matter density inhomogeneities is the principal mechanism, which defines neutron propagation. Due to the multiple scattering, the propagation of neutrons could be considered as their diffusion in the medium. Additional coherent scattering on dispersed nanoparticles increases the effective path of neutrons in matter and thus it increases the probability of radiation absorption. This process is described via the decrease of the neutron diffusion length $L_c = (3\Sigma_{tr}\Sigma_c)^{-1/2}$, where Σ_{tr} and Σ_c are the macroscopic transport cross section and the cross section of neutron absorption in matter respectively. The probability of neutron absorption is $w_a \propto 1/L_c$. For neutrons with wavelength $\lambda > \lambda_d$ we get $w_a \propto a^{-1/2}\lambda^{5/2}$.

Increase in the intensity of scattering by dispersed nanoparticles increases the number of neutrons escaping from a matter sample that appears as increase in the number of neutrons diffusively reflected from the sample. Increase in the scattering intensity is

Aleksandr Nezvanov, Université Grenoble Alpes, 2018

72 **Peculiarities of interaction and propagation of low-energy neutrons in nano-dispersed media (the example of diamond nano-powder)**

described via decrease of the neutron diffusion coefficient $D = (3\Sigma_{tr})^{-1}$. The probability of neutron scattering to large angles is $w_s \propto \Sigma_{tr}$. For $\lambda > \lambda_d$ we get $w_s \propto \lambda^4/a$. The ratio of probabilities is $w_{s/}w_a \propto \lambda^{3/2}a^{-1/2}$. Thus for small neutron energies and small characteristic sizes of dispersed nanoparticles, the probability of diffusive neutron reflection from nano-dispersed material increases sharper than the probability of neutron absorption in this material. The neutron wavelengths $\sim\lambda_d$ corresponds to energies of cold and very cold neutrons (CN and VCN respectively). The phenomenon of intense coherent elastic scattering of slow neutrons on dispersed nanoparticles allows application of materials containing nanoparticles for constructing novel efficient reflectors of VCNs and CNs. Most efficient currently VCN reflectors are based on diamond nanopowders [1], [2], [5], [7].

The principle mechanism of interaction of slow neutrons with nanopowder consists of their coherent elastic scattering on nanoparticles, which is described via introduction of effective (optical) potential of matter. We start from a simple model for matter: piled up monodispersed diamond powder consisting of round nanoparticles with the radius a, without impurities of other chemical elements. The powder packing factor is denoted as γ; it corresponds to the fraction of material volume occupied by matter; the porosity of material is $p = 1 - \gamma$. The efficient potential of the interaction of neutrons with particle matter is $V(r) = \{U_0,$ for $r \leq a \mid 0,$ for $r > a\}$, where $U_0 = \left(2\pi\hbar^2 / m\right)n \cdot b \sim 10^{-7}$ eV, m is the neutron mass, b is the neutron coherent scattering amplitude at the bound atomic nucleus [72]. For diamond this potential barrier equals $U_0 = 305$ neV.

For calculations of neutron scattering in dispersed media one often uses the perturbation theory in the form of first Born approximation for single scattering [92]. Such approach constrains sizes of dispersed particles $a^2 \ll \hbar^2/mU_0$ [9] or $a < 11.8$ nm for diamond. Solving precisely the problem, one could reliably estimate uncertainties of results derived within the Born approximation. To increase the accuracy of model description of the interaction of low energy neutrons with nanodispersed materials, first we solve precisely the scattering problem without using Born approximation.

Aleksandr Nezvanov, Université Grenoble Alpes, 2018
Peculiarities of interaction and propagation of low-energy neutrons in nano-dispersed media
(the example of diamond nano-powder) | *73*

The solution is based on precise calculation of the differential cross section of coherent elastic scattering of neutron on nanoparticle to certain direction within elementary solid angle $d\Omega$:

$$d\sigma_1(\theta, \varepsilon)/d\Omega = |f(\theta, \varepsilon)|^2, \qquad (3.1.1)$$

where θ, ε are the scattering angle and the neutron energy respectively. The amplitude of coherent elastic scattering $f(\theta, \varepsilon)$ of neutron on nanoparticle is defined as follows:

$$f(\theta,\varepsilon) = [2ik(\varepsilon)]^{-1} \sum_{l=0}^{\infty} (2l+1)\{\exp[2i\delta_l(\varepsilon)] - 1\} P_l(\cos\theta). \qquad (3.1.2)$$

Here $k(\varepsilon)$ is the wave neutron vector, $\delta_l(\varepsilon)$ is the scattering phase, $P_l(\cos\theta)$ are Legendre polynomials. There are a few equivalent methods to calculate $\delta_l(\varepsilon)$. We use the method of phase functions [93], and solve the phase equation for precisely calculating δ_l (ε):

$$\frac{d}{dr}\delta_l'(r,\varepsilon) = -[2mV(r)/\hbar^2 k(\varepsilon)]\{\cos[\delta_l'(r,\varepsilon)]j_l(kr) - \sin[\delta_l'(r,\varepsilon)]n_l(kr)\}^2;$$

the initial condition is $\delta_l'(r = 0, \varepsilon) = 0$. Here $\delta_l'(r, \varepsilon)$, $j_l(kr)$ and $n_l(kr)$ are the phase function and Riccati–Bessel functions respectively. The scattering phase is found according to formula $\delta_l(\varepsilon) = \delta_l'(r = \infty, \varepsilon)$, and thus we define precisely the differential cross section $d\sigma_1(\theta, \varepsilon)/d\Omega$. Application of the method of phase functions provides an advantage for describing scattering in dense media, as it allows directly performing quantitative estimations and comparing criteria that condition correctness of application of different approximations [94].

For the amplitude of coherent elastic scattering of neutron on nanoparticle towards the angle θ we get in Born approximation $f^B(\theta, \varepsilon) = -[m/2\pi\hbar^2]\int V(r)\exp(-i\mathbf{q}\mathbf{r})d\mathbf{r}$, where $q = 2k(\varepsilon)\sin(\theta/2)$ [9].

Detonation nanodispersed diamond is a cluster material with diamond crystal structure characterized by sizes of ~4.3 nm [95]. We will calculate values that characterize neutron propagation in nanodispersed media, and compare results of precise quantum

Aleksandr Nezvanov, Université Grenoble Alpes, 2018

74 | **Peculiarities of interaction and propagation of low-energy neutrons in nano-dispersed media (the example of diamond nano-powder)**

mechanical calculations to results of calculations within Born approximation for different neutron energies ε in the range from 3×10^{-7} to 10^{-3} eV, for diamond nanoparticle radii a in the range from 2 to 5 nm.

The comparison will be performed using four values.

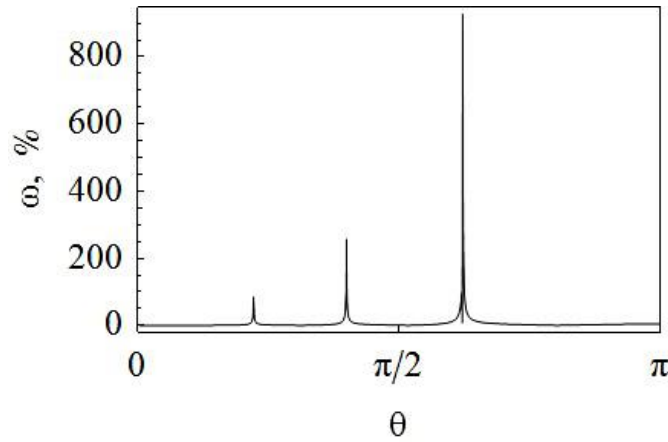First value is the differential cross section of coherent elastic scattering of neutron on diamond nanoparticle $d\sigma_1(\theta, \varepsilon)/d\Omega$ (3.1.1). The neutron wave vector is $k(\varepsilon) = \hbar^{-1}(2m\varepsilon)^{1/2}$. We will calculate normalized scattering cross sections $\chi(\theta) = |f(\theta, \varepsilon)|^2/|f_0|^2$ and $\chi^B(\theta) = |f^B(\theta, \varepsilon)|^2/|f_0|^2$, where $f_0 = f(\theta = 0, \varepsilon)$ is the value of precise amplitude of neutron "forward" scattering on nanoparticle (3.1.2). The error in the value $d\sigma_1^B/d\Omega$ calculated within Born approximation compared to the precise quantum mechanical calculation $d\sigma_1/d\Omega$ is characterized by the relative deviation $\omega(\theta) = |1 - |f^B(\theta, \varepsilon)|^2/|f(\theta, \varepsilon)|^2| \times 100\%$. Figs. 3.1.1 and 3.1.2 illustrate results of these calculations.
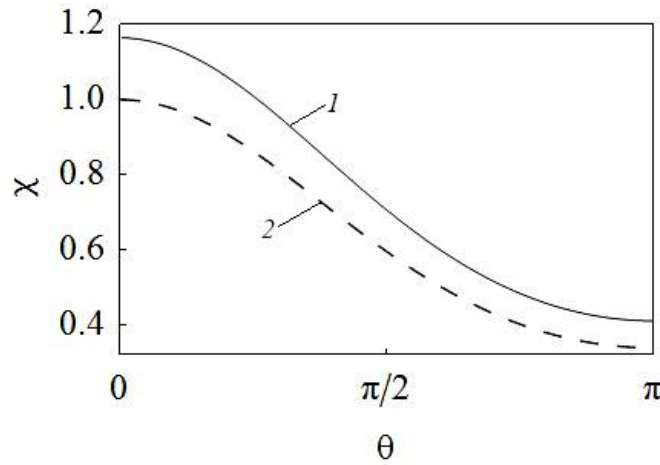
Fig. 3.1.1. Calculated normalized differential cross sections as a function of the neutron scattering angle, in relative units. $\varepsilon = 10^{-6}$ eV, the radius of diamond nanoparticle is $a = 5$ nm, $|f_0|^2 = 3.2 \times 10^{-19}$ м^2. *1* – first Born approximation $\chi^B(\theta)$; *2* – precise calculation $\chi(\theta)$.

Second calculated value is the total cross section of coherent elastic scattering of neutron on diamond nanoparticle $\sigma_1 = 2\pi \int\limits_0^\pi |f(\theta)|^2 \sin\theta \, d\theta$ or $\sigma_1 = (4\pi/k^2) \sum\limits_{l=0}^{\infty} (2l+1)\sin^2\delta_l$.

Aleksandr Nezvanov, Université Grenoble Alpes, 2018
Peculiarities of interaction and propagation of low-energy neutrons in nano-dispersed media | *75*
(the example of diamond nano-powder)

Results of precise calculation of the value σ_1 compared to calculations in Born approximation are presented in Table 3.1.

Fig. 3.1.2. Calculated value ω as a function of the neutron scattering angle θ. $\varepsilon = 10^{-4}$ eV, the radius of diamond nanoparticle is $a = 3$ nm.

Third calculated value $\sigma_{tr} = 2\pi \int_0^\pi |f(\theta)|^2 (1 - \cos\theta)\sin\theta d\theta$ is the transport cross section of coherent elastic scattering of neutron on diamond nanoparticle. Denote $\langle\mu_1\rangle = (2\pi/\sigma_1) \int_0^\pi |f(\theta)|^2 \cos\theta\sin\theta d\theta$ the mean cosine of the angle of coherent elastic scattering of neutron on nanoparticle. Then $\sigma_{tr} = \sigma_1(1 - \langle\mu_1\rangle)$. Results of precise calculations of value σ_{tr} compared to calculations within Born approximation are presented in Table 3.1.

Forth calculated value is the coefficient of reflection (albedo) R of neutrons from infinite half-space filled with monodispersed diamond nanopowder with the packing factor γ. The material is supposed to be macroscopically uniform, with the mean nanoparticle concentration equal $N_0 = 3\gamma/4\pi a^3$. We assume the structure of nanoparticle powder being disordered. Another half-space is vacuum. The neutron energy in vacuum is $\varepsilon = mv_0^2/2$; the distribution of neutron velocity directions $\mathbf{v}$ is uniform. The phase density of neutrons in vacuum is $N(\mathbf{r}, \boldsymbol{\eta}, v) = n_0(4\pi v^2)^{-1}\delta(v - v_0)$, where $v = |\mathbf{v}|$ is the value of neutron velocity in vacuum, $\boldsymbol{\eta} = \mathbf{v}/v$ is the ort of neutron velocity vector, n_0 is the density

Aleksandr Nezvanov, Université Grenoble Alpes, 2018

76 **Peculiarities of interaction and propagation of low-energy neutrons in nano-dispersed media (the example of diamond nano-powder)**

of neutron gas in vacuum. Neutrons move in material in the uniform mean field $U = \gamma U_0$, experience multiple potential (coherent) scattering on powder nanoparticles, coherent and incoherent scattering on nuclei, they could be absorbed by matter, a fraction of neutrons returns back from material to vacuum (i.e. diffusively reflected) due to coherent and incoherent processes of multiple scattering on inhomogeneities of matter density.

Neutron albedo is presented as a sum $R = R_{coh} + R_{inc}$, where R_{coh} is the coherent albedo of over-barrier reflection of neutrons from the uniform mean potential U; R_{inc} is the incoherent albedo of diffusive reflection of neutrons due to their multiple coherent and incoherent scattering on material inhomogeneities. Denote the total coefficient of passage of mono-energetic neutrons with energy $\varepsilon > U$ from vacuum to material as $D(\varepsilon)$ = $(4/3)\{[2(1-U/\varepsilon)^{3/2} - 2 + 3U/\varepsilon](\varepsilon/U)^2 - U/\varepsilon\}$, and get $R_{coh}(\varepsilon) = 1 - D(\varepsilon)$. The total albedo of incoherently reflected neutrons is $R_{inc}(\varepsilon) = D(\varepsilon)\beta(\varepsilon)$, where $\beta(\varepsilon)$ is the albedo of incoherent (diffusive) reflection of neutrons from material calculated only for the fraction of neutrons penetrating from vacuum inside material [6]. In the diffusive approximation we get $\beta(\varepsilon)$ = $[1 - \phi(\varepsilon)]/[1 + \phi(\varepsilon)]$, where $\phi(\varepsilon)$ = $(4\Sigma_c/3\Sigma_{tr})^{1/2}$; $\Sigma_c(\varepsilon) = \gamma n\sigma_c(\varepsilon)$, $\sigma_c(\varepsilon)$ is the cross section of absorption of neutron by nucleon. The macroscopic transport cross section of scattering accounting for medium density is $\Sigma_{tr}(\varepsilon) = \Sigma_c(\varepsilon) + \Sigma_s + (1 - \gamma)N_0\sigma_{tr}(\varepsilon)$, where $\Sigma_s = \gamma n\sigma_s$, σ_s is the cross section of elastic scattering of neutron on bound nucleus, $\sigma_{tr}(\varepsilon)$ is the transport cross section of coherent elastic scattering of neutron on the nanoparticle optical potential.

Finally we get: for $\varepsilon \gg U$, the neutron albedo from semi-infinite nano-dispersed material is $R(\varepsilon) = 1 - D(\varepsilon)[1 - \beta(\varepsilon)]$; for $\varepsilon \leq U$ we get $R(\varepsilon) = 1$. Results of precise calculation of albedo R compared to that in Born approximation are presented in Table 3.1 for diamond nanopowder (no chemical impurities), the porosity is $p = 0.9$.

Aleksandr Nezvanov, Université Grenoble Alpes, 2018

Peculiarities of interaction and propagation of low-energy neutrons in nano-dispersed media (the example of diamond nano-powder) | 77
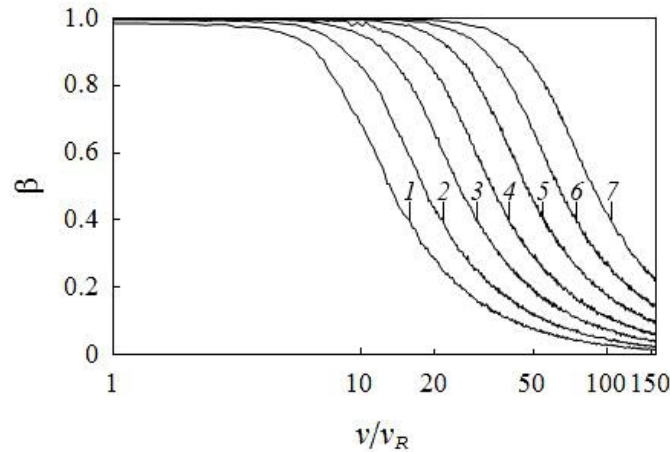
Table 3.1.

Results of calculations in Born approximation in comparison with precise quantum mechanical calculations using the method of phase functions

Particle size	Calculated values	Neutron energy ε, eV							
		3×10^{-7}	10^{-6}	3×10^{-6}	10^{-5}	3×10^{-5}	10^{-4}	3×10^{-4}	10^{-3}
$a = 2$ nm	σ_1, m^2	1.892×10^{-20}	1.793×10^{-20}	1.542×10^{-20}	9.449×10^{-21}	3.585×10^{-21}	1.112×10^{-21}	3.744×10^{-22}	1.127×10^{-22}
		1.808×10^{-20}	1.718×10^{-20}	1.487×10^{-20}	9.284×10^{-21}	3.579×10^{-21}	1.111×10^{-21}	3.743×10^{-22}	1.127×10^{-22}
	σ_{tr}, m^2	1.877×10^{-20}	1.746×10^{-20}	1.419×10^{-20}	6.849×10^{-21}	1.148×10^{-21}	1.394×10^{-22}	1.926×10^{-23}	2.092×10^{-24}
		1.793×10^{-20}	1.672×10^{-20}	1.368×10^{-20}	6.726×10^{-21}	1.151×10^{-21}	1.393×10^{-22}	1.925×10^{-23}	2.092×10^{-24}
	R, rel.un.	0.988	0.990	0.991	0.991	0.983	0.964	0.932	0.902
		0.987	0.990	0.991	0.991	0.983	0.964	0.932	0.902
$a = 3$ nm	σ_1, m^2	2.094×10^{-19}	1.858×10^{-19}	1.340×10^{-19}	5.439×10^{-20}	1.872×10^{-20}	5.681×10^{-21}	1.901×10^{-21}	5.709×10^{-22}
		1.898×10^{-19}	1.704×10^{-19}	1.266×10^{-19}	5.399×10^{-20}	1.869×10^{-20}	5.679×10^{-21}	1.900×10^{-21}	5.709×10^{-22}
	σ_{tr}, m^2	2.057×10^{-19}	1.748×10^{-19}	1.094×10^{-19}	2.313×10^{-20}	3.361×10^{-21}	3.792×10^{-22}	4.996×10^{-23}	5.276×10^{-24}
		1.894×10^{-19}	1.500×10^{-19}	1.030×10^{-19}	2.320×10^{-20}	3.363×10^{-21}	3.789×10^{-22}	4.994×10^{-23}	5.275×10^{-24}
	R, rel. un.	0.993	0.994	0.994	0.991	0.981	0.960	0.925	0.897
		0.993	0.994	0.994	0.991	0.981	0.960	0.925	0.897
$a = 5$ nm	σ_1, m^2	4.096×10^{-18}	2.975×10^{-18}	1.391×10^{-18}	4.328×10^{-19}	1.458×10^{-19}	4.398×10^{-20}	1.468×10^{-20}	4.407×10^{-21}
		3.222×10^{-18}	2.515×10^{-18}	1.336×10^{-18}	4.300×10^{-19}	1.456×10^{-19}	4.397×10^{-20}	1.468×10^{-20}	4.406×10^{-21}
	σ_{tr}, ^{2}	3.894×10^{-18}	2.470×10^{-18}	6.964×10^{-19}	8.302×10^{-20}	1.104×10^{-20}	1.227×10^{-21}	1.590×10^{-22}	1.650×10^{-23}
		3.050×10^{-18}	2.073×10^{-18}	6.831×10^{-19}	8.272×10^{-20}	1.101×10^{-20}	1.225×10^{-21}	1.589×10^{-22}	1.649×10^{-23}
	R, rel.un.	0.997	0.997	0.995	0.989	0.988	0.953	0.914	0.892
		0.996	0.996	0.995	0.989	0.988	0.953	0.914	0.892

Note. Born approximation is marked with grey.

Aleksandr Nezvanov, Université Grenoble Alpes, 2018

78   **Peculiarities of interaction and propagation of low-energy neutrons in nano-dispersed media (the example of diamond nano-powder)**

Comparative analysis of presented results of precise quantum mechanical calculations and those within Born approximation allows the following conclusions. Differential characteristics of neutron scattering on nanoparticle (the differential cross section of coherent elastic scattering) calculated within Born approximation deviate significantly from precise values in the explored range of neutron energies and sizes of diamond nanoparticles. Born approximation overestimates the probability of scattering to large angles. The accuracy of integral characteristics of scattering (total and transport cross sections, neutron albedo) calculated within Born approximation is acceptable for reliable quantitative estimations in the considered cases. The error in integral characteristics calculated within Born approximation decreases with increasing neutron energy and decreasing nanoparticle sizes.

To increase the accuracy of model description of the interaction of CNs and VCNs with diamond nanopowders, we developed a computer program for numerical Monte Carlo simulations of propagation of neutrons with energies of interest through layers of nano-dispersed powders. The simulation of interaction of neutrons with nanopowders using the method of phase functions included precise quantum mechanical calculation of cross sections of coherent elastic scattering of neutrons on nanoparticles. Fig. 3.1.3 shows calculated albedo β of incoherent (diffusive) reflection of neutrons as a function of neutron velocity v in relative units for layers of piled up diamond nanopowder of different thickness. The value of diamond critical velocity is $v_R = (2U_0/m)^{1/2} = 7.64$ m/s. To calculate each data point $\beta(v)$ in the figure, we simulated 10^4 events (neutron trajectories). Incoherent reflection of neutrons from a nanopowder layer is due to multiple potential (coherent) uncorrelated scattering of neutrons on powder nanoparticles that accompanies motion (diffusion) of neutrons in the layer and due to resulting escape of neutrons from the layer back to vacuum. The simulation is performed for monodispersed diamond powder with particle radii of 2.5 nm. The piled up density of diamond nanopowder was equal 0.35 g/cm^3. Nanoparticles are composed of carbon atoms without impurities of other chemical elements.

Aleksandr Nezvanov, Université Grenoble Alpes, 2018
Peculiarities of interaction and propagation of low-energy neutrons in nano-dispersed media
(the example of diamond nano-powder) | 79

Fig. 3.1.3. Calculated values of albedo β as a function of neutron velocity (in relative units) for layers of monodispersed diamond nanopowder. The piled up density of material is 0.35 g/cm^3; $a = 2.5$ nm; $v_R = 7.64$ m/s. The thickness of nanopowder layers is: 1 mm (*1*), 3 mm (*2*), 1 cm (*3*), 3 cm (*4*), 10 cm (*5*), 30 cm (*6*), 1 м (*7*). Nanoparticles are composed of pure carbon.

We note that efficient algorithms for precise quantum mechanical calculations have advantages in numerical simulations of realistic objects over approximating methods that require comparable efforts.

3.2. Determination of random values of neutron scattering angles

Algorithms for generation of random numbers with a specific distribution are well known and described in details in works devoted to Monte Carlo numerical methods [96], [97], [98], [99], [100]. Let us discuss the most common algorithm for simulation of continuous random values of neutron scattering angles θ within the Born approximation [101].

The function $F(\theta)$ is described as a distribution function of a random value ξ, which determines the probability that a random value of ξ will not exceed the specified value θ:

$$F(\theta) = P\{\xi \le \theta\} = \int_{-\infty}^{\theta} f(t)\, dt.$$

Then the random value ξ, which satisfies the equation $F(\xi) = \tau$, will have the distribution density $f(\theta)$. Here, τ is a random value, uniformly distributed within a range of 0 to 1 [97].

The standard algorithm of the inverse distribution method is applicable. For numerical modeling of the sampled value $\xi \in [a, b]$, the following formula is used:

$$\xi = G(\tau),$$

where τ is a uniformly distributed random number within the interval $[0, 1]$; $G(\tau)$ is the inverse function in relation to function $\tau = F(\xi)$.

For modeling neutron scattering on a spherical diamond nanoparticle in the Born approximation, $F(\theta)$ is determined as follows:

$$F(\theta) = \frac{1}{\sigma_s^B} \int_0^{\theta} d\sigma_s^B = \frac{1}{\sigma_s^B} \int_0^{\theta} 2\pi \sin t\, |f^B(\theta)|^2 dt,$$

where σ_s^B is the total cross-section of coherent elastic neutron scattering on a single nanoparticle in the Born approximation, $d\sigma_s^B$ is the differential cross-section of coherent elastic neutron scattering in direction to scattering angle t in the Born approximation; $f^B(\theta)$ is the scattering amplitude in the Born approximation.

A momentum transmitted by a nanoparticle at coherent elastic scattering [101]:

$$\boldsymbol{q} = \boldsymbol{k'} - \boldsymbol{k};\ q = 2k \sin(t/2),$$

where t is the scattering angle.

The amplitude of coherent elastic neutron scattering to angle t on a single spherical diamond nanoparticle with the radius r in the Born approximation is determined as follows:

$$f^B(t) = -\frac{2m}{\hbar^2} \int_0^{\infty} U(r) \cdot \frac{\sin(qr)}{q} \cdot r \cdot dr.$$

Aleksandr Nezvanov, Université Grenoble Alpes, 2018
Peculiarities of interaction and propagation of low-energy neutrons in nano-dispersed media
(the example of diamond nano-powder) | 81

where m is the mass of neutron, $\hbar$ is the Planck constant, and $U(r)$ is the neutron/nanoparticle interaction potential:

$$U(r) = \begin{cases} U_0, 0 \leq r \leq a \\ 0, \quad r > a \end{cases},$$

where a is the radius of a uniform diamond nanoparticle, $U_0 = (2\pi\hbar^2/m)nb \sim 10^{-7}$ eV, n is the atomic (nuclear) density of diamond nanoparticle matter, b is the coherent amplitude of bound-atom neutron scattering [72]. The diamond optical potential is $U_0 = 305$ neV.

Let us introduce the following notation $x = 2ka \cdot \sin(\theta/2)$. After calculations, we obtain:

$$F(\theta) = \frac{2\pi}{\sigma_S^B} \frac{1}{k^2} \left(\frac{mU_0 a^2}{\hbar^2}\right)^2 \left[1 - \frac{1}{x^2} + \frac{\sin 2x}{x^3} - \frac{\sin^2 x}{x^4}\right].$$

The total cross-section of coherent elastic neutron scattering on a single diamond nanoparticle in the Born approximation [9] is:

$$\sigma_S^B = \frac{2\pi}{k^2} \left(\frac{mU_0 a^2}{\hbar^2}\right)^2 \left[1 - \frac{1}{(2ka)^2} + \frac{\sin 4ka}{(2ka)^3} - \frac{\sin^2 2ka}{(2ka)^4}\right].$$

Let us set:

$$\Phi(k) = \left[1 - \frac{1}{(2ka)^2} + \frac{\sin 4ka}{(2ka)^3} - \frac{\sin^2 2ka}{(2ka)^4}\right]^{-1},$$

$$\Pi(x) = \left[1 - \frac{1}{x^2} + \frac{\sin 2x}{x^3} - \frac{\sin^2 x}{x^4}\right],$$

$$F(\theta) = \Phi(k) \cdot \Pi(x).$$

Let us define a new random value μ by relation $\mu = \cos\theta$.

Using the following transformations:

$$\cos\theta = 1 - 2\sin^2(\theta/2), \sin^2(\theta/2) = \sqrt{(1 - \cos\theta)/2} = \sqrt{(1-\mu)/2}$$

we get the following formula for $\Pi(\mu)$:

$$\Pi(\mu) = 1 - \frac{1}{2(ka)^2(1-\mu)}\left[1 - \frac{1}{ka\sqrt{2(1-\mu)}}\left(\sin\left(2ka\sqrt{2(1-\mu)}\right) - \frac{\sin^2\left(ka\sqrt{2(1-\mu)}\right)}{ka\sqrt{2(1-\mu)}}\right)\right].$$

Aleksandr Nezvanov, Université Grenoble Alpes, 2018

82 **Peculiarities of interaction and propagation of low-energy neutrons in nano-dispersed media (the example of diamond nano-powder)**

The distribution function for the random value μ within [-1,1] will appear as:

$$F(\mu) = 1 - \Phi(k) \cdot \Pi(\mu).$$

$F(\mu)$ varies from 0 to 1 with variations of the random value μ from -1 to 1.

Thus, modeling of $\mu = G(\tau)$ will let us receive a random scattering angle cosine $\mu = \cos\theta$, which will have the distribution function $F(\mu)$.

Taking into account a shell, the neutron interaction potential for a spherical diamond nanoparticle model will appear as:

$$U(r) = \begin{cases} U_c, 0 \leq r \leq R_c \\ U_s, R_c \leq r \leq R, \\ 0, \quad r > R \end{cases}$$

where R_c is the radius of the nanoparticle diamond core, $R = R_c + h$ is the nanodiamond radius considering the shell with thickness h, U_c is the diamond core potential; U_s is the nanodiamond shell potential. Solution of the equation $F(\xi) = \tau$ for a more complicated potential form can be obtained numerically.

Software implementation of the described numerical modeling algorithm included compilation of detailed tables of values for inverse functions $G(y)$, $0 < y < 1$. Using linear interpolation, the equation $\mu = G(\tau)$ was solved.

The range of values $\mu \in [-1, 1]$ was divided in N equal parts $\mu_0, \mu_1, \mu_2, \dots, \mu_N$, where $\mu_0 = -1$, $\mu_1 = \mu_0 + \Delta\mu$, $\Delta\mu = 2/N$, $\mu_N = 1$. The sequence of corresponding values of the distribution function $F(\mu_0), F(\mu_1), \dots, F(\mu_N)$ was obtained. Then the value of the random variable τ, uniformly distributed within [0, 1], was generated. Such a value of j was found that $F(\mu_{j-1}) \leq \tau \leq F(\mu_j)$.

Using linear interpolation, we obtained the value of μ_τ, angle cosine, corresponding to the value $F(\mu_\tau) = \tau$:

$$\mu_\tau = \mu_{j-1} + [\tau - F(\mu_{j-1})]T_j,$$

where $T_j = (\mu_j - \mu_{j-1})/[F(\mu_j) - F(\mu_{j-1})]$.

Aleksandr Nezvanov, Université Grenoble Alpes, 2018
Peculiarities of interaction and propagation of low-energy neutrons in nano-dispersed media | *83*
(the example of diamond nano-powder)

3.3. Conversion of spherical coordinate system and free-path simulation

At simulating the passage of neutrons through nanodispersed powders, after each action of neutron scattering in the material there are implemented successive conversions of coordinates from the local coordinate system $x'y'z'$ into the laboratory coordinate system XYZ. The latter is fixedly related to the material plate. After each action of neutron scattering a local system of coordinates $x'y'z'$ is shaped in the material. The start of coordinates coincides with the point of neutron interaction with the material, and the axis z' of the local coordinate system is directed to the neutron movement after scattering at the given point towards the free path. The local coordinate system serves for the goals characterizing the neutron scattering in the current coordinate system at every point of interaction.

Fig. 3.3.1. Neutron scattering at the point $\mathbf{r}_1$ in the laboratory system of coordinates XYZ. $\left(x_0, y_0, z_0\right)$ – the point of neutron fall on the plate; $\mathbf{\Omega}_1'$ – a new direction of neutron movement after scattering at the point $\mathbf{r}_1$.
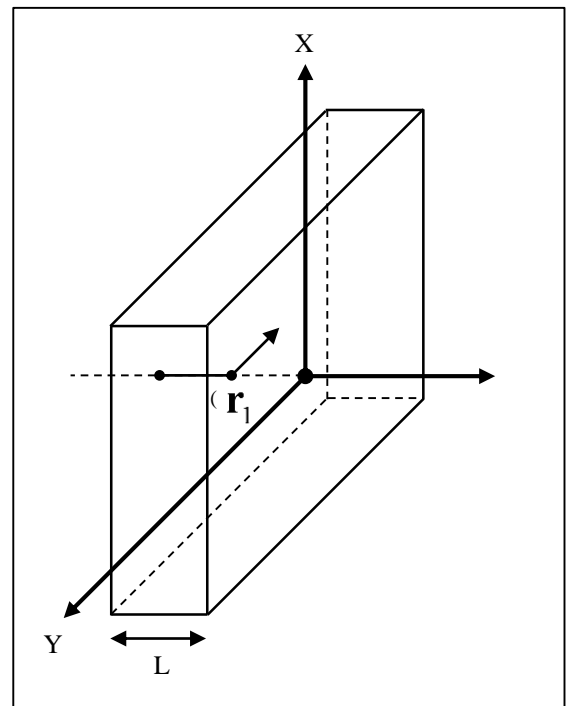
Let's outline an algorithm of neutron distribution in nanopowder, starting from the entry into the material, as well as show the relation between the local and laboratory coordinate systems.

Aleksandr Nezvanov, Université Grenoble Alpes, 2018

84 | **Peculiarities of interaction and propagation of low-energy neutrons in nano-dispersed media (the example of diamond nano-powder)**

And now let's examine the plate from nanodispersed material with a thickness L. Let the neutron fall by normal on the material border $z = -L/2$ towards the axis Z of the laboratory coordinate system. We are generating random length of neutron free-path l_1 before the interaction in the material.

The distribution function l_1 has the form of [102], [98], [96], [97], [103], [104]:

$$F(x) = 1 - \exp\left[-\Sigma \cdot x\right]; \ 0 < x < \infty,$$

in which Σ – total macroscopic cross-section of the neutron interaction with the material.

We define the length of neutron free path l_1 explicitly using the inverse function method:

$$l_1 = -(1/\Sigma)\ln\gamma \ ,$$

in which γ – the random value, equally distributed in the interval [0, 1].

In this way, the coordinates of the point $\mathbf{r_1}$ of the first neutron interaction in the material are determined in the laboratory system of coordinates XYZ:

$$\mathbf{r_1} = \left(x_0, y_0, -L/2 + l_1\right)$$

We test the point $\mathbf{r_1}$ at affiliation to the area of space occupied by a material. If the point $\mathbf{r_1}$ is in the material, we act out a kind of neutron interaction with nanoparticle in the point $\mathbf{r_1}$. Probability of the *i*-type neutron interaction with the nanoparticle is defined by the correlation $P_i = \sigma^i / \sigma$, где σ^i – microscopic cross-section of the *i*-type interaction; σ – total microscopic cross-section of the neutron interaction with the nanoparticle.

In case the neutron absorption isn't implemented, the direction of coherent elastic scattering $\mathbf{\Omega'_1}$ is acted out in the local coordinate system $x'y'z'$:

$$\mathbf{\Omega'_1} = \sin\theta'_1\cos\chi'_1 \cdot \mathbf{i'} + \sin\theta'_1\sin\chi'_1 \cdot \mathbf{j'} + \cos\theta'_1 \cdot \mathbf{k'}$$

Here θ'_1, χ'_1 – polar and azimuth scattering angles. The angle value χ'_1 is equally distributed in the interval [0, 2π]. The algorithm of acting out $\mu = \cos\theta'_1$ is defined in the section 3.2 of the thesis.

Aleksandr Nezvanov, Université Grenoble Alpes, 2018
Peculiarities of interaction and propagation of low-energy neutrons in nano-dispersed media   85
(the example of diamond nano-powder)

Next, we act out random length of the neutron free path l_2 towards the scattering $\mathbf{\Omega}_1' : \mathbf{l}_2 = l_2 \cdot \mathbf{\Omega}_1'$. The transition from local to laboratory coordinate system is defined by conversion [9], [102], [98], [96]:

$$\begin{pmatrix} x \\ y \\ z \end{pmatrix} = \begin{pmatrix} a \\ b \\ c \end{pmatrix} + \begin{pmatrix} x' & y' & z' \end{pmatrix} \begin{pmatrix} -\cos\varphi\cos\theta & \sin\varphi & \cos\varphi\sin\theta \\ -\sin\varphi\cos\theta & -\cos\varphi & \sin\varphi\sin\theta \\ \sin\theta & 0 & \cos\theta \end{pmatrix} ,$$

θ, φ – direction of the neutron movement after the scattering with regard to the laboratory coordinate system; (a,b,c) – coordinate shifting in the laboratory system with respect to the previous point of the neutron scattering in the material.

The coordinates of the next point $\mathbf{r}_2 = (x_2, y_2, z_2)$ of the neutron interaction in material in the laboratory coordinate system XYZ at the first step of simulation are identified at values $(a,b,c) = \mathbf{r}_1$; $\theta = \theta_1 = 0$, $\varphi = \varphi_1 = 0$ (from the condition of normal fall on the plate):

$$\begin{cases} x_2 = x_1 - l_2 \sin\theta_1' \cos\chi_1' \\ y_2 = y_1 - l_2 \sin\theta_1' \sin\chi_1' \\ z_2 = z_1 + l_2 \cos\theta_1' \end{cases}$$

We review the $\mathbf{r}_2$ interaction point for affiliation of the area field under examination. If neutron is in nanopowder, we define the scattering vector $\mathbf{\Omega}_1'$ in the laboratory coordinate system. In general it is recorded as following:

$$\mathbf{\Omega}_1' = \mathbf{\Omega}_{1x}' \mathbf{i} + \mathbf{\Omega}_{1y}' \mathbf{j} + \mathbf{\Omega}_{1z}' \mathbf{k} ,$$

where $\begin{pmatrix} \mathbf{\Omega}_{1x}' \\ \mathbf{\Omega}_{1y}' \\ \mathbf{\Omega}_{1z}' \end{pmatrix} = \begin{pmatrix} -\sin\theta_1'\cos\chi_1'\cos\theta_1\cos\varphi_1 - \sin\theta_1'\sin\chi_1'\sin\varphi_1 + \cos\theta_1'\sin\theta_1\cos\varphi_1 \\ -\sin\theta_1'\cos\chi_1'\cos\theta_1\sin\varphi_1 - \sin\theta_1'\sin\chi_1'\cos\varphi_1 + \cos\theta_1'\sin\theta_1\sin\varphi_1 \\ \sin\theta_1'\cos\chi_1'\sin\theta_1 + \cos\theta_1'\cos\theta_1 \end{pmatrix}.$

Here the angles θ_1, φ_1 already refer to the previous scattering vector in the laboratory coordinate system. At the first step of simulation of neutron distribution in material the scattering vector $\mathbf{\Omega}_1'$ in the laboratory coordinate system is as following:

$$\mathbf{\Omega}_1'\big|_{\theta_1=0,\varphi_1=0} = -\sin\theta_1'\cos\chi_1' \cdot \mathbf{i} - \sin\theta_1'\sin\chi_1' \cdot \mathbf{j} + \cos\theta_1' \cdot \mathbf{k}$$

Aleksandr Nezvanov, Université Grenoble Alpes, 2018

86 | **Peculiarities of interaction and propagation of low-energy neutrons in nano-dispersed media (the example of diamond nano-powder)**

Representing in the laboratory coordinate system the direction of the neutron movement Ω'_1 in material after scattering (towards the free path), we obtain a new direction $\Omega_2 \equiv \Omega'_1$ of the neutron movement in material by the moment of interaction at the next point $\mathbf{r}_2$.

We lead the axis z' of the new local coordinate system in the direction of the scattering Ω_2, related in the laboratory coordinate system with the angles θ_1, φ_1 of the previous neutron scattering in material. For this purpose we identify new values for the angles $\theta = \theta_2$, $\varphi = \varphi_2$:

$$\theta_2 = \arccos(\Omega'_{1z}), \; \varphi_2 = \begin{cases} \arctan(\Omega'_{1y} / \Omega'_{1x}), & \Omega'_{1y} > 0 \\ \pi + \arctan(\Omega'_{1y} / \Omega'_{1x}), & \Omega'_{1y} < 0 \end{cases}$$

In this way, we find orientation of axes of the new local coordinate system, the basis vectors of which at the first step of simulation are as follows:

$$\begin{pmatrix} \mathbf{i}'_2 \\ \mathbf{j}'_2 \\ \mathbf{k}'_2 \end{pmatrix} = \begin{pmatrix} \mathbf{i} & \mathbf{j} & \mathbf{k} \end{pmatrix} \begin{pmatrix} -\cos\theta_2 \cos\varphi_2 & \sin\varphi_2 & \sin\theta_2 \cos\varphi_2 \\ -\cos\theta_2 \sin\varphi_2 & -\cos\varphi_2 & \sin\theta_2 \sin\varphi_2 \\ \sin\theta_2 & 0 & \cos\theta_2 \end{pmatrix}$$

The next step of simulation in analogy we start by acting out the type of interaction with nanoparticle in the point $\mathbf{r}_2$. In case the neutron isn't absorbed, we generate the scattering angles θ'_2, χ'_2 and the length of neutron free path l_3 in material towards $\Omega'_2 \equiv \Omega_3$ in the local coordinate system. We gain the next point $\mathbf{r}_3$ of the neutron interaction with nanoparticle in both local and laboratory coordinate systems. Then, we determine the direction of neutron scattering Ω_3 in the laboratory coordinate system. Afterwards, we develop a new local coordinate system in the next point of interaction $\mathbf{r}_3$.

The cyclical realization of algorithm continues until the neutron is absorbed in the nanodispersed medium or quits its ranges.

Aleksandr Nezvanov, Université Grenoble Alpes, 2018
Peculiarities of interaction and propagation of low-energy neutrons in nano-dispersed media | 87
(the example of diamond nano-powder)

CHAPTER 4. ANALYSIS OF RESULTS OF NUMERIICAL CALCULATIONS AND COMPARISON WITH EXPERIMENTAL DATA

4.1. Reflection and passage of low-energy neutrons through thin layers of nanodiamond powder

In the work [14] there have been carried out measurements on the passage of slow neutrons with different energy through the plate of diamond nanopowder *«ultradiamond90»* of diverse thickness.

The comparison of experimental data with the calculation results has been realized. The calculations have been made using developed software complex [36], [37]. The quantitative model, developed in the current thesis, is based on the computed model.

In the experiment around the sample12 detectors are installed. These detectors have produced a geometrically right polygon (dodecagon) and covered $\approx 45\%$ of the total solid angle.
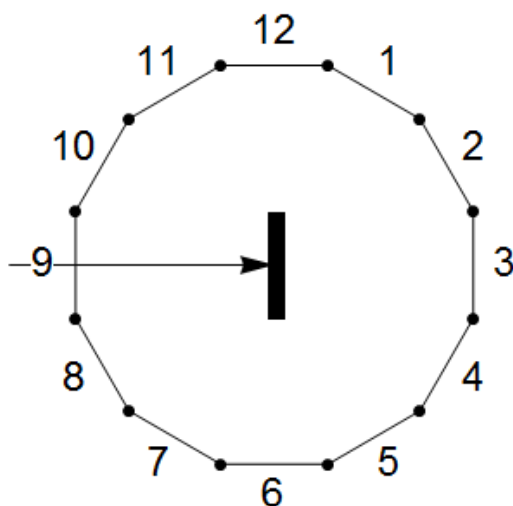
Fig. 4.0. The layout of the plate, detectors and their numeration.
The pointer indicates the direction of falling of the neutron beam normally to the plate surface. The plate with the diamond nanopowder is in the centre. The data from the detectors №№ 3, 6, 9, 12 have never been considered in the results of all the implemented measurements.

Figure 4.1 shows the results of simulation modeling of the low-energy neutron beam interaction, falling by normal to the sample surface of the diamond nanopowder
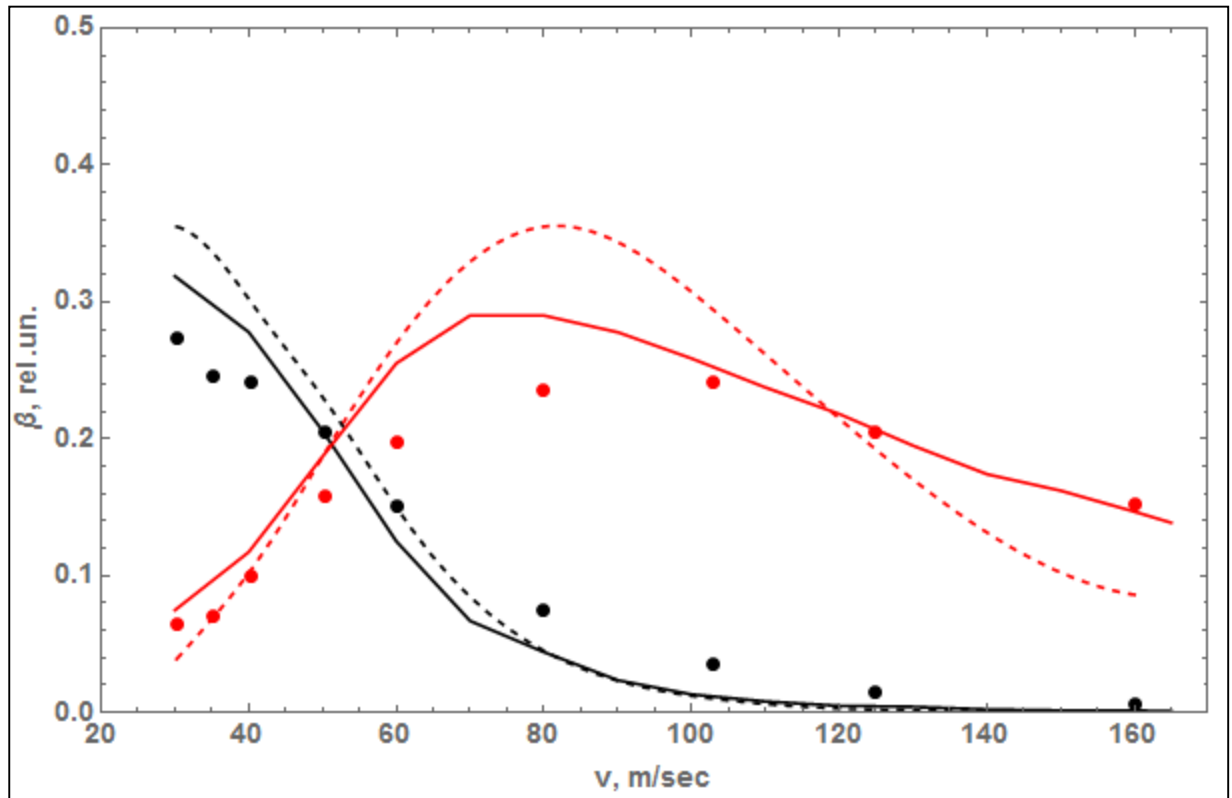
Aleksandr Nezvanov, Université Grenoble Alpes, 2018

88 | **Peculiarities of interaction and propagation of low-energy neutrons in nano-dispersed media (the example of diamond nano-powder)**

«ultradiamond90» with a thickness of 0.2 mm. The simulation results are presented as compared with the experimentally measured data, as well as with the calculated model of isolated nanoparticles without shell applied in [14].

Primarily, for the motivation of accounting necessity in the nanoparticle model of impurity shell we have completed the nanoparticle model, applied in the work [14]. The correlations of the elemental content of nanopowder (for the impurity shell substances) have been adjusted in the model; two-phase potential form of the "core-shell" interaction with neutron has been adopted; monodispersed powder has possessed an average radius of the diamond core 2.5 nm and an average size of the nanoparticle impurity shell 0.6 nm.

Consideration of the items mentioned above allowed to outline thoroughly the probability of neutron reflection from the sample for small velocities compared with the theoretical calculations based on the model from [14]. Conclusion: the matter of the nanoparticle impurity shell is necessary for a correct statement of experiment results.

The results of calculations of the neutron hit to detectors are shown in Figure 4.2 and Figure 4.3.

Aleksandr Nezvanov, Université Grenoble Alpes, 2018

Peculiarities of interaction and propagation of low-energy neutrons in nano-dispersed media
(the example of diamond nano-powder)

89

Fig. 4.1. Comparison of possibilities of neutron reflection and passage in accordance

with the velocity v. The sample thickness is 0.2 mm.

The red colour stands for the data pointing out the neutron passage to the front semisphere.

The black colour stands for the data pointing out the neutron passage to the back semisphere.

Points – experimental data [14].

- - - - - – calculation by the model of isolated particle without shell from the work [14].

———— – our calculation by the model of isolated particle with impurity shell.

Aleksandr Nezvanov, Université Grenoble Alpes, 2018

90 | ***Peculiarities of interaction and propagation of low-energy neutrons in nano-dispersed media (the example of diamond nano-powder)***

Aleksandr Nezvanov, Université Grenoble Alpes, 2018
Peculiarities of interaction and propagation of low-energy neutrons in nano-dispersed media 91
(the example of diamond nano-powder)

Fig. 4.2. Results of numerical simulation. The neutron velocity – 30 m/sec.
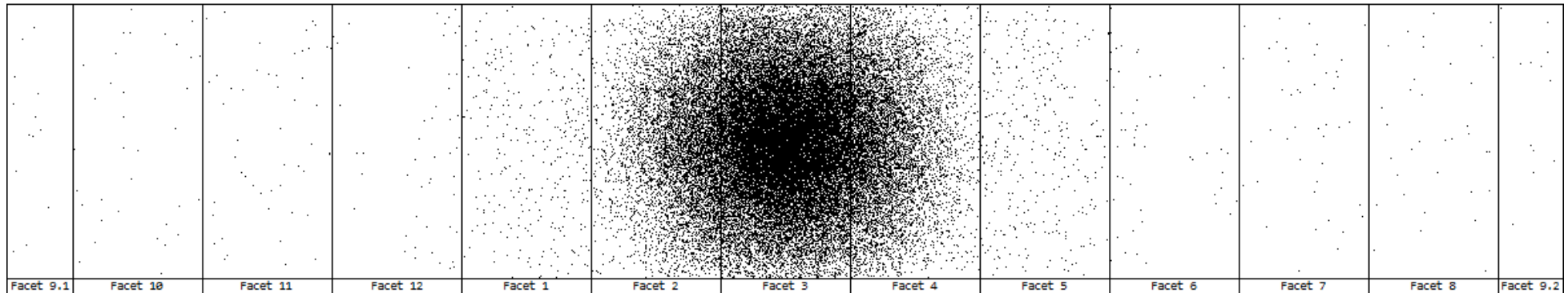
Fig. 4.3. Results of numerical simulation. The neutron velocity – 160 m/sec.

Explanatory note to figures. The results of calculations of neutron passage through the diamond nanopowder. Points – the calculated position of neutron entry into detectors. The calculation method - numerical simulation modeling by the Monte Carlo method. The experiment of the work has been simulated [14]. The thickness of the diamond nanopowder layer is 0.2 mm.

Aleksandr Nezvanov, Université Grenoble Alpes, 2018

92 | ***Peculiarities of interaction and propagation of low-energy neutrons in nano-dispersed media (the example of diamond nano-powder)***

Fig. 4.4 shows the results of numeric calculations on Model No. 1 and Model No. 2.

Model No. 1 is a model of isolated diamond nanoparticles; it is described in the work [14]. The monodispersed powder of spherical particles of radius $a = 2.5$ nm, bulk density of the nanopowder 0.6 g/cm^3.

Model No. 2 is a qualitative model developed in the thesis taking into account the effects of the medium density. The distribution of particle sizes, stated by the diamond nanopowder *«ultradiamond90»* manufacturer, has been used. The cross-sections of elastic coherent neutron scattering on nanoparticles have been calculated by the Born equation.

The chemical content of diamond nanoparticles [16]: the diamond core of nanoparticle – 72.25 wt. %; the remaining carbon (crystal and amorphous forms) – 18.06 mass. %; oxygen – 4.18 wt. %; hydrogen – 1.02 wt. %; nitrogen – 3.24 wt. %; fireproof impurities – 1.25 wt. %.

Indestructible (primary) agglomerate from nanoparticles possesses typical sizes $d_2 \sim 100 - 200$ nm and the packaging density of nanoparticle γ_1.

The parameters of the diamond nanopowder in the Model No. 2: bulk density of the nanopowder $\rho_{bulk} = 0.6$ g/cm^3; a concentration of diamond nanoparticles in the powder $N_0 = 2.37 \times 10^{24}$ m^{-3}; the packaging coefficient of diamond nanoparticles in the powder in total $\gamma = 0.209$; the thickness of impurity shell $h = 0.5$ nm; the substance density of impurity shell $\rho_{shell} = 1.6$ g/cm^3. The calculation of parameters N_0 and γ is marked out in the section 2.4.

Calculation on the Model No. 2 has been produced for four different values $\gamma_1 = 0.523$; 0.569; 0.625; 0.682. The most satisfactory acceptance with the results of experiments is reached for $\gamma_1 = 0.523$.

Calculations on the Model No. 1 give less satisfactory consent for the results of experiments and can hardly significantly improve.

Figure 4.4 (curve 5) represents the results of our calculations on Model No. 1 with the data of the work [14], which completely matched with the authors' calculations.

Aleksandr Nezvanov, Université Grenoble Alpes, 2018
Peculiarities of interaction and propagation of low-energy neutrons in nano-dispersed media | *93*
(the example of diamond nano-powder)

Graphs of angular features of monoenergetic neutron beam scattering are shown in Figure 4.5 and Figure 4.6. Neutron velocities $v = 35$ and $v = 160$ m/sec accordingly. The results of numerica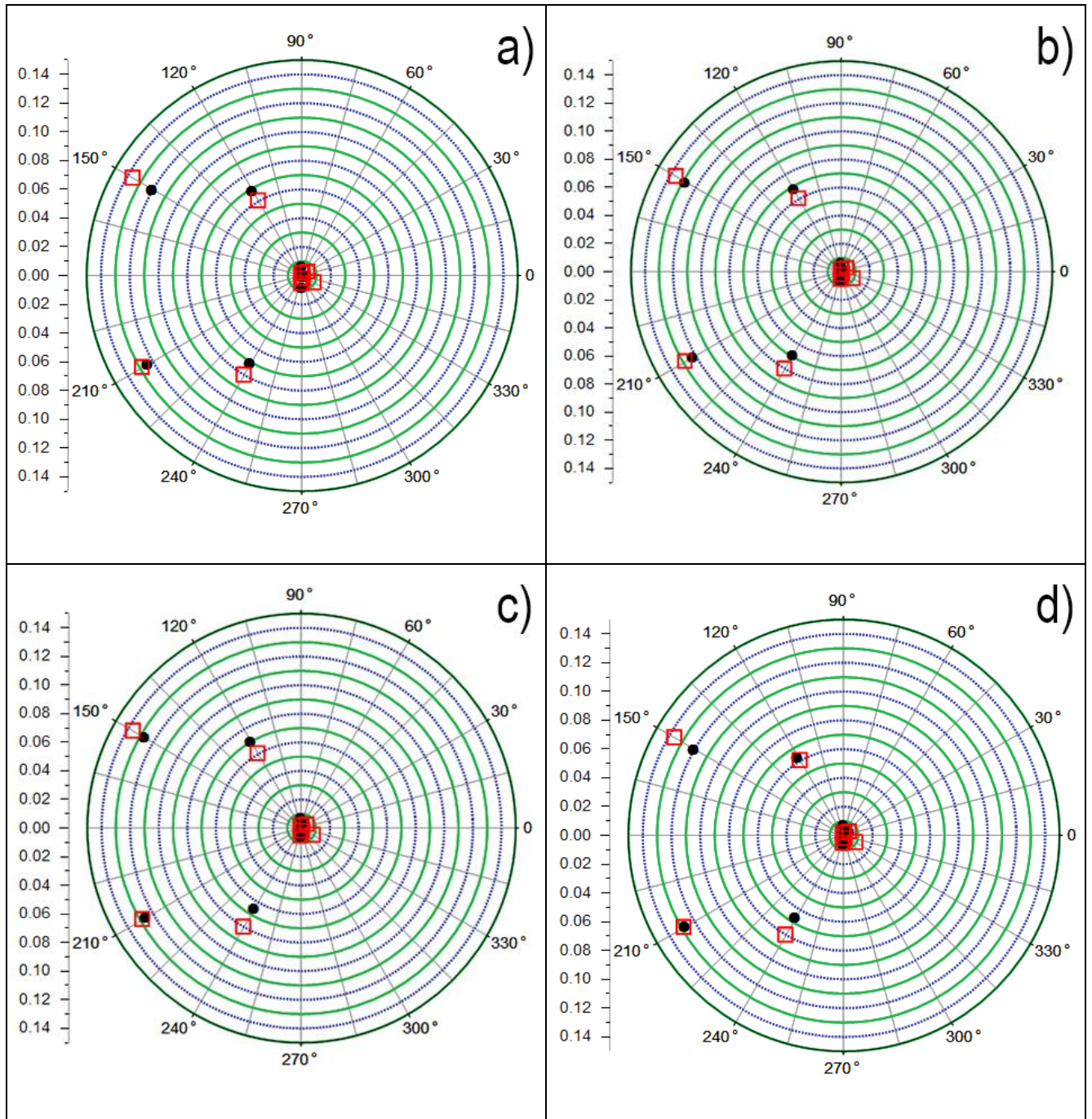l simulation were gained with the application of Model No. 2. The relative part of neutrons fallen into the detector is $\delta_D = N_D / N_B$, in which N_D is the number of neutrons fallen into the detector, N_B is the number of neutrons fallen onto the beam sample.

The plate thickness of the diamond nanopowder *«ultradiamond90»*: $h = 2\,\text{mm}$. The calculated packaging coefficients of nanoparticles in the primary agglomerate: $\gamma_1 = 0.523$ (a), $\gamma_1 = 0.569$ (b), $\gamma_1 = 0.625$ (c), $\gamma_1 = 0.682$ (d). The calculation γ_1 is realized by the distribution function of particle in the sizes $f(r)$, indicated by the manufacturer. The calculation method is outlined in the section 2.4 of the thesis.

Aleksandr Nezvanov, Université Grenoble Alpes, 2018

94 | **Peculiarities of interaction and propagation of low-energy neutrons in nano-dispersed media (the example of diamond nano-powder)**
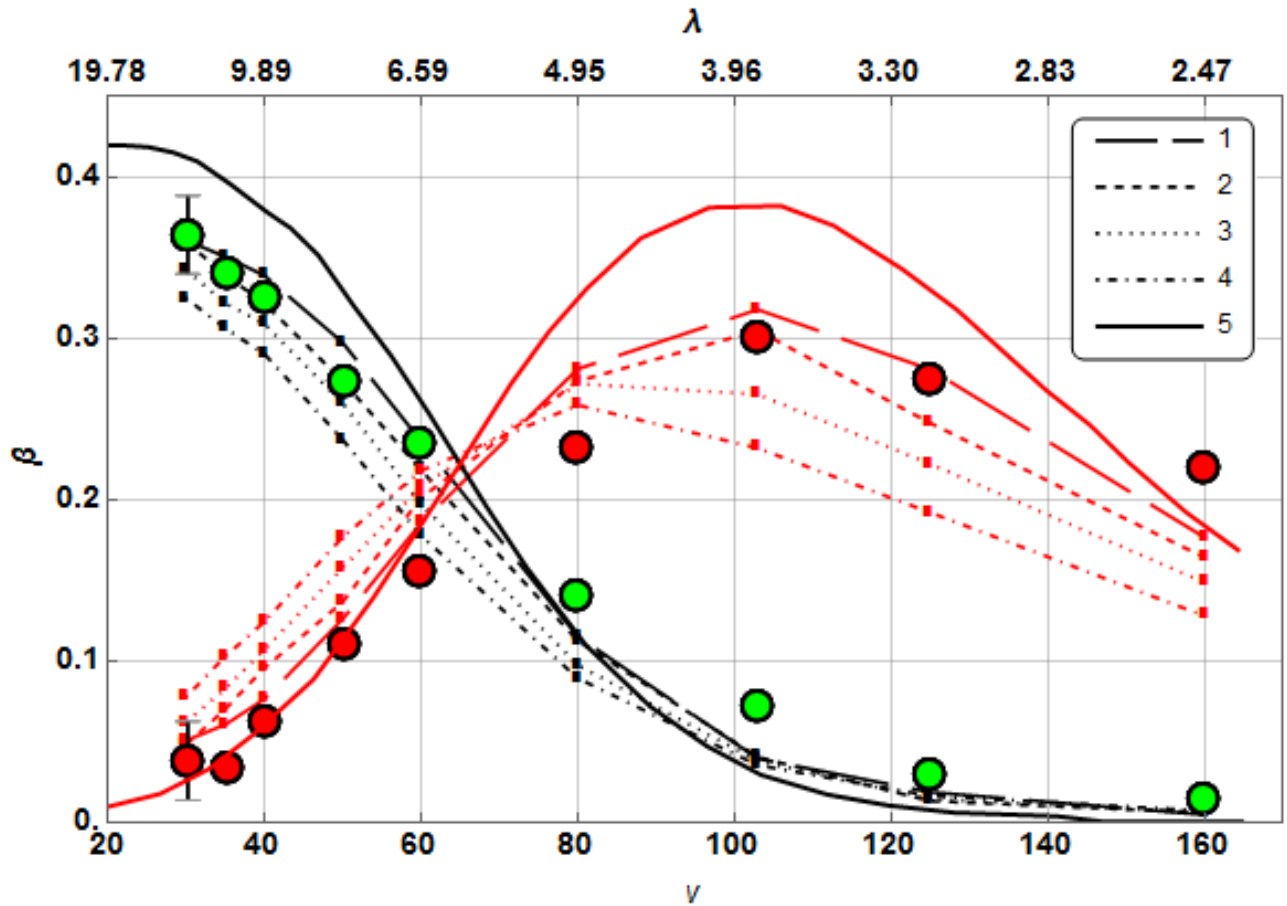
Fig. 4.4. Comparison of probabilities β of neutron reflection (in black colour) and passage (in red colour) in relation with the velocity v (the wave length λ)

Explanatory note to Figure 4.4. The sample thickness is 0.4 mm. The round points – experimental data [14] (the green colour – reflection; the red colour – passage). The curved 1-4 obtained at various value of packaging coefficient γ_1 of diamond nanoparticles in nondestructive agglomerate: $1 - \gamma_1 = 0.523$; $2 - \gamma_1 = 0.569$; $3 - \gamma_1 = 0.625$; $4 - \gamma_1 = 0.682$. The curved 5 – the numerical calculation for the model of isolated nanoparticles [14] (Model No. 1).

Aleksandr Nezvanov, Université Grenoble Alpes, 2018

Peculiarities of interaction and propagation of low-energy neutrons in nano-dispersed media | 95
(the example of diamond nano-powder)

Fig. 4.5. Dependence of the part of scattered neutrons δ_D, fallen into detectors, shown in

the scheme of Figure 4.0 (from the scattering angle).

The neutron velocity $v = 35$ m/sec. The black round points – simulation. The red square

points – experiment [14]. The nanopowder plate thickness *«ultradiamond90»* – 2 mm

$\gamma_1 = 0.523$ (a); $\gamma_1 = 0.569$ (b); $\gamma_1 = 0.625$ (c); $\gamma_1 = 0.682$ (d).
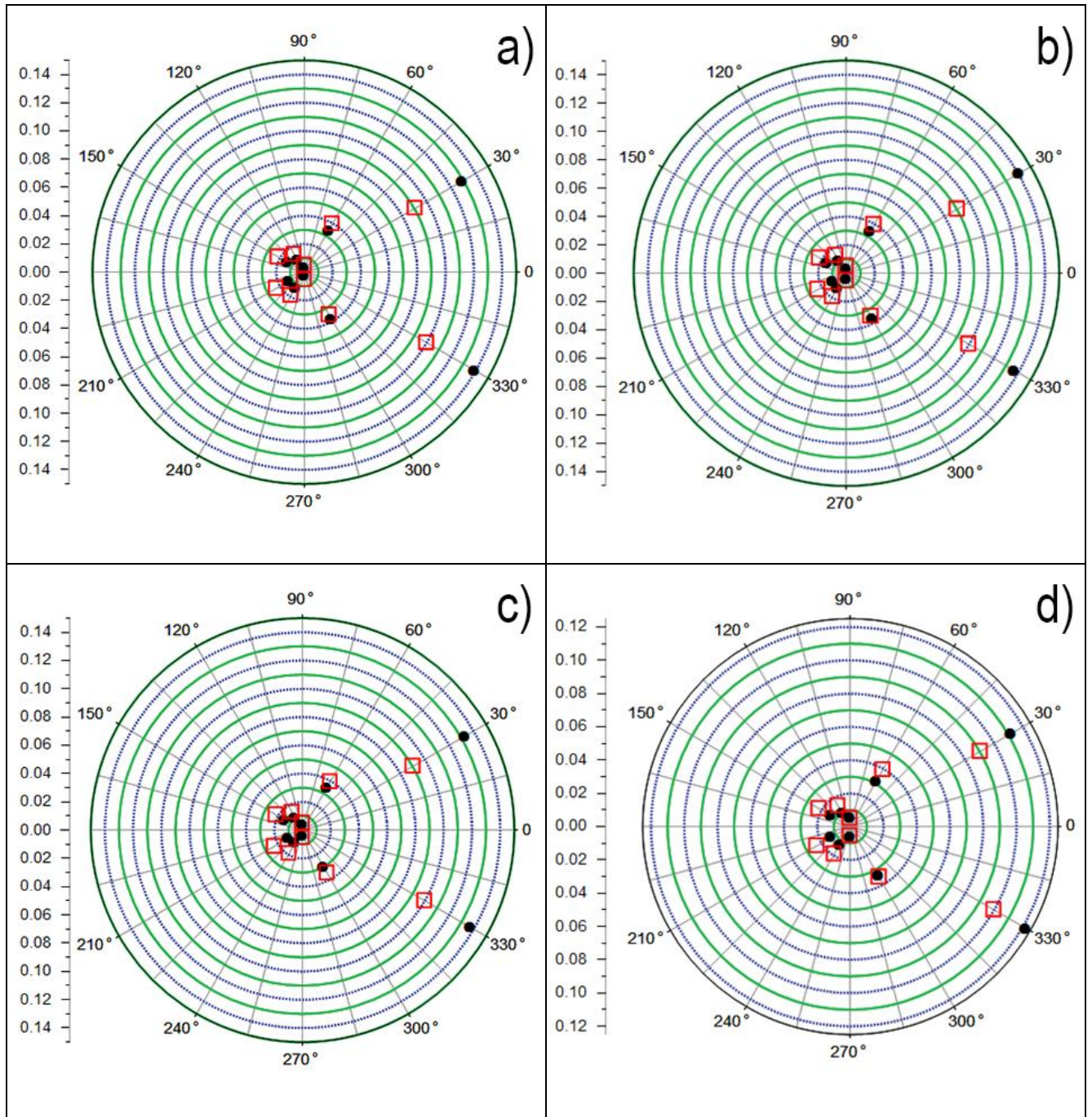
Fig. 4.6. Dependence of the part of scattered neutrons δ_D, fallen into detectors, shown in the scheme of Figure 4.0 (from the scattering angle).

The neutron velocity $v = 160$ m/sec. The black round points – simulation. The red square points – experiment [14]. The nanopowder plate thickness *«ultradiamond90»* – 2 mm $\gamma_1 = 0.523$ (a); $\gamma_1 = 0.569$ (b); $\gamma_1 = 0.625$ (c); $\gamma_1 = 0.682$ (d).

Aleksandr Nezvanov, Université Grenoble Alpes, 2018
Peculiarities of interaction and propagation of low-energy neutrons in nano-dispersed media | 97
*(the example of diamond nano-powder)*

Figure 4.7 presents the experiment data [14] on the neutron reflection and passage through the diamond nanopower *«ultradiamond90»* layer with a thickness of 0.4 mm. The numerical calculations have been carried out in relation with Model No. 2. The distribution of diamond nanoparticles in the sizes $f(r)$ has been approximated by exponential-power distribution law (see Formula (2.4.1) and Figure 2.4.1). The thickness of the impurity shell is $h = 0.5$ nm. The shell substance density – $\rho_{shell} = 1.6$ g/cm^3. The approximation parameters are defined in accordance with the section 2.4. At average radius value $R_{mean} = 1.8$ nm we have: $A = 21.33$ nm$^{-6.55}$; $\alpha = 5.55$; $\beta = 3.80$ nm^{-1}; $N_0 = 3.58 \times 10^{24}$ m^{-3}. The simulation accuracy is less than the sizes of respective points on the graph.

Parameters of the diamond nanopowder model: nanopowder bulk density $\rho_{bulk} = 0.6$ g/cm^3; packaging coefficient of diamond nanoparticles in powder in total $\gamma = 0.2274$; packaging coefficient of nanoparticles in the primary agglomerate $\gamma_1 = 0.691$.

The calculation of parameters has been realized in relation with the method in the section 2.4 for the distribution function of nanoparticles in sizes $f(r)$ (2.4.1).

As it is shown in Figure 4.7, the function of $f(r)$ kind (2.4.1) on the whole satisfactorily describes the data of experiments [14]. The variation of parameter γ_1 provides opportunities for the optimization of results.
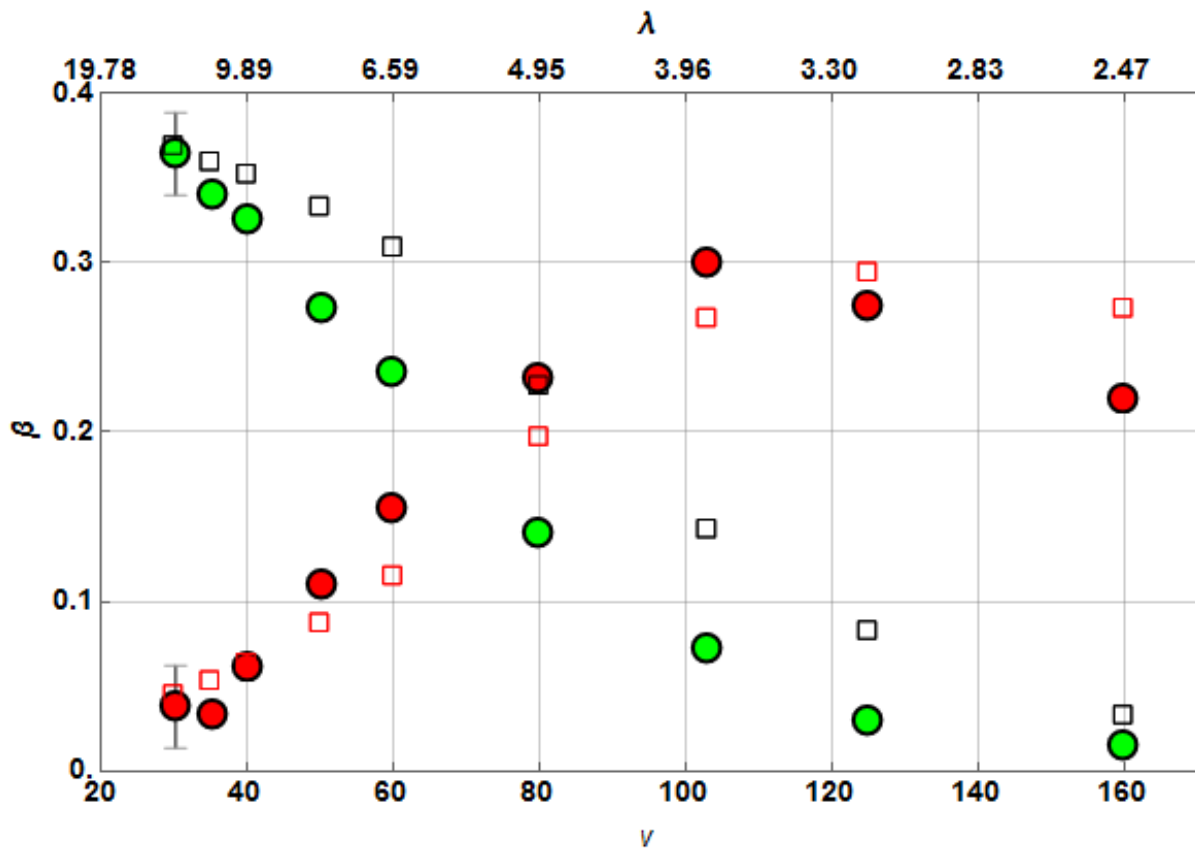
Fig. 4.7. Comparison of probabilities β of neutron reflection (green round points) and passage (red round points) in relation with the velocity v (the wave length λ) Thickness of the nanopowder plate – 0.4mm. The round points – experimental data. The square points - results of simulation modeling (the black squares – neutron reflection in detectors of the back semisphere; the red squares – neutron passage in detectors of the front semisphere.

Aleksandr Nezvanov, Université Grenoble Alpes, 2018
Peculiarities of interaction and propagation of low-energy neutrons in nano-dispersed media
(the example of diamond nano-powder) | 99

4.2. Low-energy neutron reflection and passage through thick layers of nanodiamond powder

Figure 4.8 and Figure 4.9 represent the data of experiments on slow neutron reflection and passage through layers of different thickness of the diamond nanopowder *«ultradiamond90»* of various thickness. The numerical calculations have been realized at quantitative Model No. 2. The distribution of nanopartiocles in sizes $f(r)$ has been used, provided by the manufacturer of the diamond nanopowder [15].

In our Model No. 2, the "remove" of neutrons from monoenergetic spectrum at the expense of heating and incoherent processes hasn't been taken into account) the neutron absorption has been taken into account in calculations). For thick samples, the remove processes of neutrons can make a significant contribution to the changes of measured results.

The calculation have been implemented for values $\gamma_1 = 0.523$; $\gamma_1 = 0.569$; $\gamma_1 = 0.682$; $\gamma_1 = 0.682$ of packaging coefficient of nanoparticles in nondestructible (primary) agglomerate with a size of $d_2 \simeq 100 - 200$ nm. The variation existence in calculation and experimental data at thicknesses of diamond nanopowder plate is shown in Figure 4.8 and Figure 4.9 by 2 mm and 6mm relatively.

With the increase of neutron velocity, the contribution of coherent elastic scattering on nanoparticles in a complete cross-section of neutron interaction with nanopowder decreases $\left(\sim v^{-4} \right)$ much faster than the contribution of inelastic processes $\left(\sim v^{-1} \right)$.

The neutron scattering cross-section σ_S with a wave length $\lambda = 0.44$ nm on hydrogen nuclei in diamond nanopowder is measured experimentally in the work [105]. Value $\sigma_s = (108 \pm 2)$ barn has been obtained which slightly varies with the temperature.
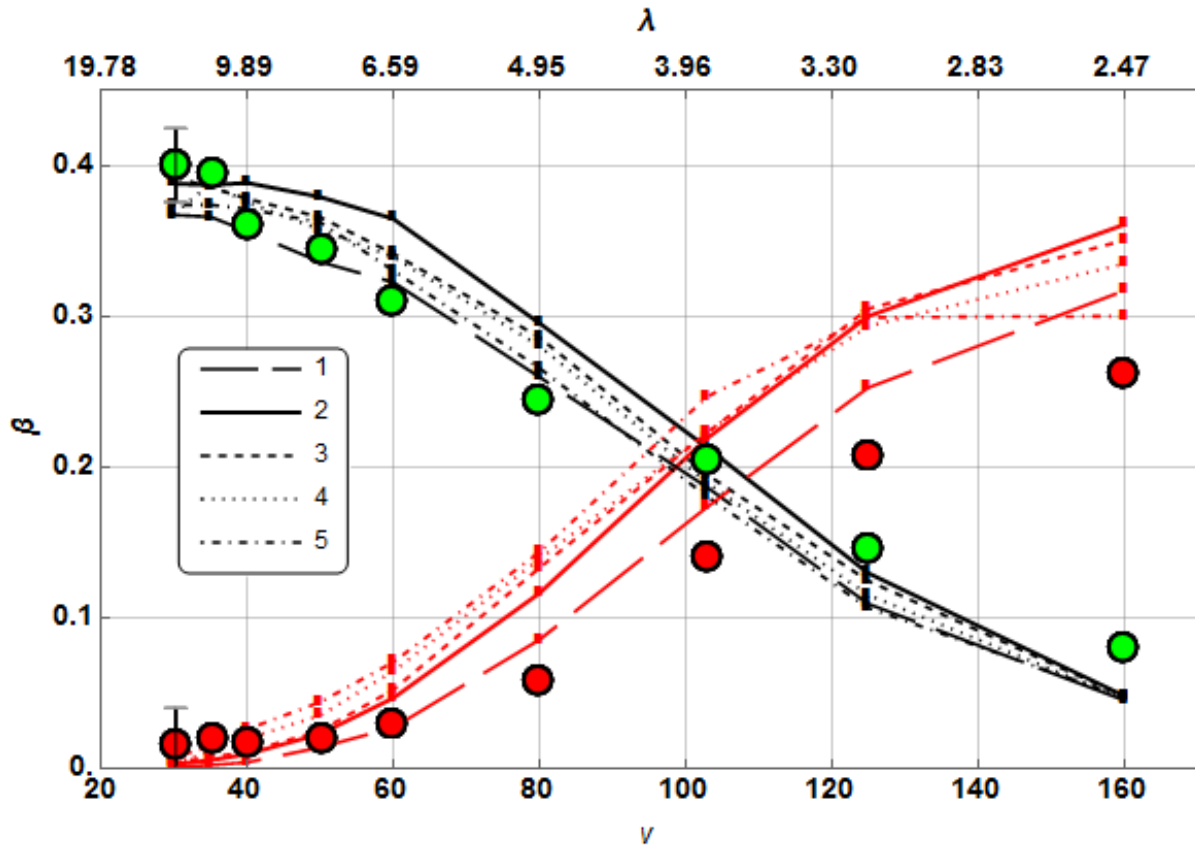
Let's suggest that the low neutron interaction with the hydrogen leads to the "remove" of the current neutron from the monoenergetic spectrum.

Aleksandr Nezvanov, Université Grenoble Alpes, 2018

100 | **Peculiarities of interaction and propagation of low-energy neutrons in nano-dispersed media (the example of diamond nano-powder)**

The constant empirical parameter $\sigma_s = (108 \pm 2)$ barn that accounts for the neutrons escape was borrowed from the work [105] and was introduced into our Model No. 2 for the interaction of slow neutrons with diamond nanopowder. Without changing any other parameters in Model No. 2, new numerical calculations were performed to define the neutron propagation in diamond nanopowder, takinng into account the introduced constant parameter σ_s. The calculation results are shown in curve 1 in Figures 4.8 and 4.9. The presented results correspond to the value $\gamma_1 = 0.682$. Calculations for other values of γ_1 differ negligeably.

Parameters of Model No. 2 are the following: the bulk density of nanopowder $\rho_{bulk} = 0.6$ g/cm^3; the concentration of diamond nanoparticles in the powder as a whole $N_0 = 2.37 \times 10^{24}$ m^{-3}; the packing index of diamond nanoparticles in powder $\gamma = 0.209$; the thickness of the impurity shell $h = 0.5$ nm; the density of the impurity shell $\rho_{shell} = 1.6$ g/cm^3.

A comparison of Figures 4.8 and 4.9 shows that the introduction of the empirical parameter σ_s, measured in the work [105], significantly improved the alignment of the experimental results from the work [14] with the numerical calculations results under Model No. 2 in the covered neutron energy range for thick layers of nanopowders of 2 mm and 6 mm.

New calculations were carried out under Model No. 2 with the introduced empirical parameter of the neutrons escape σ_s for thin layers of diamond nanopowder 0.2 mm and 0.4 mm. The calculation results for thin layers with the parameter σ_s almost do not differ from the results of previous calculations without the parameter σ_s.

Aleksandr Nezvanov, Université Grenoble Alpes, 2018

Peculiarities of interaction and propagation of low-energy neutrons in nano-dispersed media
(the example of diamond nano-powder)

101

Fig. 4.8. Comparison of the probability β of reflection (round green dots) and the passage (round red dots) of neutrons as a function of velocity v (wavelength λ). The sample thickness is 2 mm. Round dots are experimental data [14]. Curve 1 is numerical calculation with allowance for the empirical parameter σ_s of the neutrons escape. For calculated curves 2–5, the values of the packing index γ_1 of diamond nanoparticles in the primary agglomerate are the following:

$$2 - \gamma_1 = 0.523; \; 3 - \gamma_1 = 0.569; \; 4 - \gamma_1 = 0.625; \; 5 - \gamma_1 = 0.682.$$
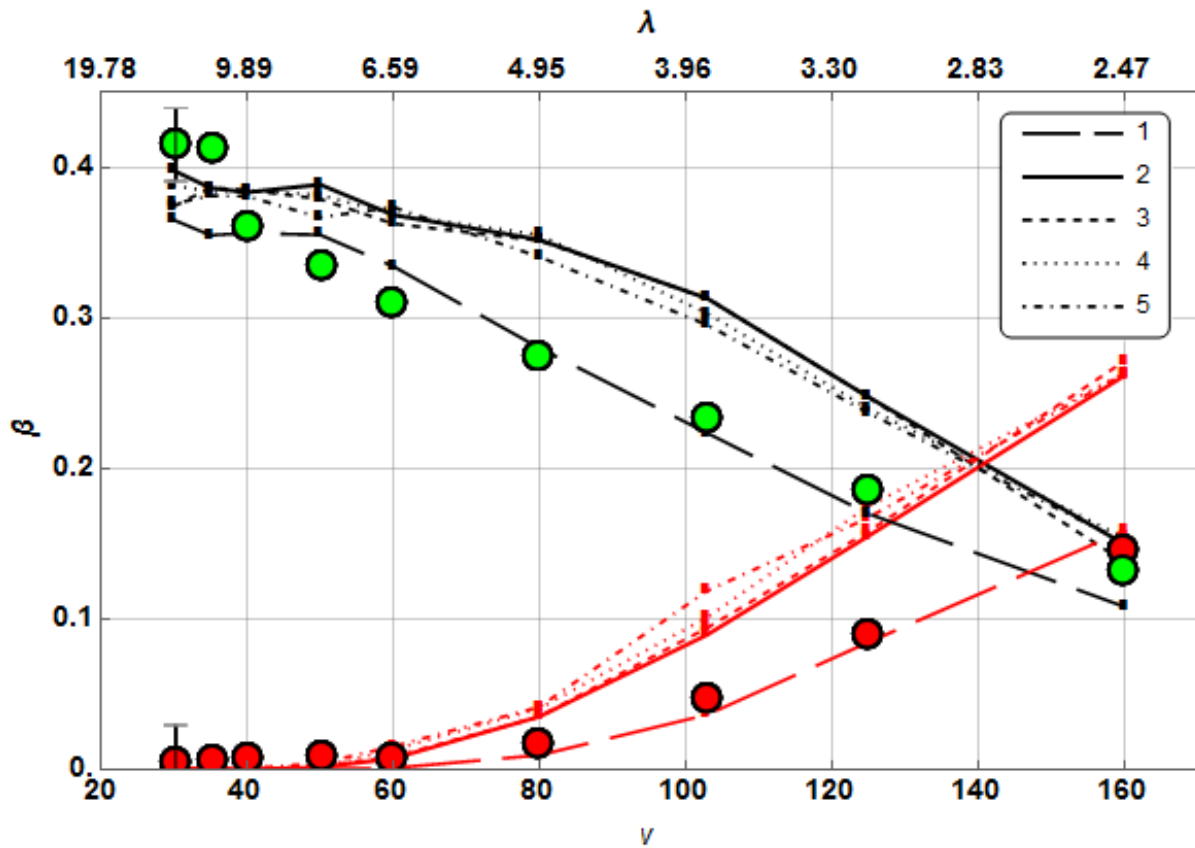
Fig. 4.9.

Comparison of the probability β of reflection (round green dots) and the passage (round red dots) of neutrons as a function of velocity v (wavelength λ).

The sample thickness is 6 mm. Round dots are experimental data [14].

Curve 1 is numerical calculation with allowance for the empirical parameter σ_s of the neutrons escape. For the calculated curves 2–5, the values of the packing index γ_1 of diamond nanoparticles in the primary agglomerate are the following:

$$2 - \gamma_1 = 0.523; \ 3 - \gamma_1 = 0.569; \ 4 - \gamma_1 = 0.625; \ 5 - \gamma_1 = 0.682.$$

Aleksandr Nezvanov, Université Grenoble Alpes, 2018
Peculiarities of interaction and propagation of low-energy neutrons in nano-dispersed media
(the example of diamond nano-powder) | *103*

4.3. The "quasi-specular" reflection of cold and very cold neutrons from a fluorinated sample of diamond nanopowder

The detonation diamond nanopowder is subjected to technological treatment by deep fluorination [35]. As a result of processing, almost all of the hydrogen is removed from the nanopowder, and the surface impurity shell is removed from the individual nanoparticles. The size of diamond nuclei of nanoparticles remain unchanged (average size ~ 4.3 nm). The surface of diamond nuclei is covered with a thin layer of fluorine atoms approximately one atom thick. The hydrogen content in diamond nanoparticles is ~ 0.2 at. %, which is 35–60 times less than before the fluorination process. The bulk density of diamond nanopowder after fluorination almost did not change: 0.29–0.30 g/cm^3 [35].

Figures 4.10 and 4.11 show the dependence of neutron scattering probability β by the surface of a fluorinated diamond nanopowder [35]. The individual dots on the graphs show the results of numerical calculations.

The scale of structural agglomerations of nanoparticles in fluorinated diamond nanopowder has not been studied. To be specific, let us assume the spatial scale homogeneity of the fluorinated nanopowder. The packing index of a fluorinated scale-homogeneous nanopowder (F-powder) as a whole is $\gamma_{hom} = 0.086$.

The size distribution function $f(r)$ of diamond nanoparticles nuclei was defined in the course of experiments on the neutrons passage through the thin layers of F-nanopowder. The function $f(r)$ is shown in Figure 4.12.

Figure 4.10 shows that at a neutron wavelength $\lambda > 1.1$ nm neutrons interact with the F-nanopowder mainly through elastic coherent scattering by nanoparticles. For $\lambda < 1.1$ nm, the main mechanism of neutron interaction with the F-nanopowder changes.

In the thesis, we consider mainly the elastic coherent scattering of neutrons by nanoparticles. Therefore, we shall further consider the scattering of neutrons with a wavelength of $\lambda > 1.1$ nm.

Aleksandr Nezvanov, Université Grenoble Alpes, 2018

104 | **Peculiarities of interaction and propagation of low-energy neutrons in nano-dispersed media (the example of diamond nano-powder)**

Table 4.1 shows the ratios $\eta = \beta_{exp} / \beta_{calc}$, where β_{exp} and β_{calc} are experimentally measured [35] and calculated values of the neutron scattering probability β for the graph data of Figure 4.10. Table 4.1 shows that the value η is almost constant. That is, there is a systematic error in calculating the values of β_{calc}.

Calculations by direct simulation have shown that the neutrons reflection from the F-nanopowder surface is carried out in the neutron diffusion mode in the F-nanopowder layer with the subsequent escape of neutrons. The probability of neutron reflection β is determined by the neutron transport cross section in the nanopowder. For loose F-nanopowder, the transport cross section of neutrons is determined by formula (2.1.48):

$$\Sigma_{tr} = N_0 \sigma_{tr} \propto \gamma \cdot a^{-1} \cdot k^{eff} \cdot \left(1 - \gamma^2\right) \cdot U_0^2 \ .$$

The analysis shows that the systematic error in the calculation of β_{calc} is mostly due to the incorrect identification of the F-nanopowder packing index.

The assumption of F-nanopowder's spatial scale homogeneity is not justified. It is possible to assume that F-nanopowder nanoparticles form agglomerations with a packing index $\gamma_1^{(F)}$, similar to the structural agglomeration of a detonation diamond nanopowder that has not undergone fluorination.

In view of this observation, the calculated values β_{calc} were renormalized by the value $\bar{\eta}$. Figure 4.11 shows the dependency of β_{calc} renormalized by the value $\bar{\eta}$ and β_{exp} on the neutron wavelength λ.

Aleksandr Nezvanov, Université Grenoble Alpes, 2018

Peculiarities of interaction and propagation of low-energy neutrons in nano-dispersed media | *105*
(the example of diamond nano-powder)

Table 4.1.

Wavelength λ, Å	Ratio $\eta = \beta_{exp} / \beta_{calc}$			Average value
	Incidence angle $\alpha = 1°$	Incidence angle $\alpha = 2°$	Incidence angle $\alpha = 3°$	
11.4	0.895	0.902	0.878	0.892
12.1	0.897	0.848	0.874	0.873
12.8	0.865	0.861	0.862	0.863
13.5	0.870	0.828	0.856	0.851
14.2	0.887	0.834	0.845	0.856
14.9	0.874	0.813	0.827	0.838
Average value	0.881	0.848	0.857	—

Total average value $\bar{\bar{\eta}} = 0.862$.

Aleksandr Nezvanov, Université Grenoble Alpes, 2018

106 | **Peculiarities of interaction and propagation of low-energy neutrons in nano-dispersed media (the example of diamond nano-powder)**
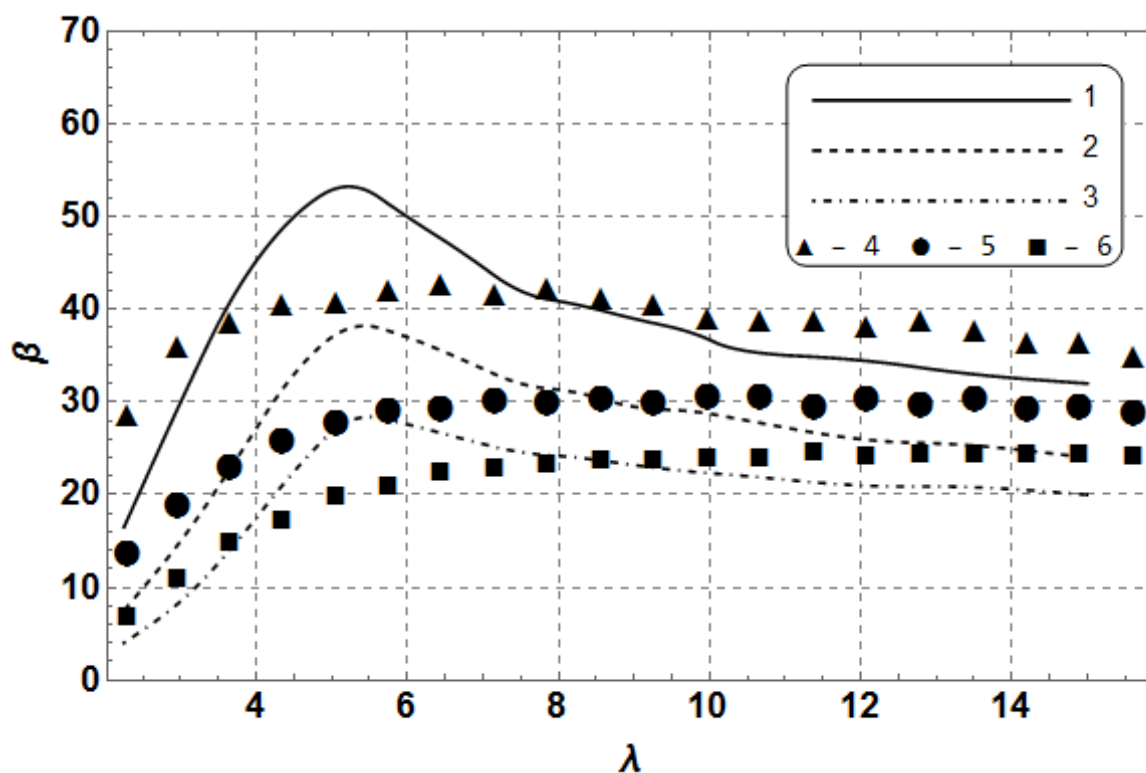
Fig. 4.10. Probabilities of neutron scattering into the detector from the surface of a fluorinated diamond nanopowder.

A neutron beam strikes the surface of the nanopowder at a sliding angles of 1° (1), 2° (2), 3° (3). The target points are 1° (4), 2° (5), 3° (6).

The neutron wavelength is λ in Å.

Aleksandr Nezvanov, Université Grenoble Alpes, 2018
Peculiarities of interaction and propagation of low-energy neutrons in nano-dispersed media | *107*
(the example of diamond nano-powder)
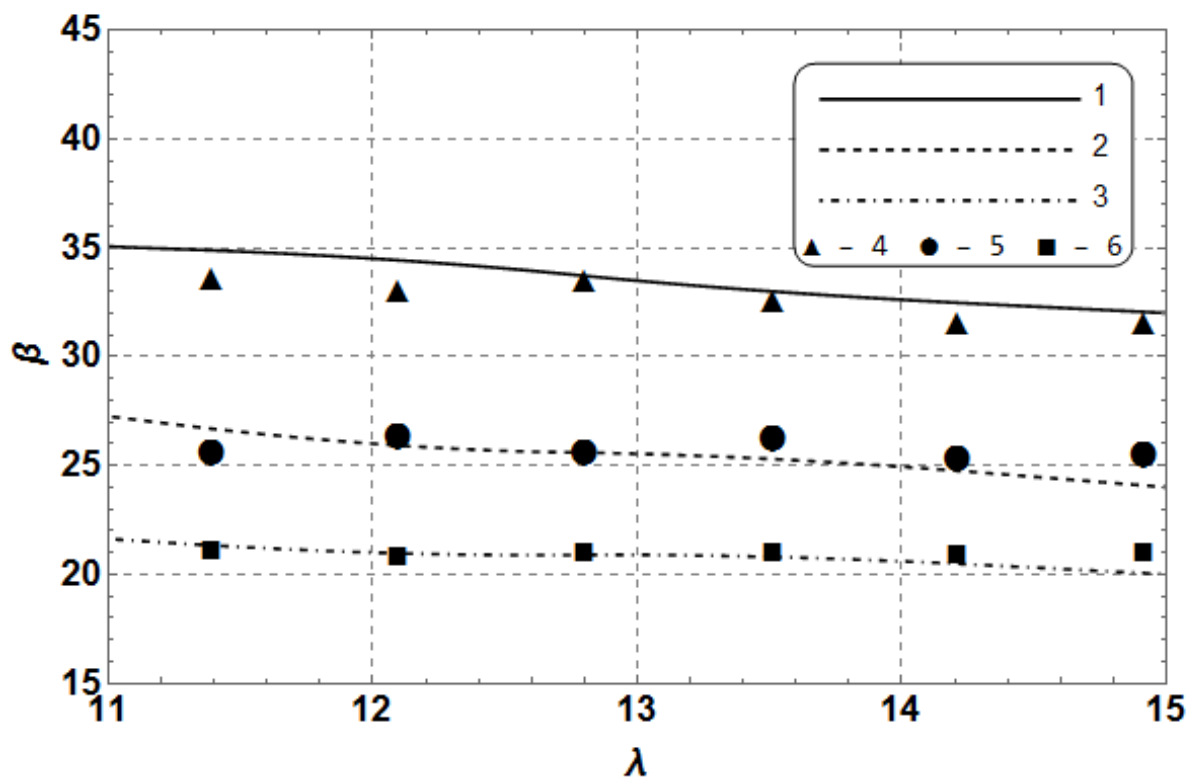
Fig. 4.11. The probability of neutron scattering into the detector from the surface of a fluorinated diamond nanopowder.

The neutron wavelength is λ in Å. See notes in 4.10. The target points β_{calc} 1° (4), 2° (5), 3° (6) are renormalized by the index $\bar{\bar{\eta}} = 0.862$.

Aleksandr Nezvanov, Université Grenoble Alpes, 2018

108 | **Peculiarities of interaction and propagation of low-energy neutrons in nano-dispersed media (the example of diamond nano-powder)**
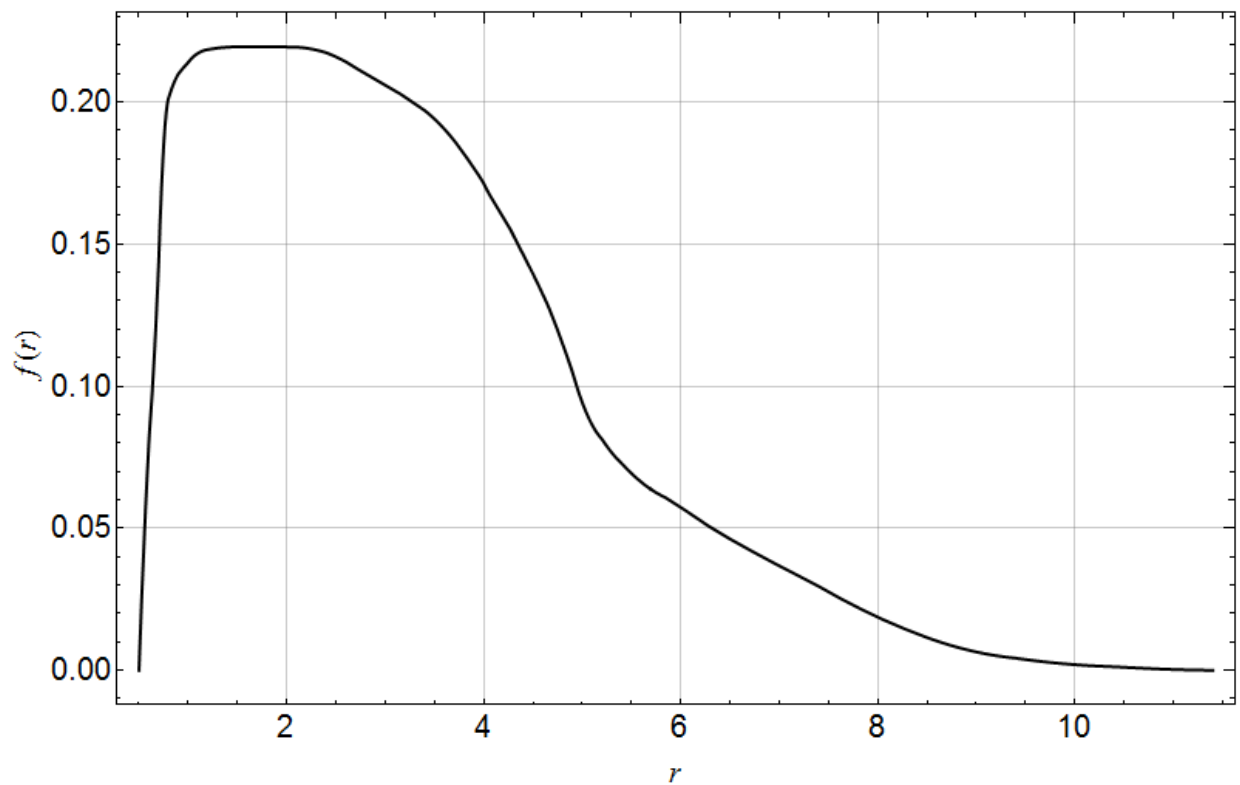
Fig. 4.12. Function of the distribution of diamond nuclei nanoparticles radii of fluorinated diamond nanopowder, r in nm.

Aleksandr Nezvanov, Université Grenoble Alpes, 2018
Peculiarities of interaction and propagation of low-energy neutrons in nano-dispersed media
(the example of diamond nano-powder) | *109*

CONCLUSION

In this thesis we studied the peculiarities of interaction and propagation of low-energy neutrons in nano-dispersed media.

In chapter 2 we suggested a neutron transfer equation in diamond nanopowders, which takes into account the internal small-scale material structure and coherent and incoherent processes of interaction between low-energy neutrons and nanopowder material. We defined the boundary conditions for the neutron transfer equation in the diffusion approximation. Additionally, we used the variation method to suggest an analytical solution for the transfer equation, which accounts for the absorption in the small-angle scattering approximation. We proposed and justified the low-energy neutron interaction model with diamond nanopowder, taking into account the features of the nanopowder structure, and the features of the coherent and incoherent interaction between neutrons and nanopowders.

In chapter 3 the algorithm was designed and a set of computer programs was implemented to calculate the interaction and propagation of neutrons in diamond nanopowders, taking into account the features of the nanopowder structure, diamond nanoparticles and the processes of coherent and incoherent interaction of neutrons with nanopowders.

In chapter 4 theoretical numerical calculations were conducted with the proposed model for the interaction of low-energy neutrons with diamond nanopowders, and the calculation results were compared with experimental results

REFERENCES

[1] V. V. Nesvizhevsky, «Interaction of neutrons with nanoparticles», *Phys. At. Nucl.*, т. 65, вып. 3, сс. 400–408, мар. 2002.

[2] V. A. Artem'ev, «Estimate of the critical parameters of a reactor with a core consisting of nanostructural meterial», *At. Energy*, т. 94, вып. 3, сс. 189–192, 2003.

[3] V. A. Artem'ev, «Estimation of critical parameters for thermal reactor with active zone made of nanostructured materials [in Russian]», *Probl. At. Sci. Technol. Ser. Phys. Nucl. React.*, вып. 1–2, сс. 7–12, 2003.

[4] V. A. Artem'ev, «Estimation of neutron reflection from nanodispersed materials», *At. Energy*, т. 101, вып. 6, сс. 901–904, дек. 2006.

[5] V. K. Ignatovich и E. P. Shabalin, «Algebraic method for calculating a neutron albedo», *Phys. At. Nucl.*, т. 70, вып. 2, сс. 265–272, 2007.

[6] V. A. Artem'ev, «The possibility of cold neutron accumulation in vessels made of nanomaterials [in Russian]», *Perspekt. Mater. Spec. Issue Funct. Nanomater. high-purity Subst.*, т. 6, вып. 1, сс. 121–125, 2008.

[7] E. V. Lychagin, A. Y. Muzychka, V. V. Nesvizhevsky, G. Pignol, K. V. Protasov, и A. V. Strelkov, «Storage of very cold neutrons in a trap with nano-structured walls», *Phys. Lett. Sect. B Nucl. Elem. Part. High-Energy Phys.*, т. 679, вып. 3, сс. 186–190, 2009.

[8] V. A. Artem'ev, «Dependence of the characteristics of a nuclear reactor on the particle size of a nanodispersed moderator», *At. Energy*, т. 101, вып. 3, сс. 675–679, сен. 2006.

[9] L. D. Landau и L. M. Lifshitz, *Quantum Mechanics. Non-Relativistic Theory*, 3-е изд. Oxford: Pergamon Press, 1991.

[10] M. L. Goldberger и K. M. Watson, *Collision theory*. New York: John Wiley and Sons, 2004.

[11] V. G. Baryshevsky, *Nuclear Optics of Polarized Media [in Russian]*. Moscow:

Aleksandr Nezvanov, Université Grenoble Alpes, 2018
**Peculiarities of interaction and propagation of low-energy neutrons in nano-dispersed media
(the example of diamond nano-powder)** | *111*

Energoatomizdat, 1995.

[12] Y. N. Barabanenkov, «Multiple scattering of waves by ensembles of particles and the theory of radiation transport», *Sov. Phys. Usp.*, т. 18, cc. 673–689, 1975.

[13] V. V. Babikov, *Method of Phase Functions in Quantum Mechanics [in Russian]*. Moscow: Nauka, 1976.

[14] V. V. Nesvizhevsky, E. V. Lychagin, A. Y. Muzychka, A. V. Strelkov, G. Pignol, и K. V. Protasov, «The reflection of very cold neutrons from diamond powder nanoparticles», *Nucl. Instruments Methods Phys. Res. Sect. A*, т. 595, вып. 3, cc. 631–636, окт. 2008.

[15] «Website of „ultradiamond90" nanopowder». [Онлайн]. Доступно на: http://www.ultradiamondtech.com/. [Просмотрено: 29-май-2010].

[16] A. L. Vereschagin, E. A. Petrov, G. V. Sakovich, V. F. Komarov, A. V. Klimov, и N. V. Kozyrev, «Diamond-carbon material and method of its production», 2041165, 1995.

[17] A. L. Vereschagin, E. A. Petrov, G. V. Sakovich, V. F. Komarov, A. V. Klimov, и N. V. Kozyrev, «Synthetic Diamond-Containing Material and Method of Obtaining It», 5,861,349, 1999.

[18] Ouyang Q., Okada K. Nano-ball bearing effect of ultra-fine particles of cluster diamond // Appl. Surf. Sci. 1994. Т. 78, № 3. С. 309–313.

[19] Palosz B. и др. Microstructure of nanocrystalline diamond powders studied by powder diffractometry // J. Appl. Phys. 2005. Т. 97, № 6. С. 064316.

[20] Palosz B. и др. Analysis of short and long range atomic order in nanocrystalline diamonds with application of powder diffractometry // Zeitschrift fur Krist. 2002. Т. 217, № 10. С. 497–509.

[21] Barnard A.S., Sternberg M. Crystallinity and surface electrostatics of diamond nanocrystals // J. Mater. Chem. 2007. Т. 17, № 45. С. 4811.

[22] Barnard A.S. Self-assembly in nanodiamond agglutinates // J. Mater. Chem. 2008. Т. 18, № 34. С. 4038.

Aleksandr Nezvanov, Université Grenoble Alpes, 2018

112 | **Peculiarities of interaction and propagation of low-energy neutrons in nano-dispersed media (the example of diamond nano-powder)**

[23] Krüger A. и др. Unusually tight aggregation in detonation nanodiamond: Identification and disintegration // Carbon N. Y. 2005. Т. 43, № 8. С. 1722–1730.

[24] Spitsyn B.V. и др. Inroad to modification of detonation nanodiamond // Diam. Relat. Mater. 2006. Т. 15, № 2–3. С. 296–299.

[25] Chang L.-Y., Ōsawa E., Barnard A.S. Confirmation of the electrostatic self-assembly of nanodiamonds // Nanoscale. 2011. Т. 3, № 3. С. 958.

[26] Artem'ev V.A., Nezvanov A.Y., Nesvizhevsky V. V. Nanotechnology for atomic energy and industry // Dautreppe 2016 demain l'énergie: Programme & résumés. Grenoble: Société Française de Physique, 2016. p. 47.

[27] A. Y. Nezvanov, V. A. Artem'ev, and V. V. Nesvizhevsky, 'Improving the accuracy of the model describing the interaction of very cold neutrons with diamond nanopowders [in Russian]', in *Meetings and Youth Conference on Neutron Scattering and Synchrotron Radiation in Condensed Matter (NSSR-CM-2014): Collected Abstracts*, 2014, p. 209.

[28] V. A. Artem'ev and A. Y. Nezvanov, 'Nanotechnology for nuclear energy and industry [in Russian]', in *Abstracts of the conference of young specialists 'Innovations in Nuclear Energy'*, 2017, pp. 362–368.

[29] A. Y. Nezvanov, 'Analysis of existing models of diamond nanoparticles [n Russian]', in *The 51st School on Condensed State Physics: Collection of abstracts and the list of participants*, 2017, p. 135.

[30] A. Y. Nezvanov, V. A. Artem'ev, and V. V. Nesvizhevsky, 'Simulations for studying the interactions of low-energy neutrons with nanodiamond powder [in Russian]', in *Proceedings of the 11th International Conference 'Carbon: Fundamental Problem, Material Science, Technology'*, 2018, pp. 335–336.

[31] Artem'ev V.A., Nesvizhevsky V.V., Nezvanov A.Yu., Proskuryakov A.L. A Solution of the Kinetic Equation for the Propagation of Radiation in Nanodispersed Absorbing Medium in the Approximation of Small Scattering Angles // Proceedings of the XXIII International Seminar on Interaction of Neutrons with Nuclei. Dubna: JINR, 2016. pp. 111–118.

Aleksandr Nezvanov, Université Grenoble Alpes, 2018
Peculiarities of interaction and propagation of low-energy neutrons in nano-dispersed media
(the example of diamond nano-powder)

113

[32]   V. A. Artem'ev and A. Y. Nezvanov, 'Nanotechnology for nuclear energy and industry [in Russian]', in *Proceedings of the conference of young specialists 'Innovations in Nuclear Energy'*, 2017, pp. 362–368.

[33]   Artem'ev V.A., Nesvizhevsky V. V., Nezvanov A.Yu. Estimations of the Inelastic Interaction of Neutrons with Nanostructures Media at Low Energies and Temperatures // Proceedings of the XXV International Seminar on Interaction of Neutrons with Nuclei. Dubna: JINR, 2018. pp. 23–30.

[34]   V. A. Artem'ev, A. Y. Nezvanov, and V. V. Nesvizhevsky, 'Precise calculations in simulations of the interaction of low energy neutrons with nano-dispersed media', *Crystallogr. Reports*, vol. 61, no. 1, pp. 84–88, 2016.

[35]   Nesvizhevsky V.V., Dubois M., Gutfreund Ph., Lychagin E.V., Nezvanov A.Yu. and Zhernenkov K.N. Effect of nanodiamond fluorination on the efficiency of quasispecular reflection of cold neutrons // Phys. Rev. A. American Physical Society, 2018. Vol. 97, i. 2. pp. 1–8. DOI: 10.1103/PhysRevA.97.023629.

[36]   A. Y. Nezvanov, 'Monte Carlo Neutron Transport in Nanodispersed Diamond Powder in using of Born approximation (MCNT-NDP-B)', 2015618099, 2015.

[37]   A. Y. Nezvanov, 'Monte Carlo Neutron Transport in Nanodispersed Diamond Powder within Precise Calculation (MCNT-NDP-PC)', 2016612455, 2016.

[38]   V.A. Artem'ev, V.A. Sazonov, V.I. Koshkin, V.N. Fridlyanov, A.L. Proskuryakov, Yu.M. Borovin. Investigation of the patterns of the dynamics of nanotechnology development in the world in the period 1900-2012. // Mechanical engineering and engineering education, 2013, № 4, pp. 70-80.

[39]   Hulman A. Economic development of nanotechnologies: a review of indicators. Forsyte, 2009, Vol. 3, № 1 (9), p. 30-47.

[40]   Nanotechnology as a key factor in the new technological order in the economy. Ed. Academician of the Russian Academy of Sciences S.Yu. Glazyev and Professor V.V. Kharitonov. - M .: "Trovant". 2009. – 304 c.

[41]   V.A. Artemyev, V.I. Koshkin, V.A. Sazonov, V.N. Fridlyanov, A.L. Proskuryakov, Yu.M. Borovin. Research of directions of development of

Aleksandr Nezvanov, Université Grenoble Alpes, 2018

114 | **Peculiarities of interaction and propagation of low-energy neutrons in nano-dispersed media (the example of diamond nano-powder)**

nanotechnologies in the nuclear industry and technology. // Mechanical engineering and engineering education, 2012, № 4, pp. 9-17.

[42] I. D. Morokhov, L. I. Trusov, and V. N. Lapovok, *Physical phenomena in ultra-dispersed substances [in Russian]*. Moscow: Energoatomizdat, 1984.

[43] V. I. Tkachenko, V. A. Yupenkov, Y. A. Krikun, A. A. Ryabovol, V. A. Artem'ev, and V. P. Alekhin, 'Diploma №4. The phenomenon of anomalous attenuation of X-ray radiation by ultradispersed media [in Russian]', *Bull. High. Attestation Comm. Russ. Fed.*, vol. 5–6, p. 44, 1994.

[44] V. A. Artem'ev, S. V. Chuklyaev, Y. A. Krikun, V. I. Tkachenko, V. A. Yupenkov, and V. V. Chulkov, 'Passage of X-rays through ultradispersed systems', *At. Energy*, vol. 78, no. 3, pp. 184–189, Mar. 1995.

[45] V. A. Artem'ev and N. I. Sokolovskii, 'Evaluation of X-ray attenuation by ultradisperse media', *At. Energy*, vol. 81, no. 6, pp. 874–879, Dec. 1996.

[46] V. A. Artem'ev, 'Attenuation of x rays by ultradisperse media', *Tech. Phys. Lett.*, vol. 23, no. 3, pp. 212–213, Mar. 1997.

[47] Алёхин В.П., Артемьев В.А., Крикун Ю.А., Соколовский Н.И., Ткаченко В.И., Юпенков В.А. О прохождении рентгеновского излучения через мелкодисперсные среды. // Сборник научных трудов сотрудников института / Под ред. А.М. Рябышева. Москва: МАСИ (ВТУЗ-ЗИЛ), 1995. С. 60–63.

[48] Алёхин В.П., Артемьев В.А., Крикун Ю.А., Соколовский Н.И., Ткаченко В.И., Юпенков В.А. О взаимодействии рентгеновского излучения с высокодисперсными средами // Сборник научных трудов сотрудников института / Под ред. А.М. Рябышева. Москва: МАСИ (ВТУЗ-ЗИЛ), 1995. С. 64–67.

[49] Алёхин В.П., Артемьев В.А., Катращук Г.К., Крикун Ю.А., Соколовский Н.И., Ткаченко В.И., Юпенков В.А. О взаимодействии рентгеновского излучения с ультрадисперсными средами. // Сборник научных трудов сотрудников института / Под ред. А.М. Рябышева. □ Москва: МАСИ (ВТУЗ-ЗИЛ), 1995. С. 68–71.

Aleksandr Nezvanov, Université Grenoble Alpes, 2018
Peculiarities of interaction and propagation of low-energy neutrons in nano-dispersed media
(the example of diamond nano-powder) | *115*

[50] Алёхин В.П., Артемьев В.А., Крикун Ю.А., Соколовский Н.И., Ткаченко В.И., Юпенков В.А. Рентгенографический контроль многослойных конструкций сложной формы. // Сборник научных трудов сотрудников института / Под ред. А.М. Рябышева. ☐ Москва: МАСИ (ВТУЗ-ЗИЛ), 1995. С. 71–73.

[51] Алёхин В.П., Артемьев В.А., Катращук Г.К., Соколовский Н.И., Крикун Ю.А., Ткаченко В.И., Юпенков В.А. Рентгеноконтрастные материалы для медицины // Сборник научных трудов сотрудников института / Под ред. А.М. Рябышева. Москва: МАСИ (ВТУЗ-ЗИЛ), 1995. С. 74–75.

[52] Алехин В.П., Артемьев В.А., Катращук Г.К., Крикун Ю.А., Соколовский Н.И., Ткаченко В.И., Юпенков В.А. Перспективные новые защитные материалы при лучевой диагностике // Сборник научных трудов сотрудников института / Под ред. А.М. Рябышева. ☐ Москва: МАСИ (ВТУЗ-ЗИЛ), 1995. С. 75–76.

[53] Артемьев В.А., Алёхин В.П. Распространение рентгеновского излучения в ультрадисперсных материалах. // Международный аэрозольный симпозиум IAS-3. Секция «Ультрадисперсные порошки». Москва: Аэрозольное общество, 1996. С. 17–18.

[54] Алексеев Ю.С., Артемьев В.А., Джур Е.А. и др. Аномалии рентгеновского излучения и их использование в промышленности. // Системні технології. Регіональний міжвузівський збірник наукових праць. Дніпропетровськ: ДНВП «Системні технології», 2002. С. 3–9.

[55] Чукляев С.В., Грудский М.Я., Артемьев В.А. Вторично-эмиссионные детекторы ионизирующих излучений. Москва: Энергоатомиздат, 1995. ☐ 368 с.

[56] Marenkov O S and Komyak N I, Handbook of Photon Interaction Coefficients in X-ray Photometric Analysis (Leningrad, Energoatomizdat, 1988).

[57] Grigor'ev I S and Melikhov E Z (eds.), Handbook of Physical Quantities (Moscow, Energoatomizdat, 1991).

Aleksandr Nezvanov, Université Grenoble Alpes, 2018

116 | *Peculiarities of interaction and propagation of low-energy neutrons in nano-dispersed media (the example of diamond nano-powder)*

[58] Kaloshkin S D et al. (2012). J. Alloys Comp. 536S, S522.

[59] Artem'ev V A (2002). At. Energ. 93, 665.

[60] Ignatovich V K, Nesvizhevsky V V (2014). At. Energ. 116,132.

[61] Kalashnikov N P, Remizovich V S and Ryazanov M I, Collisions of Fast Charged Particles in Solids (Moscow, Atomizdat, 1980).

[62] Волков К.В., Даниленко В.В., Елин В.И. Синтез алмаза из углерода продуктов детонации ВВ // Физика горения и взрыва. 1990. Т. 23, № 3. С. 123–125.

[63] Vereschagin A.L. и др. Properties of ultrafine diamond clusters from detonation synthesis // Diam. Relat. Mater. 1994. Т. 3, № 1–2. С. 160–162.

[64] Даниленко В.В. Синтез и спекание алмаза взрывом. Москва: Энергоатомиздат, 2003. 272 с.

[65] Даниленко В.В. Из истории открытия синтеза наноалмазов // Физика твердого тела. 2004. Т. 46, № 4. С. 581–584.

[66] Даниленко В.В. Особенности синтеза детонационных наноалмазов // Физика горения и взрыва. 2005. Т. 41, № 5. С. 104–116.

[67] Гуревич И.И., Тарасов Л.В. Физика нейтронов низких энергий / под ред. Шкляр С.Я. Москва: Наука, 1965. 608 с.

[68] Киттель Ч. Введение в физику твёрдого тела / под ред. Гусева А.А. Москва: Наука, 1978. 792 с.

[69] Займан Д. Модели беспорядка. Теоретическая физика однородно неупорядоченных систем: Пер. с англ. Москва: Мир, 1982. □ 592 с.

[70] Чудновский А.Ф. Теплообмен в дисперсных средах / под ред. Новожилов Ю.В. Москва: ГИТТЛ, 1954. 444 с.

[71] Ханнинк Р., Хилл А. Наноструктурные материалы / под ред. Баурова Н.И. Москва: Техносфера, 2009. 488 с.

[72] Игнатович В.К. Физика ультрахолодных нейтронов. Москва: Наука, 1986. □ 272 с.

Aleksandr Nezvanov, Université Grenoble Alpes, 2018
Peculiarities of interaction and propagation of low-energy neutrons in nano-dispersed media
(the example of diamond nano-powder) | *117*

[73] Зельдович Я.Б. Хранение холодных нейтронов // Журнал Экспериментальной и Теоретической Физики. 1959. Т. 36, № 6. С. 1952–1954.

[74] Степанов А.В. Оптический потенциал для ультрахолодных нейтронов. // Физика элементарных частиц и атомного ядра. 1976. Т. 7, вып. 4. С. 989-1038.

[75] Татарский В.И. Распространение волн в турбулентной атмосфере / под ред. Шмидт В.В., Гладнева Л.И. Москва: Наука, 1967. pp. 548 с.

[76] Рытов С.М., Кравцов Ю.А., Татарский В.И. Введение в статистическую радиофизику. Часть 2. Случайные поля. Москва: Н, 1978. pp. 464 с.

[77] Апресян Л.А., Кравцов Ю.А. Теория переноса излучения: статистические и волновые аспекты. Москва: Наука, 1983. pp 215 с.

[78] Foldy L.L. The Multiple Scattering of Waves. I. General Theory of Isotropic Scattering by Randomly Distributed Scatterers // Phys. Rev. 1945. Vol. 67, No. 3–4. P. 107–119.

[79] Lax M. Multiple Scattering of Waves // Rev. Mod. Phys. 1951. Vol. 23, P. 287–310.

[80] Lax M. Multiple Scattering of Waves. II. The Effective Field in Dense Systems // Phys. Rev. 1952. Vol. 85, No. 4. P. 621–629.

[81] Исимару А. Распространение и рассеяние волн в случайно-неоднородных средах. Т. 1. Москва: Мир, 1981. 285 с.

[82] Исимару А. Распространение и рассеяние волн в случайно-неоднородных средах. Т. 2. Москва: Мир, 1981. 322 с.

[83] Абрикосов А.А., Горьков Л.П., Дзялошинский И.Е. Методы квантовой теории поля в статистической физике. Москва: Добросвет, 1998. 514 с.

[84] Ашкрофт Н.В., Мермин Н.Д. Физика твердого тела. Т. 1. Москва: Мир, 1979. 399 с.

[85] Фейнберг С.М., Шихов С.Б., Троянский В.Б. Теория ядерных реакторов. Т. 1. Элементарная теория реакторов. М.: Атомиздат, 1978.

Aleksandr Nezvanov, Université Grenoble Alpes, 2018

118 | ***Peculiarities of interaction and propagation of low-energy neutrons in nano-dispersed media (the example of diamond nano-powder)***

[86] Avdeev M. V., Aksenov V.L., Rosta L. Pressure induced changes in fractal structure of detonation nanodiamond powder by small-angle neutron scattering // Diam. Relat. Mater. 2007. Vol. 16, N 12. P. 2050–2053.

[87] Илиева К.Д., Казарновский М.В. Нестационарный перенос нейтронов. Теория и приложение / под ред. Старирадева Б. София: Издательство Болгарской Академии Наук, 1984. 138 с.

[88] Цвайфель П. Физика реакторов / под ред. Малявина О.М. Москва: Атомиздат, 1977. 280 с.

[89] Гуревич И.И., Протасов В.П. Нейтронная физика. Москва: Энергоатомиздат, 1997. 416 с.

[90] Абромовиц М., Стиган И.А. Справочник по специальным функциям с формулами, графиками и таблицами. Москва: Наука, 1979. 832 с.

[91] Ландау Л. Д., Лифшиц Е. М. Механика. М.: Наука, 1973.

[92] Свергун Д.И., Фейгин Л.А. Рентгеновское и нейтронное малоугловое рассеяние. М.: Наука, 1986.

[93] Бабиков В.В. Метод фазовых функций в квантовой механике. М.: Наука, 1976.

[94] Артемьев В.А., Витовский Н.А., Михнович В.В. // Физика и техника полупроводников. 1989. Т. 23. С. 1395.

[95] Алексенский А.Е., Байдакова М.В., Вуль А.Я., Давыдов В.Ю., Певцова Ю.А. Фазовый переход алмаз – графит в кластерах ультрадисперсного алмаза // Физика твердого тела. 1997. Т. 39. С. 1125–1134.

[96] Спанье Д., Гелбард Э. Метод Монте-Карло и задачи переноса нейтронов. Москва: Атомиздат, 1972. С. 272.

[97] Соболь И.М. Численные методы Монте-Карло / ed. Пирогова Г.Я. Москва: Наука, 1973. С. 312.

[98] Бусленко Н.П., Голенко Д.И., Соболь И.М. и др. Метод статистических испытаний (метод Монте-Карло). М.: Физматлит, 1962.

Aleksandr Nezvanov, Université Grenoble Alpes, 2018
Peculiarities of interaction and propagation of low-energy neutrons in nano-dispersed media
(the example of diamond nano-powder)

119

[99]   Михайлов Г.А., Войтишек А.В. Численное статистическое моделирование. Методы Монте-Карло: учебное пособие для студентов вузов. Москва: Издательский центр "Академия," 2006. С. 368.

[100] Кольчужкин А.М., Учайкин В.В. Введение в теорию прохождения частиц через вещество. Москва: Атомиздат, 1978. С. 256.

[101] Давыдов А.С. Квантовая механика. 3rd ed. СПб: БХВ-Петербург, 2011. С. 704.

[102] Бусленко Н.П., Шрейдер Ю.А. Метод статистических испытаний (Монте-Карло) и его реализация на цифровых вычислительных машинах. Москва: Физматгиз, 1961. 228 с.

[103] Франк-Каменецкий А.Д. Моделирование траекторий нейтронов при расчете реакторов методом Монте-Карло. Москва: Атомиздат, 1978. 96 с.

[104] Ермаков С.М., Михайлов Г.А. Статистическое моделирование. 2-е изд. М.: Наука, 1982. 296 с.

[105] Krylov A.R. et al. Study of bound hydrogen in powders of diamond nanoparticles // Crystallogr. Reports. 2011. Vol. 56, 7. pp. 1186–1191.

[106] Poole C.P.J., Owens F.J. Introduction to Nanotechnology. Hoboken, New Jersey: John Wiley and Sons, 2003. 388 с.

[107] Roduner E. Size matters: why nanomaterials are different // Chem. Soc. Rev. 2006. Т. 35, № 7. С. 583.

[108] Baidakova M., Vul' A. New prospects and frontiers of nanodiamond clusters // J. Phys. D. Appl. Phys. 2007. Т. 40, № 20. С. 6300–6311.

[109] Vul' A.Y. Innovative superhard materials and sustainable coating // Proc. of NATO Advanced Research Workshop. Kyiv, 2004. С. 29.

[110] Долматов В.Ю. Детонационные наноалмазы: синтез, строение, свойства и применение // Успехи химии. 2007. Т. 76, № 4. С. 375–397.

[111] Долматов В.Ю. К вопросу об элементном составе и кристаллохимических параметрах детонационных наноалмазов // Сверхтвердые материалы. 2009. Т. 3. С. 26–33.

[112] Ji S. и др. FTIR study of the adsorption of water on ultradispersed diamond powder surface // Appl. Surf. Sci. 1998. T. 133, № 4. C. 231–238.

[113] Batsanov S.S. и др. Giant dielectric permittivity of detonation-produced nanodiamond is caused by water // J. Mater. Chem. 2012. T. 22, № 22. C. 11166.

[114] Сакович Г.В., Комаров В.Ф., Петров Е.А. Синтез, свойства, применение и производство наноразмерных синтетических алмазов. Часть 1. Синтез и свойства // Сверхтвердые материалы. 2002. T. 3. C. 3.

[115] Volkov D.S., Proskurnin M.A., Korobov M. V. Elemental analysis of nanodiamonds by inductively-coupled plasma atomic emission spectroscopy // Carbon N. Y. 2014. T. 74. C. 1–13.

[116] Еняшин А.Н., Ивановский А.Л. Атомная структура, стабильность и электронное строение икосаэдрических наноалмазов и онионов // Физика твердого тела. 2007. T. 49, № 2. C. 378–383.

[117] Raty J.Y., Galli G. Ultradispersity of diamond at the nanoscale // Nat. Mater. 2003. T. 2, № 12. C. 792–795.

[118] Eidelman E.D. и др. A stable suspension of single ultrananocrystalline diamond particles // Diam. Relat. Mater. 2005. T. 14, № 11–12. C. 1765–1769.

[119] Shenderova O.A., Zhirnov V. V., Brenner D.W. Carbon Nanostructures // Crit. Rev. Solid State Mater. Sci. 2002. T. 27, № 3–4. C. 227–356.

[120] Ōsawa E. Monodisperse single nanodiamond particulates // Pure Appl. Chem. 2008. T. 80, № 7. C. 1365–1379.

[121] Vul' A., Baidakova M., Dideikin A. Carbon nanomaterials. Series: Advanced Materials and Technolohies. 2-е изд. / под ред. Gogotski Y., Presser V. Boca Raton: CRC Press, 2013. 251-278 c.

[122] Osswald S. и др. Control of sp2/sp3 Carbon Ratio and Surface Chemistry of Nanodiamond Powders by Selective Oxidation in Air // J. Am. Chem. Soc. 2006. T. 128, № 35. C. 11635–11642.

[123] Panich A.M. и др. Nuclear magnetic resonance study of ultrananocrystalline diamonds // Eur. Phys. J. B. 2006. T. 52, № 3. C. 397–402.

Aleksandr Nezvanov, Université Grenoble Alpes, 2018
Peculiarities of interaction and propagation of low-energy neutrons in nano-dispersed media | 121
(the example of diamond nano-powder)

[124] Алексенский А.Е. и др. Структура алмазного нанокластера // Физика твердого тела. 1999. Т. 41, № 4. С. 740–743.

[125] Ōsawa E. и др. Consequences of strong and diverse electrostatic potential fields on the surface of detonation nanodiamond particles // Diam. Relat. Mater. 2009. Т. 18, № 5–8. С. 904–909.

[126] Fang X. и др. Nonaromatic Core−Shell Structure of Nanodiamond from Solid-State NMR Spectroscopy // J. Am. Chem. Soc. 2009. Т. 131, № 4. С. 1426–1435.

[127] Avdeev M. V. и др. The spatial diamond-graphite transition in detonation nanodiamond as revealed by small-angle neutron scattering // J. Phys. Condens. Matter. 2013. Т. 25, № 445001. С. 7.

[128] Aksenov V.L. Neutron studies of carbon nanostructures // Nanotechnologies Russ. 2011. Т. 6, № 7–8. С. 407–418.

[129] Tomchuk O. V. и др. Small-angle scattering from polydisperse particles with a diffusive surface // J. Appl. Crystallogr. 2014. Т. 47, № 2. С. 642–653.

[130] Томчук А.В. и др. Малоугловое рассеяние нейтронов фрактальными кластерами в водных дисперсиях наноалмазов // Письма в ЭЧАЯ. 2011. Т. 8, № 10. С. 24–28.

[131] Avdeev M. V. и др. Aggregate structure in concentrated liquid dispersions of ultrananocrystalline diamond by small-angle neutron scattering // J. Phys. Chem. С. 2009. Т. 113, № 22. С. 9473–9479.

[132] Stelmakh S. и др. Internal Structure of Diamond Nanocrystals by Modeling and PDF Analysis // MRS Proc. 2013. Т. 1554.

[133] Богатырева Г.П. и др. Поверхностные и электрофизические свойства наноалмаза детонационного синтеза // Сверхтвердые материалы. 1999. № 6. С. 42–46.

[134] Кулакова И.И. и др. Химические свойства ультрадисперсных детонационных алмазов // Сверхтвердые материалы. 2000. № 1. С. 46–53.

Aleksandr Nezvanov, Université Grenoble Alpes, 2018

122 | *Peculiarities of interaction and propagation of low-energy neutrons in nano-dispersed media (the example of diamond nano-powder)*

[135] Mochalin V., Osswald S., Gogotsi Y. Contribution of Functional Groups to the Raman Spectrum of Nanodiamond Powders // Chem. Mater. 2009. Т. 21, № 2. С. 273–279.

[136] Ястребов С.Г., Иванов-Омский В.И. Функция распределения ультрадисперсных алмазов по размерам // Письма в ЖТФ. 2008. Т. 34, № 6. С. 73–79.

[137] Жарков А.С., Петров Е.А., Анасьева Е.С. Синтез, свойства и перспективы применения детонационных наноалмазов // Фундаментальные проблемы современного материаловедения. 2013. Т. 10, № 3. С. 430–436.

[138] Оленин А.Ю. Механизмы формирования металлических наночастиц // Российские нанотехнологии. 2012. Т. 7, № 5–6. С. 53–55.

[139] Романов Н.А., Номоев А.В., Калашников С.В. Исследование функций распределения наночастиц по размерам. Механизм образования наночастиц, полученных методом испарения электронным пучком // Вестник бурятского государственного университета. 2013. Т. 3. С. 93–99.

[140] V.V. Nesvizhevsky, G. Pignol, K.V. Protasov, Nanoparticles as a possible moderator for an ultracold neutron source, Int. J. Nanoscience 6 (2007) 485-489.

[141] E.V. Lychagin, A.Yu. Muzychka, V.V. Nesvizhevsky, G.V. Nekhaev, G. Pignol, K.V. Protasov, A.V. Strelkov, Coherent scattering of slow neutrons at nanoparticles in particle physics experiments, Nucl. Instr. Meth. A 611 (2009) 302-305.

[142] V.V. Nesvizhevsky, R. Cubitt, E.V. Lychagin, A.Yu. Muzychka, G.V. Nekhaev, G. Pignol, K.V. Protasov, A.V. Strelkov, Application of diamond nanoparticles in low-energy neutron physics, Materials 3 (2010) 1768-1781.

[143] R. Cubitt, E.V. Lychagin, A.Yu. Muzychka, G.V. Nekhaev, V.V. Nesvizhevsky, G. Pignol, K.V. Protasov, A.V. Strelkov, Quasi-specular reflection of cold neutrons from nano-dispersed media at above-critical angles, Nucl. Instr. Meth. A 622 (2010) 182-185.

Aleksandr Nezvanov, Université Grenoble Alpes, 2018
Peculiarities of interaction and propagation of low-energy neutrons in nano-dispersed media
(the example of diamond nano-powder) | *123*

[144] V.V. Nesvizhevsky, Reflectors for VCN and applications of VCN, Rev. Mex. Fis. 57 (2011) 1-5.

[145] V.V. Nesvizhevsky, U. Koester, M. Dubois, N. Batisse, L. Frezet, A. Bosak, L. Gines, O. Williams, Fluorinated nanodiamonds as unique neutron reflector, Carbon 130 (2018) 799-805.